Subcellular Localization of Benzoate:Coenzyme A Ligases in Plants

Diploma Thesis

at the

Max-Planck-Institute for Chemical Ecology, Jena

and

Department of Biology and Pharmacy,
Friedrich Schiller University, Jena

submitted by

Katrin Gruner

supervised by

Prof. Dr. Jonathan Gershenzon
PD. Dr. Klaus-J. Appenroth

Jena, January 2008

Table of contents

Table of contents II

Table of figures V

Table of tables VII

1 Introduction 1

1.1 General Introduction 1

1.2 Background 2

1.2.1 The biosynthesis of benzoic acid in plants 2

1.2.2 The biosynthetic pathways of benzoic compounds in Petunia 3

1.2.3 The function of Benzonate:Coenzyme A Ligase (BZL) 5

1.2.4 Benzonate:Coenzyme A Ligase (BZL) in *Clarkia breweri* and *Arabidopsis thaliana* 6

1.2.5 At1g65880 knockout mutants Salk_094196 and GABI_565B09 7

1.3 Peroxisomes 7

1.3.1 The role of peroxisomes in plant metabolism 8

1.3.2 Targeting of proteins to peroxisomes 9

1.3.3 The function of glyoxisomes in degradation of fatty acids: β-oxidation and glyoxylate cycl 10

1.4 Current Aims 11

1.4.1 Mutant complementation test 12

1.4.2 Subcellular localization of *A. thaliana* BZLs using a density gradient 13

1.4.3 At1g65890 promoter activity time course 13

2 Materials and Methods 14

2.1 Materials 14

2.1.1 Organisms 14

2.1.2 Chemicals 15

2.1.3 Antibiotics and Pesticides 17

2.1.4 Enzymes / buffers 17

2.1.5 Kits 18

2.1.6 Equipment....18
2.1.7 Software....20
2.2 Methods....21
2.2.1 Molecular biological methods....21
2.2.1.1 Isolation of RNA....21
2.2.1.2 cDNA synthesis....21
2.2.1.3 Amplification of nucleic acids....21
2.2.1.4 DNA gel electrophoresis....29
2.2.1.5 Cloning and transformation of competent *Eschericha.coli* cells....30
2.2.1.5.1 Transformation of *Agrobacterium tumefaciens*....33
2.2.1.6 Isolation of plasmid DNA from *Escherichia coli*....34
2.2.1.7 DNA digests with restriction enzymes....34
2.2.1.8 DNA sequencing....35
2.2.2 Plant treatments....36
2.2.2.1 *Arabidopsis thaliana* growth conditions....36
2.2.2.2 *In planta* Transformation of *Arabidopsis thaliana* with *Agrobacterium tumefaciens* by vacuum infiltration....36
2.2.2.3 Seed sterilization....37
2.2.2.4 Screening of transformed *Arabidopsis thaliana* seeds on selective plates....38
2.2.2.5 Histological analysis of GUS gene expression....38
2.2.3 Biochemical methods....39
2.2.3.1 Screening for glucosinolate content via High Pressure Liquid Chromatography (HPLC)....39
2.2.3.1.1 Purification of sulfatase for glucosinolate analysis....40
2.2.3.2 Protein expression in *E. coli*....40
2.2.3.3 Protein extraction from *E. coli*....41
2.2.3.4 SDS-Polyacrylamide-Gelelectrophoresis (SDS-Page)....42
2.2.3.5 Western immunoblot analysis....43
2.2.3.6 Peroxisome extraction....45
2.2.3.7 Enzyme assays....47
2.2.3.7.1 Catalase activity assay....48
2.2.3.7.2 Fumarase activity assay....48
2.2.3.7.3 Isocitrate lyase activity assay....49

3 Results....51

3.1 Results of the mutant complementation test 51
3.1.1 Design of transgenic lines 51
3.1.2 3- and 4-benzoyloxyglucosinolate screening in transgenic plants via HPLC-based analysis 54
3.1.3 Verification of transcription activity for transgene constructs 61
3.1.4 Confirmation of promoter activity using eGFP 64
3.2 Subcellular localization of Arabidopsis BZL using a density gradient 65
3.2.1 Verification of expression of the transgenic Arabidopsis BZL genes exhibiting a 5' HA-tag via RT-PCR 66
3.2.2 Verification of proper Antibody-binding 67
3.2.3 Verification of proper marker enzyme activity 69
3.2.4 Verification of the isolation of peroxisomes from *Arabidopsis thaliana* ...70
3.2.5 Isolation of peroxisomes from transgenic *Arabidopsis thaliana* carrying an overexpressed tagged BZL gene....72
3.3 Results of the At1g65890 promoter activity time course 73

4 Discussion 84
4.1 At1g65890 promoter activity time course....84
4.2 Mutant Complementation....88
4.3 The subcellular localization of Arabidopsis BZL using a density gradient 93
4.4 Future perspectives 95

5 Abstract.... 97

6 Abbreviations VIII

7 Literature.... X

Appendix.... XVI

Aknowledgement XXIII

Selbstständigkeitserklärung XXIV

Table of figures

Figure 1: The proposed biosynthetic pathways leading to some benzenoid compounds in petunia (*Petunia hybrida*) flower tissue. 4
Figure 2: The enzymatic reaction of BA to benzoyl-CoA catalyzed by BZL is ATP and CoA dependent. 6
Figure 3: Sucrose/Percoll gradient separation of peroxisomes. 46
Figure 4: An overview of the procedure described in section 3.1.1. 53
Figure 5: An overview of the transgenic selection procedure. 54
Figure 6: Representative HPLC-DAD traces of seed glucosinolate analysis. 59
Figure 7: Concentrations of 3- and 4-benzoyloxyglucosinolates (3BZOgls and 4BZOgls) in transgenic plants. 61
Figure 8: Screening of transgenic Arabidopsis plants by RT-PCR 63
Figure 9: Screening of the pDESTTM::880Prom::eGFP gene fusion construct in transgenic Arabidopsis plants. 64
Figure 10: At1g65880 promoter::eGFP studies on embryonic tissue of A. thaliana. eGFP activity. 65
Figure 11: Screening of transgenic BZL in A. thaliana plants. 67
Figure 12: Immunoblot analysis of transgenic BZLs carrying an unrelated HA-tag. 68
Figure 13: Immunoblot analysis of transgenic BZLs carrying an introduced N-terminal HA-tag. 69
Figure 14: Peroxisome isolation on a percoll/sucrose density gradient. 70
Figure 15: Marker enzyme assays on isolated peroxisome fractions obtained using a sucrose percoll gradient 72
Figure 16: Histochemical analysis of At1g65890 promoter::gusA gene fusion expression. 75
Figure 17: Histochemical analysis of At1g65890 promoter::gusA gene fusion expression. 76
Figure 18: Histochemical analysis of At1g65890 promoter::gusA gene fusion expression. 77

Figure 19: Histochemical analysis of At1g65890 promoter::gusA gene fusion expression in transgenic plants of different developing stages and of untransformed Col-0 controls. 80
Figure 20: Histochemical analysis of At1g65890 promoter::gusA gene fusion expression in 31 day old transgenic plants and of a 31 day untransformed Col-0 control plant. 82
Figure 21: Histochemical analysis of At1g65890 promoter::gusA gene fusion expression in 31 day old transgenic leaves and of 31 day old untransformed Col-0 control leaves. 83
Figure 22: At1g65880 promoter sequence. XVI
Figure 23: At1g65890 promoter sequence. XVII
Figure 24: At1g65880 BZL sequence. XVIII
Figure 25: At1g65890 BZL sequence. XIX
Figure 26: Sequence of a putative *Clarkia breweri* BZL gene. XX
Figure 27: Sequence of a putative *Petunia hybridia* BZL gene XXI
Figure 28: Sequence of the *badA* gene of *Rhodopseudomonas palustris.* XXII

Table of tables

Table 1: Oligonucleotides used in PCR reactions.....23
Table 2: Oligonucleotides used in “touch-up” PCR reactions.....28
Table 3: Restriction enzymes and buffers. 34
Table 4: An overview of the rescue mutant results.....55

1 Introduction

1.1 General Introduction

Plants are sessile organisms. They can not hide or run away from their enemies. Therefore, they have developed other strategies to protect and defend themselves in order to interact with their abiotic and biotic environment. One of these strategies is the utilization of various chemical compounds commonly referred as plants' secondary metabolites. The diversity of structures within the different classes of secondary metabolites yields a wide range of functional diversity as well. A distinguishing characteristic between primary and secondary metabolites is that the functions of secondary metabolites are not involved in general maintenance and growth of a plant. Secondary plant compounds are known to be important for the survival and propagation of the plant as they mediate the plants' response to environmental cues. Therefore, secondary plant metabolites serve as attractants to pollinators, as inhibitors of herbivore attack, as toxins, and many more. The production of these compounds typically takes place in specific organs, tissues, or cell types and at specific developmental stages.

According to their basic structure and the metabolic pathways leading to them secondary metabolites can be distinguished into different classes, e.g. nitrogen-containing compounds, phenylpropanoids and benzenoids, flavonoids, and terpenes. Glucosinolates represent a major group of nitrogen containing secondary metabolites. Glucosinolates are nitrogen- and sufur-rich compounds derived from amino acid. They are widely known for their strong flavors of the genus *Brassica* like mustard, oilseed and vegetable crops. It is believed that glucosinolates and/or mainly their hydrolysis products serve as defensive toxic compounds and are used for protection from generalist herbivores and pathogens and as attractants to specialist herbivores (Reichelt et al., 2002). Hydrolysis products are made upon plant damage through the action of myrosinases (Bones and Rossiter, 1996; Rask et al., 2000). Glucosinolates occur in all plant organs and undergo quantitative and qualitative changes throughout plant development (D'Auria and Gershenzon, 2005). The highest overall glucosinolate level is found in the seeds, where they rise up to 3 % of the total seed weight. Furthermore, seeds in contrast to vegetative

tissue exclusively contain benzoyloxyglucosinolates (Petersen et al., 2002; Brown et al., 2003). Benzoyloxyglucosinolates are made via esterification of methionine-derived hydroxylglucosinolates with benzoyl-CoA (Graser et al., 2001; Reichelt et al., 2002). It is of commercial interest to reduce glucosinolates levels in agricultural important oil-seeds to increase the feed value but at the same time to also increase glucosinolates in vegetative tissue for defence. The widely studied model plant *Arabidopsis thaliana* as a representative of *Brassica* and with a high diversity and content of glucosinolates provides an opportunity to study the underlying biosynthetic pathways of glucosinolates and to finally test the fitness low-glucosinolates oilseed *Brassica* varieties.

1.2 Background

1.2.1 The biosynthesis of benzoic acid in plants

The aromatic metabolite benzoic acid (BA) is a biosynthetic building block of numerous benzoyl and benzyl groups in plants' secondary metabolism. Benzenoid compounds, such as salicylic acid (SA), gallic acid, benzoic acid (BA) itself, cocaine, taxol, salicin, and many more, can be found playing diverse roles ranging from fragrances components, aromas, cell wall constituents, signaling molecules, defensive compounds against pathogens, and pigments up to phytoalexins. The biochemical pathways leading to these compounds are widely studied but despite its simple structure and widespread occurrence, the biosynthesis of BA and its thioester benzoyl-CoA is not well understood.

The biosynthesis of plant benzenoid compounds originates either from phenylalanine (Phe) or directly through the shikimate/chorismate pathway. The shikimate/chorismate pathway was first discovered in bacteria (Serino et al., 1995; Gehring et al., 1997). There is evidence this direct pathway also exists in plants (Werner et al., 1997; Wang et al., 2001). For example, salicylic acid biosynthesis in *Arabidopsis thaliana* is directly derived from isochorismate in response to pathogen attack (Wildermuth et al., 2001). In order to obtain benzenoids from L-phenylalanine the first step, the deamination to *trans*-cinnamic acid (*t*-CA). Phenylalanine ammonia lyase (PAL) catalyzes this step. There are two major routes proposed resulting in the cleavage of two carbons from the side

chains: The CoA-dependent, *β*-oxidative pathway leading to benzoyl-CoA and the CoA-independent, non-oxidative pathway leading to benzoic acid (Wildermuth, 2006). Furthermore, benzenoid compounds become altered in their stability, solubility, membrane permeability and activity through modifications by methylation, glucosylation, or activation with Coenzyme A (CoA) in order to regulate them. Therefore, BA and benzoyl-CoA are a source for many benzenoid compounds through further modifications.

1.2.2 The biosynthetic pathways of benzoic compounds in Petunia

In plants, phenylpropanoid metabolism is a major source of aromatic secondary metabolites. In 2004 the biosynthetic pathways leading to some benzenoid compounds were proposed for *Petunia hybrida* petal tissue (see figure 1; (Boatright et al., 2004)). Phenylpropanoid metabolism is complex and consists of several branching pathways for supplying the plant with a bulk of compounds primarily involved in secondary metabolism such as structural cell components (e.g. lignin and suberin), pigments (e.g. flavonoids and antocyanins), and aromatic and volatile phenylpropanoids/benzenoids (contribute to the aroma of fruits and the floral scent). Several enzymes responsible for the formation of benzenoid compounds, the final steps of the branching phenylpropanoid metabolism, were isolated and characterized, e.g. benzoyl-CoA:benzyl alcohol benzoyl transferase (BEBT; (D'Auria et al., 2002)), acetyl-CoA: benzyl alcohol benzoyl acetyltransferase (BEAT; (Dudareva et al., 1998b)), *S*-adenosyl-L-Met:benzoic acid/salicylic acid (BSMT/SAMT; (Dudareva et al., 1998b; Ross et al., 1999; Dudareva et al., 2000; Murfitt et al., 2000; Negre et al., 2003)).
However, surprisingly little is known about the interconnections, the biochemical pathways leading to the simple benzenoid compounds like BA and benzoyl-CoA for example.

In the phenylpropanoid metabolism the benzenoid compounds are obtained from the amino acid phenylalanine. The well known enzyme PAL catalyzes the first step, the deamination of the amino acid L-phenylalanine to *trans*-cinnamic acid. The following degradation of the side chain of CA by two carbons to achieve benzoate compounds occurs via two major proposed routes. The CoA-dependent, *β*-oxidative pathway leads to benzoyl-CoA via activation of *t*-CA by the formation of the cinnamoyl-CoA ester and the key intermediate phenylpropanoid acid CoA ester (figure 1, blue route). This route

mirrors *β*-oxidation as the name implies. Alternatively, the CoA-independent, non-*β*-oxidative pathway leads to BA via benzaldehyde with the key intermediate *p*-hydroxybenzaldehyde (figure 1, black route). Additionally, a combination of the two pathways, a CoA-dependent and non-*β*-oxidative pathway, is also conceivable (figure 1, red arrows).

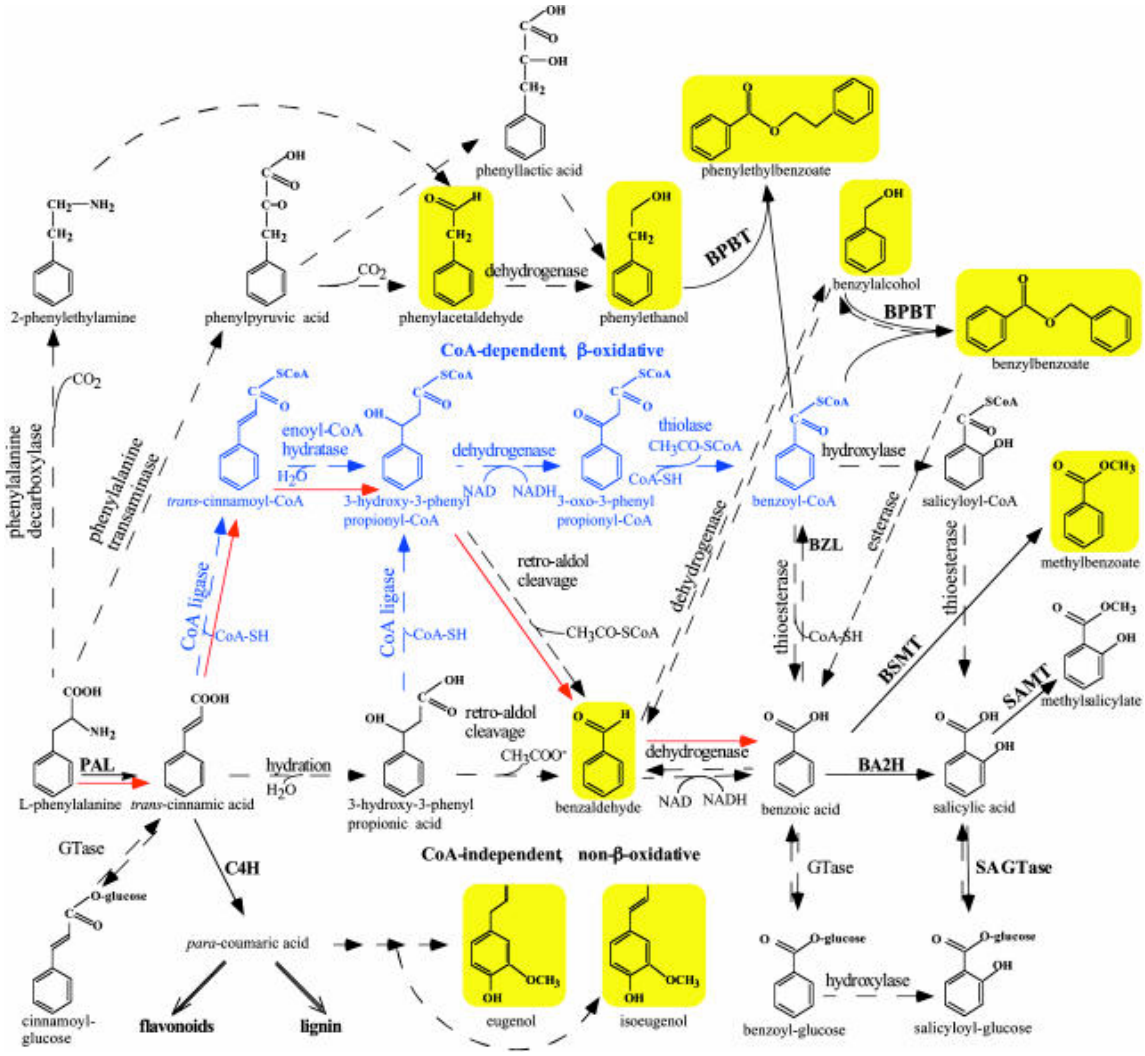

Figure 1: The proposed biosynthetic pathways leading to some benzenoid compounds in petunia (*Petunia hybrida*) flower tissue.
Starting with the deamination of L-phenylalanine to *trans*-CA by PAL, the pathway splits into two major routs for side chain shortening by two carbons. The CoA-dependent, β-oxidative pathway is shown in blue, whereas the CoA-independent, non-β-oxidative pathway is shown in black. A possible combination of the two is shown with red arrows. Broken arrows indicate possible steps not yet described. A yellow background marks volatile benzenoid/phenylpropanoid-related compounds in petunias floral scent. BSMT and SAMT, *S*-adenosyl-L-Met:benzoic acid/salicylic acid and salicylic acid carboxyl methyltransferase, respectively; BA2H, benzoic acid 2-hydroxylase; BZL, benzoate:CoA ligase; C4H, cinnamic acid-4-hydroxylase; SA GTase, UDP-Glc:salicylic acid glucosyltransferase. (Boatright et al., 2004)

In petunia flower tissue, both pathways are involved in the formation of benzenoid compounds. It is likely that both and even different ways of side chain shortening exist in different plants or side by side in the same plant as in petunia. One pathway, the CoA-dependent, β-oxidative pathway, results in the direct formation of the activated compound benzoyl-CoA. However, the involvement of BZL, the enzyme that can catalyze the thioesterification of BA to benzoyl-CoA (see figure 1 and 2), still needs to be verified.

1.2.3 The function of Benzonate:Coenzyme A Ligase (BZL)

What is the activity of BZL needed for? The CoA-dependent, β-oxidative route of the phenylpropanoid metabolism directly yields the formation of benzoyl-CoA. Even if only the CoA-dependent, β-oxidative pathway proves to be active the activity of BZL is still needed. The general abundance of thioesterase activity in plants, the enzyme catalyzing the reverse reaction from benzoyl-CoA to BA (Obel and Scheller, 2000), indicates one reason. Another reason is that CoA esters can not permeate through membranes (Verleur et al., 1997). But the CoA activation of BA is necessary for acyltransferase reactions, which are incorporated into secondary metabolites yielding secondary compounds like cocaine, taxol, some modified glucosinolates and others. Acyltransferase requires benzoyl-CoA as a substrate to catalyze benzoylation of secondary compounds (Yang et al., 1997; Dudareva et al., 1998b; Walker et al., 2000; Graser et al., 2001).

The enzyme BZL catalyzes the enzymatic reaction from BA to its activated form benzoyl-CoA (figure 2). The reaction is CoA and ATP dependent. BZL is a member of the superfamily of acyl-activating enzymes (AAEs; (Shockey et al., 2003)). The reaction catalyzed by AAEs comprises two steps: The formation of an acyl-AMP intermediate while releasing pyrophosphate and the formation of acyl-CoA ester while releasing AMP. Thioesterase, a widespread enzyme in plants, catalyzes the reverse reaction from benzoyl-CoA to BA (figure 2; (Obel and Scheller, 2000)).

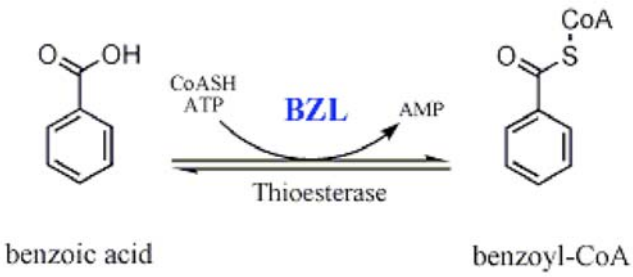

Figure 2: The enzymatic reaction of BA to benzoyl-CoA catalyzed by BZL is ATP and CoA dependent.
The reverse reaction is catalyzed by the enzyme thioesterase.

1.2.4 Benzonate:Coenzyme A Ligase (BZL) in *Clarkia breweri* and *Arabidopsis thaliana*

A BZL was partially purified and characterized from *Clarkia breweri* flowers (Beuerle and Pichersky, 2002). The enzyme in Clarkia catalyzes the formation of benzoyl-CoA and anthraniloyl-CoA, important intermediates for subsequent acyltransferase reactions in plant secondary metabolism. The native enzyme is active as a monomer with a molecular mass of approximately 59-64.5 kDa, and it has K_m values of 45, 95, and 130 µM for benzoic acid, ATP, and CoA, respectively. BZL is most active in a pH range of 7.2-8.4. Its activity is strictly dependent on certain bivalent cations like Mg^{2+} and Mn^{2+} and it is an AMP-forming enzyme. Overall, its properties suggest that it is related to the family of CoA ligase enzymes that includes the plant enzyme 4-hydroxycinnamate: CoA ligase.

Although enzymatic activity was purified from Clarkia floral tissue, DNA or protein sequence data are not yet known for any plant BZL. A HPLC-based screen of mutagenized *Arabidopsis thaliana* lines identified two genes, At1g65880 and At1g65890, potentially encoding plant BZLs (Kliebenstein et al., 2007). The acyl-activating enzyme (AAE) family members (Shockey et al., 2003), are tandemly duplicated with >90 % nucleotide sequence identity. Available expression data suggest one or both genes are most highly expressed in developing seeds (Zimmermann et al., 2004). In fact, Col-0 *bzo1*, a mutation located in the region of the At1g65880 gene, shows altered seed-specific accumulation of benzoyloxyglucosinolates in an HPLC-based analysis. 3-benzoyloxyglucosinolate is missing and the precursor compound 3-

hydroxypropylglucosinolate is increased compared to Col-0 (Kliebenstein et al., 2007). Benzoyloxyglucosinolates in *A. thaliana* seeds are derived through esterification of hydroxylglucosinolates with benzoyl-CoA (Graser et al., 2001; Reichelt et al., 2002). Finally, both proteins encoded by At1g65880 and At1g65890 behaved as BZLs in enzymatic assays containing BA, ATP and CoA when expressed in a heterologous vector system. The purified enzyme formed bezoyl-CoA (figure 2; (Kliebenstein et al., 2007); unpublished data by John D'Auria). Furthermore, subcellular prediction programs (PSORT, (Nakai and Horton, 1999); TargetP, (Emanuelsson et al., 2000); and AraPerox, (www.araperox.uni-goettingen.de, (Reumann et al., 2004))) indicate a possible targeting of the two BZLs to the peroxisomes. Both genes exhibit the carboxyl-terminal tripeptide motif SRL, one of the major peroxisomal targeting signals type 1 (PTS1; (Reumann, 2004)). Such localization signals suggest synthesis of BA via *β*-oxidation, because peroxisomes and especially seed specific glyoxysomes are known to be the main sites of *β*-oxidation in plants.

1.2.5 At1g65880 knockout mutants Salk_094196 and GABI_565B09

Salk_094196 (Alonso et al., 2003) and GABI_565B09 (Rosso et al., 2003) are two T-DNA insertion lines with disruptions of the coding region of the Col-0 At1g65880 gene. The two commercially available knockout lines lack the production of 3- and 4-benzoyloxyglucosinolate in embryonic tissue due to a loss of function of the At1g65880 gene. The At1g65880 gene encodes a seed specific BZL catalyzing the esterification of BA with Coenzyme A (figure 2). Since activation of benzoic acid is essential for the following esterification of hydroxyglucosinolates to benzoyloxyglucosinolates, the loss of this function will therefore result in downstreap effects. These effects can be shown by analysis of the seed glucosinolate content via HPLC-DAD (see figure 6B and C in results 3.1.2).

1.3 Peroxisomes

Peroxisomes are small cellular organelles of 0.5 to 1.5 µm in diameter with a single membrane surrounding a dense matrix. They are found ubiquitous in eukaryotic cells.

Unlike chloroplasts and mitochondria, peroxisomes do not possess their own genome. All their matrix proteins are encoded within the nucleus, synthesized on free ribosomes in the cytosol, and post-translationally transported into the peroxisomes (in review (Olsen et al., 1993)). Peroxisomes can originate in the endoplasmatic reticulum (ER) or simply by division of pre-existing peroxisomes (Orth et al., 2007). Proteins required for peroxisome biogenesis are termed peroxins (pex). Peroxins are involved in many aspects of membrane biogenesis and maintenance, including matrix protein import, peroxisome division/proliferation, and organelle inheritance (Crookes and Olsen, 1999). Peroxisomes differentiate into metabolically specialized variants specific to the tissue and the developmental stage, such as leaf peroxisomes in mature leaves, glyoxisomes in germinating seeds, nodule- and senescent-specific peroxisomes, as well as hardly characterized unspecialized peroxisomes.

1.3.1 The role of peroxisomes in plant metabolism

Peroxisomes are involved in a variety of important physiological functions, which predominantly are spread over multiple cellular organelles. Primarily peroxisomes compartmentalize oxidative metabolic reactions and their toxic by-products. The basic metabolic functions of plant peroxisomes are: β-oxidation of unsaturated fatty acids and branched amino acids (Brickner and Olsen, 1998; Zolman et al., 2001), participation in photorespiration, and the immediate detoxification of hydrogen peroxide (H_2O_2) and other reactive oxygen species (ROS) through catalase and other auxiliary antioxidative enzymes at the site of production. Despite these basic functions, peroxisomes are also believed to be involved in plant senescence (Orth et al., 2007) and they are proposed to be involved in the biosynthesis of the plant hormones auxin and jasmonic acid (Sanders et al., 2000; Stintzi and Browse, 2000; Feussner and Wasternack, 2002; Strassner et al., 2002; Koo et al., 2006) and in sulfur and nitrogen metabolism (Eilers et al., 2001; Nakamura et al., 2002; Nowak et al., 2004; Reumann et al., 2004). Evidence is emerging that peroxisomes are also involved in specific defence mechanisms against pathogen attack (Taler et al., 2004; Koh et al., 2005; Lipka et al., 2005). Although they share common features (hydrogen peroxide-producing oxidases and catalase), peroxisomes are very variable and flexible in their contents due to their specialized metabolic function (Olsen, 1998). Metabolically specialized plant peroxisomes are present at different

stages in the life cycle and they possess a different composition of enzymes for their physiological role (Brickner and Olsen, 1998). Glyoxysomes provide young not yet autotrophic seedlings of higher plants with nutrition for growth by mobilizing storage lipids via β-oxidation and the glyoxylate cycle (Olsen et al., 1993; Brickner et al., 1997; Brickner and Olsen, 1998; Olsen, 1998). In green tissue leaf-type peroxisomes are present. They contain enzymes needed for photorespiration (Olsen et al., 1993; Brickner and Olsen, 1998; Olsen, 1998). Peroxisomes in root cells contain enzymes involved in the nitrogen metabolism (Olsen, 1998; Johnson and Olsen, 2001). And unspecialized peroxisomes without defined metabolic roles can be present in all plant organs (Olsen et al., 1993; Olsen, 1998). In response to varying specific needs of the cell peroxisomes are capable of undergoing interconversion from one into another (Olsen et al., 1993).

1.3.2 Targeting of proteins to peroxisomes

Peroxisomes do not have their own organellar DNA. All peroxisomal proteins are nuclear encoded and translated in the cytosol. Therefore, peroxisomal proteins have to be targeted to and translocated across or into the peroxisomal membrane. For addressing them to the peroxisomes the proteins carry a specific **p**eroxisomal **t**argeting **s**ignal (PTS). Two types of signals are well defined. The majority of proteins targeted to peroxisoms exhibit a noncleaved carboxyl-terminal tripeptide of the prototype SKL or conservative variations thereof, the PTS1 (Gould et al., 1987; Gould et al., 1989; Reumann, 2004). In contrast, few proteins possess a PTS2. The cleavable PTS2 consists of a conserved nine amino acid consensus sequence usually within 20-30 amino acids of the amino terminus (R[LI]x_5HL; (Swinkels et al., 1991; Glover et al., 1994; Reumann, 2004)).

Lots of proteins are involved in the translocation of peroxisomal matrix proteins with a PTS1 or 2. The whole process is not yet understood, however it is believed that proteins with a PTS1 are recognized in the cytosol by the soluble receptor Pex5 (Van der Leij et al., 1993; Kragler et al., 1998; Wimmer et al., 1998) and the soluble Pex7 binds PTS2-proteins as their specific receptor (Marzioch et al., 1994; Rehling et al., 1996). For each signal there is a separate pathway of the initial steps of import into the peroxisomal matrix. Both targeting pathways merge at the receptor Pex14 at the surface of the peroxisome. Pex14 interacts with both, the PTS1- and the PTS2-receptors, to build a single

protein import complex (Albertini et al., 1997; Brocard et al., 1997; Komori et al., 1997). Chaperones may also interact with the PTS-protein to control their conformation for proper import (Crookes and Olsen, 1999). The import is energy dependent and requires ATP or GTP hydrolysis and also Mg^{2+}, which is preferred over other cations and has multiple functions in this pathway (Brickner and Olsen, 1998).

1.3.3 The function of glyoxisomes in degradation of fatty acids: *β*-oxidation and glyoxylate cycle

Most seeds contain in a small space all the resources necessary for the developing embryo to grow for the first couple of days. Therefore highly efficient packaging of energy rich compounds is required. Many species of higher plants store lipids in form of oils and triglycerides, containing mostly unsaturated fatty acids in the seed. In order to recover the energy from fatty, several oxidative steps must occur which will ultimately yield saccharose, the transportable metabolite. Initially, lipases coupled to the surface of the oleosomes (single membrane lipid bodies) catalyze the decomposition of triglycerides into water soluble glycerol and fatty acids. Glycerol, oxidized to its corresponding aldehyde, directly accesses glycolysis, whereas the resulting fatty acids are degraded to C_2-units (acetates) by repeated *β*-oxidation at the inner glyoxisome membrane, the peroxisome specialized for lipid degradation. Glyoxisomes are prevalent in germinating seeds, especially those rich in storage lipids. All enzymes involved in complete degradation of fatty acids to produce acetyl-CoA and later succinate from two acetate residues in the glyoxylate cycle are found in glyoxisomes.

The *β*-oxidation pathway consists of five enzymatic reactions involving the activities of acyl-CoA synthetase, acyl-CoA oxidase, enoyl-CoA hydratase and 3-hydroxyacyl-CoA dehydrogenase as part of a multifunctional protein complex, and ketoacyl-CoA thiolase resulting in acetyl as final product. During the glyoxylate cycle the conversion of two acetate residues into succinate catalyzed by peroxisomal citrate synthase, isocitrate lyase, malate synthase, and malate dehydrogenase takes place. Catalase is one of the enzymes which eliminate H_2O_2, a damaging reactive oxygen species which is a by-product of the *β*-oxidation pathway. The further metabolization of fatty acids to saccharose continues in the mitochondria, where succhinate becomes oxidised to oxalacetate,

and in the cytosol, where oxalacetate becomes decarboxylised to phosphoenolpyruvate. Finally, saccharose is produced through an inversed glycolysis. (Schopfer and A., 2006)

1.4 Current Aims

This work focuses on the subcellular localization of benzonate:CoA ligase (BZL) in plants. BZL participates in a small but important step in the production of benzoyloxy-glucosinolates. Seed-specific benzoyloxyglucosinolates are made via esterification of methionine-derived hydroxylglucosinolates with benzoyl-CoA (Graser et al., 2001; Reichelt et al., 2002). Benzoyl-CoA, in turn, is derived by the action of BZL (see figure 2) among other possible pathways. BZL has been hypothesized to be part of the phenyl-propanoid metabolism ((see figure 1; (Boatright et al., 2004)). Past research has mainly focused on the final steps of the phenylpropanoid pathway. However, not much is known about the biochemical pathways of the simple intermediate benzenoid compounds such as benzoyl-CoA and benzoic acid (BA). The β-oxidative like pathway of the phenylpropanoid metabolism requires β-oxidation like enzymes and is most likely located in the peroxisomes. The non-β-oxidative pathway in contrast is most likely located in the cytosol. The activated compound benzoyl-CoA as a direct product of the β-oxidative pathway serves as a building block in many down-stream enzymatic reactions participating in secondary metabolism. BA the product of the non-β-oxidative pathway in contrast to benzoyl-CoA can permeate through membranes and is therefore the most likely transportable compound (Verleur et al., 1997). Furthermore, thioesterase, a very common enzyme in plants, catalyzes BA from benzoyl-CoA (Obel and Scheller, 2000). These reasons make the action of BZL indispensable for the plant.

While the *A. thaliana* BZLs encoded by the genes At1g65880 and At1g65890 ((Kliebenstein et al., 2007); unpublished data by John D'Auria) containe a potential major PST1 (SRL; (Reumann, 2004)) at the carboxyl-terminus and therefore subcellular prediction programs indicate their targeting to the peroxisomes the verification of this prediction remains to be done. Prediction programs are limited in their sensitivity and specifity. False positives are common. This is due to limited knowledge of the identity and function of auxiliary targeting elements, the small size of the PTS1 and the possibility of improper exposure on the surface of the folded protein preventing recognition by

Pex5 (Emanuelsson et al., 2003). Moreover the lower hierarchy of a carboxyl-terminal PTS1 compared to N-terminal non-peroxisomal targeting signals can also lead to ambiguous targeting predictions (Neuberger et al., 2003). Therefore, such a prediction is a strong indicator but not a sufficient criterion for unambiguous localization of the protein to the peroxisomal matrix. This makes it necessary to actually show experimentally that a predicted protein is indeed targeted to peroxisomes. Establishing that BZL localizes to the peroxisomes would provide strong evidence for the potential role of the *β*-oxidative like pathway of bezenoid biosynthesis in plants.

I used two different approaches to ascertain the subcellular localization of BZL to the peroxisomes in *A. thaliana*. In addition, I conducted a separate round of experiments to understand the activity of the At1g65890 promoter in more detail.

1.4.1 Mutant complementation test

The mutant complementation test provides an indirect way to show BZL localization in plants to the peroxisomes. In order to determine if those putative BZL genes carrying a potential PTS1 signal can complement a known BZL knockout phenotype, five different constructs of the At1g65880 promoter::(potential) BZL gene constructs in an At1g65880-knockout background were made. Included within this experiment were the tandemly duplicated *A. thaliana* genes At1g65880 and At1g65890, potential BZL genes from *Clarkia breweri* and *Petunia hybrida*, both found via sequence homology search using the *A. thaliana* genes and cloned by John D'Auria, and a published BZL gene from the bacterium *Rhodopseudomonas palustris* (Egland et al., 1995). The *A. thaliana* genes and the gene from Clarkia exhibit a potential major PTS1 of the type SRL. The genes from Petunia and the bacterium do not contain any obvious PTS1 or other peroxisomal targeting signal. The hypothesis I wished to test was that only the (putative) BZL genes with a PTS1 substitute the function of the At1g65880 gene in the T-DNA insertion lines Salk_094196 (Alonso et al., 2003) and GABI_565B09 (Rosso et al., 2003). It would be a strong indicator for the functional site of plant BZL in the peroxisomes. Due to the loss of function of the At1g65880 gene both knockout mutants lack the seed-specific production of 3- and 4-benzoyloxyglucosinolates. A substitution of the knocked-out At1g65880 gene by an alternative active BZL would give a phenotype

containing 3- and 4-benzoyloxyglucosinolates in the transgenic seeds in HPLC-based analysis.

1.4.2 Subcellular localization of *A. thaliana* BZLs using a density gradient

In order to demonstrate localization of plant BZLs to the peroxisomes, peroxisomes of transgenic *A. thaliana* plants constitutively overexpressing an At1g65880 or At1g65890 gene were isolated via a percoll/sucrose gradient. The gene constructs contained a 5' terminal fused unrelated HA-tag from *Human influenza virus*. Marked antibodies against the unrelated HA-tag identify transgenic tagged BZL in the content of the isolated peroxisomes separated on a protein gel. Finding the tagged BZL in the purified peroxisome fraction would provide direct evidence of the localisation of *A. thaliana* BZL in the peroxisomes.

1.4.3 At1g65890 promoter activity time course

The At1g65890 promoter activity time course is an additional approach that was undertaken during the course of this work. Even though the available expression data suggest the tandemly duplicated genes At1g65880 and At1g65890 are most highly expressed in embryonic tissue (Zimmermann et al., 2004) and the At1g65880 gene was shown to play an important role in accumulation of seed-specific benzoyloxyglucosinolates (Kliebenstein et al., 2007), the role of At1g65890 remains unclear. Therefore, an At1g65890 promoter::GUS fusion construct was made in order to localize the potential site(s) of expression of this particular gene during the development of the plant. This additional project was performed in order gain a better understanding as to the potential roles At1g65890 BZL may play *in planta*.

2 Materials and Methods

2.1 Materials

2.1.1 Organisms

Bacterial strains

Agrobacterium tumefaciens GV 3850 (Spec^{+}, Rif.$^{+}$)	(Zambryski et al., 1983)
Escherichia coli TOP 10	Invitrogen (Germany)
Escherichia coli BL 21 (DE 3)	Novagen (USA)

Plants

Arabidopsis thaliana ecotype Columbia-0	Arabidopsis Biological Resource Center (ABRC, http://www.arabidopsis.org/abrc), USA
Arabidopsis thaliana	
At1g65880 T-DNA knockout strains:	
SALK_094196 (N594196) (Alonso et al., 2003)	Arabidopsis Biological Resource Center (ABRC, http://www.arabidopsis.org/abrc), USA
GABI_565B09 (Rosso et al., 2003)	Nottingham Arabidopsis Stock Centre (NASC, http://arabidopsis.info), UK

2.1.2 Chemicals

Agar-Agar	Roth (Germany)
Agarose	BioRad (Germany)
Bovine serum albumin (BSA)	New England Biolabs (USA)
Bromophenol blue	Sigma (Germany)
Cellulose	Bioserv (USA)
Chloroform	Roth (Germany)
Dimethyl sulfoxide (DMSO)	Sigma (Germany)
DEAE Sephadex A-25	Sigma (Germany)
Dichloroisocyannoic acid Sodium salt Dihydate (Bleach)	Fluka/Sigma (Germany)
Dithiothreitol (1,4-) (DTT)	Roth (Germany)
Dried milk powder, nonfat	Appli Chem (Germany)
Ethylendiamintetra acetic acid (EDTA)	Sigma (Germany)
Ethanol unvergällt, reinst	Roth (Germany)
Ethanol vergällt	Roth (Germany)
Ethidiumbromide	Roth (Germany)
Formaldehyde	Roth (Germany)
Glacial acetic acid (100% acetic acid)	Roth (Germany)
Glycerol	Roth (Germany)
Glycine	Roth (Germany)
Isopropanol (2-propanol)	Roth (Germany)
Magnesium chloride	Roth (Germany)
Morpholinoethanesulfone acid (MES)	Sigma (Germany)
β-Mercaptoethanol	Sigma (Germany)

Methanol	Sigma-Aldrich (Germany)
MOPS (3-(N-Morpholino)propanesulfonic acid)	Sigma (Germany)
Murasheege Skoog salts (M & S salts)	Duchefa (The Nethelands)
Nitrogen, liquid	Air Liquide (France)
Plant agar	Duchefa (The Nether-lands)
Peptone	Roth (Germany)
Potassium phosphate	Sigma (Germany)
Silwet L-77	Witco Europe
Sinalbin (p-hydroxybenzylglucosinolate)	Bioraf (Denmark) www.glucosinolates.com
Sodium chloride	Roth (Germany)
Sodium Dodecyl Sulfate (SDS)	Sigma (Germany)
Sodiumdihydrogenphosphate Monohydrate (NaH2PO4)	Roth (Germany)
diSodiumhydrogenphosphate Dihydrate (Na2HPO4)	Roth (Germany)
Sucrose	Duchefa (The Nether-lands)
Tris acetate EDTA (TAE) Concentrate 50 x, modi-fied	Millipore (USA)
N,N,N’,N’-teramethylethylendiamin (TEMED)	Sigma (Germany)
Tris(hydroxymethyl)aminomethane (Tris)	Roth (Germany)
Tris HCl stock solution 1M	Sigma (Germany)
Triton X-100	Merck (Germany)
X-Gluc	Duchefa (The Nether-lands)

2.1.3 Antibiotics and Pesticides

Gentamicin	Roth (Germany)
Glufosinate-ammonium (BASTA)	Sigma (Germany)
Kanamycin	Roth (Germany)
Rifampicin	Sigma (Germany)
Spectinomycin	Duchefa (The Netherlands)
Timentin	Duchefa (The Netherlands)

2.1.4 Enzymes / buffers

Catalase from bovine liver (10,000-40.000 U/mg protein)	Sigma (Germany)
Fumarase from porcine heart (300-500 U/mg protein)	Sigma (Germany)
Isocitrate lyase from *Bacillus stearothermophilus* (5 U/mg protein)	Sigma (Germany)
Lysozyme	Sigma (Germany)
Proteinkinase K	Invitrogen (Germany)
RNase	Sigma (Germany)
Sulfatase	Sigma (Germany)

2.1.5 Kits

ABI PRISM® BigDye™ terminators	Applied Biosytems (USA)
DyeEx™ 2.0 Spin Kit	Quiagen (Germany)
Gateway® BP Clonase™ II enzyme mix	Invitrogen (Germany)
Gateway® LR Clonase™ II enzyme mix	Invitrogen (Germany)
NucleoSpin® Plasmid	Macherey-Nagel (Germany)
RNeasy® Plant Mini Kit	Quiagen (Germany)
SuperScript™ III Reverse Transcriptase	Invitrogen (Germany)
TOPO TA Cloning® Kit for Sequencing	Invitrogen (Germany)

2.1.6 Equipment

Agilent 1100 DAD HPLC System	Hewlett-Packart
Axiovert 200 (microscope)	Zeiss (Germany)
Camera NIKON Coolpix 995	NIKON
Centrifuge AvantiTM J-25	Beckman Coulter(USA)
Centrifuge AvantiTM J-20 XP	Beckman Coulter(USA)
Centrifuge 5415R	Eppendorf (Germany)
Climatic growth chamber for plants	York (USA)
Gene Genius gel documentation system	Merck (Germany)
Incubator CERTOMAT® BS-1	B. Braun Biotech International (Germany)
Incubator/Growth chamber Modell CU-36L5	Percival (USA)
Incubator for Bacteria B6120	Heraeus

Incubator InnovaTM 4230 Refrigerated Incubator Shaker	New Brunswick Scientifics (USA)
KL 1500 LCD (illuminators)	Zeiss (Germany)
PCR Thermo CyclerT gradient	Biometra® GmbH (Germany)
PCR Thermo CyclerT personal	Biometra® GmbH (Germany)
Sequencer ABI PRISM® 3100 Genetic Analyzer	GMI (USA)
Spectrophotometer (UV/Visible) Ultrospec 2100pro	Amersham Biosciences (Germany)
Stemi 2000-C	Zeiss (Germany)
Stemi SV 11	Zeiss (Germany)
Ultracentrifuge OptimaTM L-90K	Beckman (USA)
Ultrawave Homogenisator Sonoplus HD2070	Bandelin (Germany)
UV-VIS Recording Spectrophotometer UV-2501 PC	SHIMADZU (Germany)
Waring Commercial Blender	Waring Commercial (USA)
Water purification System	Millipore (USA)

2.1.7 Software

Carl Zeiss Vision	Axio Vision Rel 4.4
ChemOffice 2004	ChemDraw Ultra 8.0
	ChemFinder Ultra 8.0
Data Trans	(self made programm)
Thomson EndNote	Endnote 9
HP ChemStations	
Invitrogen	Vector NTI Advanced 10
Microsoft Office	Excel
	Powerpoint
	Word
Shimadzu	UVProb Version 1
Ulead	PhotoImpact

2.2 Methods

2.2.1 Molecular biological methods

2.2.1.1 Isolation of RNA

Isolation of the total RNA from *Arabidopsis thaliana* plant tissue was carried out with the RNeasy® Plant Mini Kit (Quiagen, Germany). RNA was extracted from 50 to 100 mg fresh plant material according to the manufactures specifications. The plant material was frozen in liquid nitrogen right after harvest and stored at -80 °C for a short time or used for grinding up the tissue to powder with a small mortar and a pestle right away. 450 µl of Buffer RLC (β-Mercaptoethanol added) was added to 100 mg tissue powder of silique/embryonic tissue and 450 µl Buffer RLT (β-Mercaptoethanol added) was used with all other plant tissue (e.g. seedlings). The optional step 9a of an extra centrifugation to fully remove ethanol was included. The elution step of the RNA in 30-50 µl RNase-free water was repeated. The resulting RNA was frozen at -80 °C for further use or used for first-strand cDNA synthesis subsequent.

2.2.1.2 cDNA synthesis

First-Strand cDNA Synthesis was performed according to the manufactures specifications of the SuperScript™ III Reverse Transcriptase Kit (Invitrogen, Germany). Maximum of RNA was added to the 20 µl reaction. RNaseOUT™ was excluded from the reaction. The resulting first-strand cDNA was used in the following PCR reaction.

2.2.1.3 Amplification of nucleic acids

The amplification of specific DNA fragments was achieved with the polymerase chain reaction (PCR). A typical PCR reaction mix consisted of the following: template DNA, a forward and a reverse primer, all four dNTPs, a polymerase, reaction buffer, water to a total volume, and salt if needed. A Pfu-DNA polymerase is a thermo stable enzyme isolated from the bacterium *Pyrococcus furiosus*. It can synthesize large DNA fragments with a low error rate because of a strict “proofreading” activity (3’exonuclease activity).

Therefore, this enzyme was applied when it was important to reduce polymerase induced errors in the sequence. Taq polymerase, while having a higher error rate, adds ATPs to the 3' end of the synthesized strand. The "A-overhang" was necessary for subcloning into a "T-overhang" providing vector. The buffer used in the reaction came with the polymerase. Primers (see table 1) were designed with the software Vector NTI Advanced 10 (Invitrogen, Germany) and synthesized from Invitrogen (Germany).

The PCR consists of three major steps: Denaturizing of the two DNA strands, annealing of the specific primer to the DNA, and synthesis of the new stands. The annealing temperature depends on the length and melting temperature of the selected primers, which I standardized to 54 °C. The synthesis time varies according to the length of the expected fragment. A Taq polymerase takes 1 min per 1000 bp and a Pfu polymerase takes 25 % longer for the same amount. The PCR was done automatically with a programmed thermocycler.

"Colony PCR" was performed to check bacterial colonies with the right insertion subsequent to a transformation. Therefore, DNA was added to the PCR reaction mix by using an autoclaved tooth pick to pick up a little bit of the colony. The program used was the same as for standard PCR.

25 µl Standard PCR reaction		25 µl Colony check PCR reaction	
19.75 µl	H_2O grade II	20.75 µl	H_2O grade II
2.5 µl	10 x Taq polymerase buffer	2.5 µl	10 x Taq polymerase buffer
1.0 µl	DNA*	0.5 µl	dNTP mix (10 mM)
0.5 µl	dNTP mix (10 mM)	0.5 µl	forward primer (10 pmol/µl)
0.5 µl	forward primer (10 pmol/µl)	0.5 µl	reverse primer (10 pmol/µl)
0.5 µl	reverse primer (10 pmol/µl)	0.25 µl	Taq Polymerase
0.25 µl	Taq Polymerase		

* cDNA pur, plasmid DNA 1:10 diluted

Standard cycling program

5 min	96 °C	
30 sec	96 °C	30 to 35 Cycles
30 sec	54 °C	
up to 3 min*	72 °C	
7 min	72 °C	
storing at	4 °C	

* Amplification time varies depending on the length of the expected fragment: 1 min/1000 bp

Table 1: Oligonucleotides used in PCR reactions.

Displayed are all primers used for standard PCR and "colony PCR" reactions and for sequencing. Oligonucleotide sequences are shown in 5' to 3' orientation. All primers were synthesized by Invitrogen (Germany), except 890 fwd, 890 rev, 890 middle Seq and 890 middle Seq reverse, which were produced by Operon (Germany).

Template	**Primer name**	**Primer sequence (5' to 3')**	**Annealing temp.**
pDONR™ Vector	pDONR fwd	TGG CAG TTC CCT ACT CTC GC	54 °C
	pDONR rev	AAT GTA ACA TCA GAG ATT TTG AGA CAC G	54 °C
pEarlyGate201 Vector	OCS 3' Rev	GAT GTC GCT ATA AAC CTA TTC AGC A	54 °C
pH9GW Vector	T7 prom	TAA TAC GAC TCA CTA TAG GGG AAT TG	54 °C
	T7 term	TAT GCT AGT TAT TGC TCA GCG GTG	54 °C
pEarlyGate201::35S::HA-gene	pEARLEY201_35_HA_fwd	ACA TTT ACA ATT ACC ATG TAC CCA TAC GAT	54 °C

pDest^{TM}:: At1g65880 Promoter	pDEST880_fwd	CAT TAC ACA AAG TAG AAG AAG AAG AAG AAG AT	54 °C
At1g65880 Promoter	880 Pro Seq F1	GAA CCA ACT GGA TGT GGA TCA TAA	54 °C
	880 Pro Seq R1	AGG TTG ATC CAT ACA TTT GTA TCC A	54 °C
At1g65880	880 Seq 1	TCC AAG AAC GAT GTG GTA TCA GTT A	54 °C
	880 Seq 2	CTC CCC TCT GGA TGA GAC ACT C	54 °C
	880 Seq 3	CTA AGA TGC TTA TCC CTT GCC TG	54 °C
	880 Seq 4	TGT TGA GGT CGA GAA TGT TCT TTA T	54 °C
	880 Mid Seq	AGG AAA TTC ACT TGA CCT GTC ACC	54 °C
	880 Mid Seq Rev	GGT GAC AGG TCA AGT GAA TTT CCT	54 °C
	880 Seq R4	CTA GAC GAC AAC AAC GGT CAT AGG T	54 °C
	880 Rev	AAG CCG CGA AAT AAA ATG TCC AAC C	54 °C
At1g65890 (A-AE12)	890 Fwd	ATG GAT AAT TTG GCG TTA TGT GAA G	54 °C
	890 Seq F4	GGT GAG ACT AAT AAT GAA GAT CGT GAA GA	54 °C
	890 middle Seq	AGA CTA CGA GTG TCT CAT CCA GAG G	54 °C

	890 middle Seq Rev	CTG CTT CCT TTC ATA ACG ATT TCT C	54 °C
	890 Seq R4	GAT ATG AGA GAA GCG GCT AGA CGA	54 °C
	890 Rev	GGGA GAT GTA TAA TCT CAA AGC CGC	54 °C
Clarkia breweri BZL gene	Cbr1_N01 Fwd	ATG GAT GTA CTT CCA AAG TGT AGC GCA	54 °C
	Cbr1_N01 Seq F1	CGT ATC CCG TTG ACC TCC GC	54 °C
	Cbr1_N01 Seq F4	GAG CAT TGA GAG TCT AGG GTT CCA	54 °C
	clarkiaBZL Seq R1	CAT GAT TTC GCC CAT TGT GGT A	54 °C
	Cbr1_N01 Seq R2	AAC CTC ATC GCC CCG AAA CC	54 °C
	Cbr1_N01 Seq R3	ACA CCA CTC CTT TCG GCT CC	54 °C
	Cbr1_N01 Seq R4	GAA GCG GAG ATG CTC GTA AAT CA	54 °C
	Cbr1_N01 ORF Rev	GTG ATT ATC TTG CTT AAA GTC GAG ATT G	54 °C
R. palustris BZL gene	BZL forward	ATG AAT GCA GCC GCG GTC ACG CCG CCA CCC	54 °C
	BZL Seq F1	GTC AAT ACG CTG CTG ACG GC	54 °C
	BZL Seq R1	GAG CCG CAA CGC CAC CTG GT	54 °C
	BZL Rev	TCA GCC CAA CAC ACC CTC GC	54 °C

Petunia BZL putative gene	Pet BZL Seq F1	CAG GGG CTG TGC TAA ACA CAA T	54 °C
	Pet BZL Seq F2	ATT GTT GAC GAC GAG TGG GAT	54 °C
	Pet BZL Seq F3	CAA TTT GAA GGC TAG ACA AGG AAT C	54 °C
	Pet BZL Seq R1	CTG TAG TTT CTT TAC TTT CCC AGT TCC	54 °C
	Pet BZL ORF F	ATG GAC GAG TTA CCA AAA TGT GGA G	54 °C
	Pet BZL ORF R	AAT CTC CTA CAG ACG AGC TGG CAA ATC	54 °C
eGFP	eGFP F1	ATG GTG AGC AAG GGC GAG GAG CTG TTC	54 °C
	eGFP R1	CCC TGG TGA ACC GCA TCG AGC TGA A	54 °C
At1g27450	APT1 F	GTG AGA CAT TTT GCG TGG GAT TTG	54 °C
	APT1 R	ACT TTA GCC CCT GTT GGA GTC TAC	54 °C

For adding extra unrelated sequences to a gene of interest a “touch up” PCR was performed. The reaction, utilizing Pfu polymerase for correct synthesis, consisted of 2 steps. In the first step, part of a 27 bp long HA-tag sequence (5’- tacccatacgatgttccagattacgct -3’) was added to RNA based isolated and into vector cloned genes At1g65880 and At1g65890 via the forward primers (tag at the 5’ prime end of the forward primer). The HA-tag is a sequence originated from the virus *Herpes simplex* and therefore foreign to *A. thaliana*. Later it can be used to identify the product of the transgene in plants. The second step served as addition of the residual part of the HA-tag to the sequence. As template DNA 1 µl of the previous PCR was applied. Because of the

overhanging sequence, the program had to be chanced a little bit, so that the primers containing the extra sequence at the 5' prime end can bind easier to the DNA. The first three cycles had a lower primer annealing temperature for easier binding followed by regular 35 cycles with higher annealing temperature for specific binding.

25 µl touch up PCR reaction

18.5 µl	H_2O grade II
2.5 µl	10 x Pfu Ultra^{TM} HF Reaction Buffer
1.0 µl	$MgCl_2$ (25 mM)
1.0 µl	DNA (1^{st}: vector DNA containing the gene, 2^{nd}: DNA from the 1^{st} PCR reaction)
0.5 µl	dNTP mix (10 mM
0.5 µl	forward primer (10 pmol/µl) containing extra sequences
0.5 µl	reverse primer (10 pmol/µl) against the very end of the gene
0.5 µl	Pfu DNA Polymerase Ultra

Cycling program of touch up PCR

2 min	96 °C	
30 sec	96 °C	3 Cycles
30 sec	52 °C	
2.30 min	72 °C	
30 sec	96 °C	35 Cycles
30 sec	60 °C	
2.30 min	72 °C	
7 min	72 °C	
storing at	4 °C	

Table 2: Oligonucleotides used in "touch-up" PCR reactions.

Displayed are the primers used for attaching the HA-tag to At1g65880 and At1g65890 sequences. Oligonucleotide sequences are shown in 5' to 3' direction. All primers were synthesized by Invitrogen (Germany).

Template	Primer name	Primer sequence (5' to 3')	Annealing temp.
At1g65890 (AAE12)	AAE12 HA-tag-frag Fwd	ATA CGA TGT TCC AGA TTA CGC TAT GGA TAA TTT GGC GTT ATG TG	60 °C
At1g65890; At1g65880	Tag-Frag-Rev	AAT CAA CCA CTT TGT ACA AGA AAG CTG GGT	54 °C
At1g65880	880-HA-tag-Frag Fwd	ATA CGA TGT TCC AGA TTA CC TAT GGA TGA TTT GGC ATT ATG TG	60 °C
PCR products from PCR with HA-tag primers	Tag-Frag Adapter Fwd	GGG GAC AAG TTT GTA CAA AAA AGC AGG CTT CTA CCC ATA CGA TGT TCC AGA TT	65 °C

PCR chemicals

dNTP mix, 10 mM	Fermentas (Germany)
$MgCl_2$, 25 mM	Amersham Biosciences (Germany)
PCR buffer, 10 x	Amersham Biosciences (Germany)
Pfu DNA Polymerase Ultra	Stratagene (USA)
Pfu Ultra^{TM} HF Reaction Buffer, 10 x	Stratagene (Germany)
Taq DNA Polmerase	Promega (Germany)

2.2.1.4 DNA gel electrophoresis

To check for DNA fragment size DNA was separated electrophoretically on 1.2 % agarose gels containing 0.5 mg ethidiumbromide / 100 ml. The agarose was solved in 0.5 x modified TAE buffer. DNA fragments were separated on the gel with the use of an electrophoresis chamber, filled with modified TAE buffer, on 100 to 130 volts for 20 to 30 minutes. A DNA ladder (5 µl per slot of a 1 kb and/or a 100 bp ladder) was used for identification of fragment size and DNA was loaded with loading dye (1:5). The documentation was done with the GeneGenius Bio Imaging System (Merck, Germany).

50 x TAE buffer (PCR)

242 g	Tris
57.1 ml	glacial acetic acid
100 ml	0.5 M EDTA pH 8.0
x ml	H_2O grade II to 1000 ml

DNA loading dye (PCR)

0.025 %	bromophenol blue
30 %	glycerol
in	0.5 x TAE

Ladder working mix

100 µl	ladder
700 µl	H_2O grade III
200 µl	6 x loading dye (bromophenol blue)

Electophoresis chemicals

DNA Ladder 1 kb	Invitrogen (Germany)
DNA Ladder 100 bp	Invitrogen (Germany)

2.2.1.5 Cloning and transformation of competent *Eschericha.coli* cells

TOPO TA Cloning®

PCR products with a 3'-desoxy-adenosine overhang were subcloned into the pCR®4-TOPO (bacterial cloning vector of 3957 bp containing kan^R and amp^R, Invitrogen) as part of the TOPO TA Cloning® Kit for Sequencing (Invitrogen, Germany) according to the manufactures specifications of chemical transformation. Instead of a 6 µl TOPO® Cloning reaction half reaction was enough to for using 2 µl for the transformation of the competent One Shot® Top 10 *E. coli* cells. Transformed cells recovered for half an hour in 200 µl SOC-media at 37 °C shaking. The cells were plated on prewarmed selective LB agar plates (containing antibiotics, usually Kan, for selection) and incubated at 37 °C over night. The resulting colonies were checked for positive insertion via "colony PCR".

LB medium

10 g	peptone
5 g	yeast extract
5 g	NaCl
x ml	H_2O grade II to 1000 ml

adjust with NaOH to pH 7.5
autoclave

LB agar

add 1.5 % (w/v) agar to LB medium
autoclave

SOC medium

20 g	tryptone
5 g	yeast extract
0.5 g	NaCl
10 ml	0.25 M KCl
5 ml	2 M $MgCl_2$
20 ml	1 M glucose
x ml	H_2O grade II to 1000 ml

adjust with NaOH to pH 7.0
autoclave

The Gateway® Cloning system

The Gateway® Technology is an easy, rapid and highly efficient system for introducing DNA sequences into a multiple vector cloning system using the site-specific recombination system of the bacteriophage *lamba (1)* and the *E. coli*-encoded protein Integration Host Factor. To use the system the starting DNA sequence has to contain *att*B sites for the first BP reaction. The entry clone (pDONRTH) for the reaction needs the additional *att*P sites. And the destination vector in the LR reaction has to have the *att*L sites.

The Gateway® cloning was performed with the two kits Gateway® BP Clonase^{TM} II enzyme mix and Gateway® LR Clonase^{TM} II enzyme mix (Invitrogen, Germany). Both kits were used according to specifications of the manufacturer accept for using a 4 µl-half reaction instead of the full 8 µl. The entry vector of choice in the BP reaction was pDONR^{TM} 207 (gent^{R}). The transformation was done with chemical competent One Shot® *E. coli* cells after the same scheme as for the TOPO TA Cloning® system and resulting colonies were checked for positive transformation and correct sequence by sequencing. The positive entry vector constructs, isolated from 4 ml over night LB medium containing gentamicin, were applied in the LR reaction. The destination vector of choice was pH9GW (a bacterial expression vector of 5359 bp derived from pET-28a(+), containing the T7-promoter, a N-terminal HIS-Tag and a kan^{R}). The construct was first transformed into chemically competent One Shot® Top 10 *E. coli* cells like before. After characterization by repeated sequencing, they were brought into chemical competent BL21(DE3) *E. coli* cells (Novagen, USA) for overexpression of the gene of interest. Therefore, 50 µl frozen cells were thawed on ice and mixed with 1 µl of the isolated construct, up to 30 min incubated on ice and transformed after the same scheme as for the TOPO TA Cloning® system. Both, resulting transform Top 10 colonies from the LR and the BP reaction, were used to prepare glycerol stock (850 µl culture mixed with 150 µl pure glycerol, frozen at -80 °C).

TE buffer

10 mM	Tris
0.1 mM	EDTA
in	H_2O
adjust to pH 8.0	

Vectors

pCR®4-TOPO	Invitrogen (Germany)
Gateway™ pDEST™ Vector	Invitrogen (Germany)
Gateway™ pDONR™ 207 Vector	Invitrogen (Germany)
pEarlyGate201	Craig Pikaard and Keith Earley; The Arabidopsis Biological Resource Center at the Ohio State University, USA
pH9GW (derived from pet28) expression	Joe Noel; Salk Institute, San Diego CA, USA

Antibiotic solutions

Gentamicin	Stock 50 mg/ml Final concentration 50 µg/ml
Kanamycin	Stock 50 mg/ml Final concentration 50 µg/ml
Rifampicin	Stock 20 mg/ml Final concentration 20 µg/ml
Spectinomycin	Stock 100 mg/ml Final concentration 100 µg/ml
Timentin	Stock 125 mg/ml Final concentration 125 µg/ml

2.2.1.5.1 Transformation of *Agrobacterium tumefaciens*

Agrobacterium tumefaciens strain GV 3850 ($spec^+$, rif^+) was chosen to transform *A. thaliana* plants for the following reasons:

1. The strain GV 3850 holds a helper plasmid with *vir*-gene functions necessary for T-DNA transfer.
2. The plasmid also features antibiotic resistances for selection.

To make the *A. tumefaciens* cells competent for transformation, a starter culture with 2 ml of YEP medium containing the appropriate antibiotics was inoculated with GV 3850 cells. The culture was incubated at 28 °C while shaking at 220 rpm over night. The next day, the starter culture was used to inoculate a 50 ml YEP culture (containing the same antibiotics) in a 250 ml flask. The culture was incubated for approximately 5 h (until OD_{600} 0.6-1.0) at 28 °C shaking on 220 rpm. The cells were centrifuged at 5000 rpm for 5 min, the supernatant was discarded, and the pellet was resuspended in 10 ml of ice cold 20 mM $CaCl_2$. 100 µl aliquots of the competent cell solution were frozen in liquid nitrogen and stored at -80 °C for further use.

To transform the cells, 1 µg plasmid DNA was added to 100 µl of the competent cells (if frozen, they were thawed on ice first) and mixed gently. Unless otherwise noted, all steps were performed on ice or at 4 °C. The tube containing the cells plus the DNA was then frozen in liquid nitrogen for 5 min and thawed at 37 °C for 3 to 6 min. This step was repeated and the cells were then chilled on ice for 30 min. Next 1 ml of YEP medium was added and the cells were incubated at 28 °C shaking for at least 2 h. After spinning down the cells for 1 min at 10,000 rpm and pouring off the supernatant, they were resuspended in 100 µl YEP an transferred to an agarose plate containing the same appropriate antibiotics as before plus antibiotics selective for the introduced plasmid DNA. The plates were incubated inverted for two days at 28 °C and colonies checked for positive transformation (colony PCR) before they were used to transform *A. thaliana*.

<u>YEP medium</u>

10 g	peptone
10 g	yeast extract
5 g	NaCl

adjust with 1 M NaOH to pH 7.5

2.2.1.6 Isolation of plasmid DNA from *Escherichia coli*

The NucleoSpin® Plasmid kit (Macherey-Nagel GmbH & Co. KG, Dueren, Germany) was used to extract and clean plasmid DNA from 4 ml *E. coli*. culture (5 ml over night culture: LB containing the appropriate antibiotics, incubated at 37 °C and 220 rpm shaking). The optional washing with AW buffer was performed and highly pure DNA was eluted with 50 µl buffer AE.

2.2.1.7 DNA digests with restriction enzymes

The following digest reaction was incubated at 37 °C and stopped after 1 h by chilling the reaction on ice. The size of the resulting fragments was checked eletrophoretically.

20 µl Restriction enzyme digest

200 – 500 ng	DNA
2 µl	10 x NEB buffer (different salt concentration)
0.2 µl	BSA (0.1 mg/ml NEB) added if necessary
2 Units	restriction enzyme
x µl	H_2O grade II to 20 µl

Table 3: Restriction enzymes and buffers.

All restriction enzymes and buffers used were obtained from NEB (New England Biolabs, USA). The table shows the restriction enzyme used, the appropriate buffer, the enzyme concentration delivered, and whether BSA was added to the reaction or not.

Restriction enzyme	**Buffer provided**	**Enzyme concentration [U/µl]**	**BSA added**
EcoR I	NEB Nr. 2	20	yes
EcoR V	NEB Nr. 3	20	yes
Hind III	NEB Nr. 2	20	no
Nco I	NEB Nr. 2	10	no
Nde I	NEB Nr. 4	20	no

Pst I	NEB Nr. 3	20	yes
Xba I	NEB Nr. 2	20	yes

2.2.1.8 DNA sequencing

The sequencing was done by the principles of the chain termination reaction described by Sanger *et al.* (1977) using the ABI PRISM® BigDye™ terminator kit (Applied Biosytems, USA). The BigDye™–Mix contains buffer, dNTPs, DNA-Polymerase, and for the chain termination reaction needed, the four fluorescent dye marked didesoxynucleotides. The linear PCR reaction also contained the template DNA and compared to regular PCR reaction only one short oligonucleotide primer (table 1) complementary to the template. The reaction was performed as followed:

<u>20 µl Sequencing reaction</u>

150 – 200 ng	plasmid DNA
2 pmol	sequencing primer
4 µl	BigDye™–Mix
4 µl	BigDye™ Terminator 5 x Sequencing Buffer AB
x µl	H_2O grade II to 20 µl

<u>Cycling program</u>

5 min	96 °C	
10 sec	96 °C	} 35 Cycles
20 sec	54 °C	
4 min	60 °C	
storing at	4 °C	

In order to analyze the sequences, the reaction had to be purified first. This was done by the principle of gel filtration through the use of DyeEx™ 2.0 spin columns (Quiagen, Germany). The gel separation and analyzing of the terminated fragments was done with the capillary sequencer ABI PRISM® 3100 (length of capillaries 50 cm) by Bettina Ra-

guschke. Further analyzing of the sequences was performed with the software Vector NTI Advanced 10 (Invitrogen).

2.2.2 Plant treatments

2.2.2.1 *Arabidopsis thaliana* growth conditions

Plants were grown in climatic controlled chambers (York) under a long day cycle of 16 h light period with 150 µmol photons $s^{-1}m^{-2}$ at 21 °C, 55 % relative humidity. They were planted into a autoclaved (30 min at 80 °C) soil mixture known as "Arabidopsis mix" (80 % duff (pH 6-6.5), 10 % vermiculite (1-2 mm grain size), 10 % sand (burned), 0.1 % Osmocote mini (16 % nitrogen, 8 % phosphate, 11 % potassium), and 0.1 % triabon (16 % nitrogen, 8 % phosphate, 12 % potassium). For single plants 7 x 7 x 8 cm pots were used and for five plants 9 x 9 x 9.5 cm pots were used respectively. To increase the number of inflorescences, initial bolts were cut back and allowed to re-grow.

2.2.2.2 *In planta* Transformation of *Arabidopsis thaliana* with *Agrobacterium tumefaciens* by vacuum infiltration

Two days before the actual transformation procedure a 25 ml YEP culture (including selective antibiotics: spec., rif., kan.) of the transgenic *Agrobacterium* (strain GV 3850 ($spec^+$, rif^+)) was started and incubated overnight at 28 °C shaking at 220 rpm. The culture was used to inoculate a 250 ml YEP culture under the same conditions the next day. After 24 h, the culture was centrifuged for 15 min at 4300 x g at room temperature. The remaining pellet was resuspended in 250 ml infiltration medium. A vacuum desiccator was prepared with the 250 ml infiltration solution and an inverted *A. thaliana* plant. Four week old flowering plants, grown under long day conditions, were used for transformation. The plants were put into the desiccator in such a way that the flowers were covered by the infiltration solution and avoiding wetting of the soil. The desiccator was then sealed and vacuum was applied. After the infiltration solution formed rigorous bubbles and these bubbles just began to drop again, vacuum was released quickly. The wet plants were placed on a tray horizontally and covered with a plastic cover to allow them to dry and recover for one full day.

Infiltration medium (vaccum infiltration)

2.1 g	M&S salts (including B5 vitamins, 0.5 x)
50 g	sucrose (5 %)
10µl	6-benzylaminopurine (BAP, stock: 1 mg/ml DMSO, 0.044 µM)
0.2 ml	silwet L-77 (0.02 %)
x ml	H_2O grade II to 1000 ml

2.2.2.3 Seed sterilization

Seeds were sterilized by adding three to five fold volumes of bleach (2 % (w/v) Dichloroisocyannoic acid Sodium salt Dihydrate) to a tube containing 100 to 500 seeds. The seeds were incubated with bleach for 5 min. To ensure a complete removal of the bleach three steps of washing with the same amount of sterilized H_2O (grade III) were performed. All steps were performed by vortexing to ensure full coverage of each seed with liquid, a short centrifugation step at low speed to pellet the seeds, and removal of the liquid. Seeds were tried on sterilized Whatman paper and sprinkled on Petri dishes with selective MS medium. Single seed placement was accomplished by adding 0.1 % sterile agarose to the seeds and by using a glass pipette.

Seeds also were sterilized by using another method. 100 to 500 seeds were first washed in three to five fold volumes of 70 % Ethanol and in 100 % Ethanol afterward. Both washings were performed by vortexing to ensure full coverage of each seeds with liquid, a short centrifugation step on low speed to pellet the seeds, and removal of the liquid. The seeds were dried in a sterile bench for 2^+ h and used for sprinkling them onto plates containing selective MS medium.

MS sucrose agar

0.43 %	M&S salts
1 %	sucrose
5 mM	MES
adjust with KOH to pH 6.0	
0.8 %	Plant agar
x ml	H_2O grade II to 1000 ml
autoclave	

125 µg/ml Timentin
25 µg/ml Glufosinate-ammonium (BASTA)

2.2.2.4 Screening of transformed *Arabidopsis thaliana* seeds on selective plates

Mature seeds were harvested and cleaned from green plant parts. After sterilization (see before) they were planted onto selective MS medium containing 25 µg/ml BASTA and 125 µg/ml timentin. A negative control consisting of Col-0 seeds was also planted on each plate. The plates were sealed with tape, incubated for two days at 4 °C to synchronize germination, and transferred to Percival growth chambers (24 °C). Ten day old plants were counted for ratio of living green plants to yellowish dead plants. Plants of interest were transferred to soil then and grown under long day conditions.

2.2.2.5 Histological analysis of GUS gene expression

Background:

The bacterial *gus*A gene fused to a specific promoter was used as a reporter for the activity of the promoter in plants transformed with the fusion product. The *gus*A gene encodes for the *β*-glucuronidase, which cleaves certain sugar molecules. The colourless compound X-Gluc (called X-GluA), when cleaved by the GUS enzyme, generates an intense blue indigo dye.

All following steps were also performed for Col-0 as negative control.

Staining of the transgenic GUS-plants:

The GUS staining solution was prepared fresh before each experiment. It contained 0.5 mg X-Gluc per ml final volume. The substrate was dissolved in 0.2 % dimethyl sulfoxide (DMSO). The remaining solution was made up to a 50 mM sodium phosphate buffer pH 7.0 with 0.05 % Triton X-100 detergent and then filtersterilized. Whole seeds, seedlings, and plants, or parts of plants were incubated in the staining solution for 4 h at 37°C.

Chlorophyll extraction:

After incubation, the staining solution was removed and replaced by 70 % ethanol to stop the assay and to extract the chlorophyll from the tissue to become the blue staining more visible.

Recording of the results:

The results of the staining were recorded using an Axiovert 200 microcope and a stereomicroscope Stemi SV 11, both connected to a camera and to the software Axio Vision. Alternatively pictures were taken with a digital camera.

GUS staining buffer

50 mM Sodium Phosphate Buffer pH 7.0
0.05 % Triton X-100
autoclave

GUS staining solution

0.5 % X-Gluc (hexammonium salt), suspend in:
0,5 % DMSO, solve in:
x ml GUS staining buffer

2.2.3 Biochemical methods

2.2.3.1 Screening for glucosinolate content via High Pressure Liquid Chromatography (HPLC)

Transgenic seeds were screened for their glucosinolate content by HPLC. Therefore, 96 tube arrays were filled with three steel balls (3 mm in diameter) per well. A spatula tip of seeds (approx. 20 to 30 mg) was filled into a tube. Besides the probes of interest, negative (blanks and knockout mutant seeds) and positive controls (Col-0) were also induced on each plate. 1 ml of 80 % Methanol containing 0.05 mM of internal standard sinalbin (p-hydroxybenzylglucosinolate) was added to each tube and after sealing the array seed solution was homogenized by the use of paint shaker (4 min). After centrifu-

gation for 10 min at 4300 rpm supernatant (contains glucosinolates) was transferred onto DEAE sephadex 1ml polypropylene fritted deep well plates (nunc™, Germany). Filter plates were prepared by filling dry DEAE sephadex with the help of a commercial available hole-plate onto each filter, adding 0.8 ml grad III H_2O for pouring, and a washing step with 0.5 ml 80 % methanol. Filter plates were loaded with 600 µl of the supernatant of the probes. Afterwards filter have been washed with 0.5 ml 80 % methanol, 0.5 ml H_2O (grade III) , and 0.5 ml 0.02 mM MES buffer pH 5.2 (NaOH).25 µl Sulfatase was added to each filter and the array was incubated in the refrigerator (4 -7 °C) overnight. The next day glucosinolates were eluted with 1 ml of water (grade III). The glucosinolate solution was then analyzed with the Hewlett-Packart Agilent 1100 DAD HPLC System on Supelcosil LC18 150 x 2.1 mm with 5 µm of silica particle diameter column. The method used had an injection volume of 20 µl and a flow of 0.25 ml/min on a continuous gradient of 0 to 42 % acetonitrile in 14 min (resolvents: acetonitril and H_2O). Data was evaluated with HP ChemStations and Excel after transferring the data to a text file by using the program Data Trans.

2.2.3.1.1 Purification of sulfatase for glucosinolate analysis

700 mg crude sulfatase was carefully dissolved in 30 ml grade III H_2O with the aid of a glass rod. 30 ml absolute EtOH was added and the solution mixed. After centrifugation at 4000 rpm for 20 min the supernatant was transferred into a new centrifuge bottle and 90 ml absolute EtOH was added, mixed, and centrifuged again at 3500 rpm for 15 min. This time the pellet was kept and the supernatant discarded. The pellet was dissolved in 25 ml H_2O grade III and aliquots were frozen at – 20 °C for further use.

2.2.3.2 Protein expression in *E. coli*

For protein expression in *E. coli* the Overnight Express™ Autoinduction System from Novagen was chosen. According to manufactories information's this system works with pET and other IPTG-inducible bacterial expression system without the need to monitor cell growth but the yield of a high-level protein expression. Media components are responsible for differentially metabolism for a high density growth and an automatically induced protein expression from the *lac* promoters.

The expression protocol toke three days all together. The protocol was started with the transformation of BL21(DE3) *E. coli* cells with a characterized pH9GW::gene vector and as control also an empty pH9GW plasmid the first day. If the protocol was started from a glycerol stock of the same kind of cells a 5 ml LB medium containing the appropriate antibiotic kanamycin culture was infected. Both, plate and liquid culture were cultured at 37 °C over night (shaking). The next day 50 ml Overnight Express Instant TB Medium containing kanamycin in a sterile 250 ml flask was infected either with a colony of the newly transformed cells or with 500 µl of the starter culture. The culture was incubated for 24 h at 18 °C shaking for proper expression. Protein extraction followed the third day.

Overnight Express Instant TB Medium

15 g Overnight Express Instant TB Medium (Novagen, USA)
2.5 ml glycerol
x ml H_2O grade II to 250 ml
cook in microwave (short)

2.2.3.3 Protein extraction from *E. coli*

Protein expressed from transgenic BL21(DE3) *E. coli* cells was extracted from 50 ml Overnight Express Instant TB cultures. All work was done at 4 °C or on ice. The yield of the overnight culture centrifuged for 10 min at 8000 x g. The pellet was weighed and one gram pellet was resuspended in 10 ml lysis buffer including 60 µl lysozyme (50 mg/ml). The solution was shock frozen in liquid nitrogen and thawed in a 37 °C water bath for a better yield of protein. The thawed solution was sonificated for three times 3 min each and up to 70 % power. Between the sonification cycles little breaks were made. The solution with the broken cells was centrifuged for 10 min at 20000 x g. Supernatant containing soluble proteins was separated from the pellet and frozen at -20 °C for a soon following use in western immunoblot analysis. The pellet was dissolved in the same amount of lysis buffer as the supernatant was removed and also frozen at -20 °C for a soon following use in western immunoblot analysis.

Lysis buffer working solution

make fresh

95 ml	1 x lysis buffer A
5 ml	100 mM DTT solution

1 x Lysis buffer A

50 ml	1 M Tris-HCL pH 7.5 (50 mM)
30 ml	5 M NaCl (150 mM)
2 ml	0.5 ECTA pH 8.0 (1 mM)
1 ml	100 % Triton X-100 (0.1 %)
100 ml	100 % glycerol (10 %)

100 mM DTT solution

make fresh

0.154 g	DTT
in 10 ml	H_2O grade II

2.2.3.4 SDS-Polyacrylamide-Gelelectrophoresis (SDS-Page)

Proteins were separated electophoretically in polyacrylamide gels under denaturizing conditions in the presence of SDS. Polyacrylamid3 gels were used from Bio-Rad (Germany), Ready Gel (4-20% Tris HCl). Before the protein samples were brought on the gel, they were dissolved in 4 x protein loading buffer and cooked for 10 min at 100 °C. The denaturized probes together with a protein marker (Bench Mark™ Pre-Stained Protein Ladder, Fermentas, Germany) were loaded into the gel slots. To find out about the right ideal amount of loaded sample different amounts of each (5, 10 and 15 µl) were loaded. The gel was run in 1 x SDS running buffer in a BioRad Miniprotean apparatus for about 1.5 h at a constant voltage of 100 V. The protein gels were used for immunoblot analysis.

4 x Protein loading buffer

5 ml	collection gel buffer
4 ml	glycerol
0.8 g	SDS
2 ml	β-Mercaptoethanol
1 % (g/v)	bromophenol blue

10 x SDS Running buffer

30.3 g	Tris
144 g	glycine
10 g	SDS
x ml	H_2O grade II to 1000 ml

2.2.3.5 Western immunoblot analysis

Transblot

To do the immuno staining of a protein gel, it was blotted to nitrocellulose membrane first. Therefore, a so called blot-gel sandwich was assembled in a tray arranged as followed: red electrode – sponge pad – filter paper – membrane – gel – filter paper – sponge pad – white electrode. Pads, filter paper and nitrocellulose membrane were prewetted in transfer buffer before. A Trans-blot cell was assembled with chilled transfer buffer a frozen cooling pack, a magnetic stir bar and the sandwich in the right direction. The blot was run stirring at 4 °C with 100 V constant voltage for 1-2 h.

Transfer buffer

100 ml	10x transfer buffer stock
200 ml	methanol
x ml	H_2O grade II to 1000 ml

10 x Transfer buffer stock

30.3 g	Tris (0.25 mM)
144 g	glycine (1.92 M)
x ml	H_2O grade II to 1000 ml

Antibody incubation

The trans-blotted membrane was put in blocking solution for 1 h slight shaking. After discarding the old blocking solution, new 10 ml blocking solution was added to the membrane and a chosen concentration of primary antibodies were added (anti-HA pro-

duced in rabbit, Sigma). To find out about the ideal concentration the antibody was used 1:1000, 1:3000 and 1:5000 diluted. The membrane was incubated with the primary antibodies for 2 h at RT slight shaking or over night at 4 °C slight shaking. After incubation the membrane was washed three times for 5 min in TTBS followed by a short incubation in blocking solution. For incubation with different concentrations of the secondary antibody (monoclonal anti-rabbit IgG with a couplet alkaline phosphatase, Sigma) new 10 ml blocking solution and secondary antibody (1:5000, 1:10000 and 1:15000) was added. The incubation was done as before 2 h at RT slight shaking or over night at 4 °C slight shaking followed by three times washing for 5 min in TTBS.

Blocking solution

2-5 g	dry milk
100 ml	TTBS

Tween-tris-buffered saline (TTBS)

10 ml	Tris pH 7.5 (20 mM)
15 ml	5 M NaCl (150 mM)
5 ml	10 % Tween 20 (0.1 %)
x ml	H_2O grade II to 500 ml

Alkaline phosphataste reaction

The alkaline phosphatase reaction was done at RT. The blot was rinsed in alkaline phosphatase buffer, and then the membrane was incubated with 10 ml AP substrate buffer with slight shaking for 1-30 min until bands were clearly visible. The membrane was rinsed with water and dried on air.

AB substrate buffer

10 ml	alkaline phosphatase buffer
17 µl	Nitroblue tetrazolium (NBT)
17 µl	5-bromo-4-chloro-3-indolylphosphate (BCIP)

Alkaline phosphataste buffer

10 ml	1 M Tris pH 9.5 (100 mM)
2 ml	5 M NaCl (100 mM)
0.5 ml	1 M $MgCl_2$ (5 mM)
x ml	H_2O grade II to 100 ml

2.2.3.6 Peroxisome extraction

The following protocol was used to isolate peroxisomes from *A. thaliana* tissue. The protocol is a modified version of the proposed protocol for isolation of glyoxysomes of pumpkin cotyledons (Olsen and Harrison-Lowe, 2005).

For localization of At1g65880- and At1g65890-BZL function to the peroxisomes it was necessary to isolate the peroxisomes from the focused plant tissue. Therefore 5 g leaf tissue from about 6 weeks old plants was homogenized in 50 ml cold 1 x grinding buffer working solution (= 1:10 dilution) with the help of a Waring blender (3 short bursts of ~3 sec on low speed). All steps of the protocol were performed at 4 °C or on ice. The homogenate then was filtered through Miracloth (folded in half) and the filtrate centrifuged for 10 min at 3000 x g to remove tissue debris accumulated in the pellet. In a following centrifugation step for 20 min at 10500 x g the previous supernatant got separated into a pellet containing the peroxisomes and small broken organelles and the supernatant containing bigger organelles as mitochondria and chloroplasts respectively. Therefore the supernatant was discarded carefully and the pellet resuspended in 300 µl 1 x resuspension buffer working solution with a paintbrush. The peroxisome-cell debris solution was used to carefully overlay the top of a gradient. The gradient was build from 1.5 ml of 2 M sucrose solution on the bottom carefully overlaid with 10 ml 28 % percoll solution, prepared in 14 x 89 mm centrifuge tube (Beckman, USA). It got centrifuged for 30 min at 18000 x g in a swinging-bucket rotor without the brake. After centrifugation a yellowish band of peroxisomes was visible at the percoll/sucrose surface as shown in figure 3.

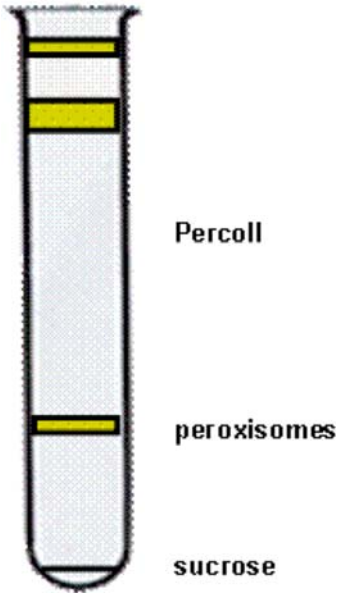

Figure 3: Sucrose/Percoll gradient separation of peroxisomes.

To purify the obtained peroxisomes fractions and especially the 'peroxisome' fraction were collected separately with a pipette. The 'peroxisomes' were diluted 3- to 5-fold with 1 x resuspension buffer (usually 1.5 – 2 ml) and centrifuged once more for 16 to 20 min at 7000 x g in a swinging-bucket rotor. The supernatant got removed carefully and the invisible pellet was gently resuspended in 300 µl of 1 x resuspension buffer. The yield was used for enzyme assays to ensure the isolation of peroxisomes and furthermore for western-immuno blot analyzes.

Controls: To ensure that the obtained solution consists of peroxisomes supernatants and other fraction also got collected for doing enzyme assays with them. Furthermore a crude plant tissue homogenate in 1 x grinding buffer working solution was also used to test with marker enzymes.

<u>2 x Grinding buffer stock solution</u>

17.844 g	tetrasodiumpyrophosphate (Na4P2O7, 40 mM)
0.744 g	EDTA (2 mM)
109.32 g	D-mannitol (0.6 M)

up to 1000 ml with H2O grade III

adjust to pH 7.5 with glacial acetic acid

<u>1 x Grinding buffer working solution</u>

make fresh	
25 ml	2 x grinding buffer stock
25 ml	H2O grade III
50 mg	BSA (1mg/ml)

2 x Resuspension buffer stock solution

4.776 g	HEPES (20 mM)
109.32 g	D-mannitol (0.6 M)
up to 1000 ml with H_2O grade III	
adjust to pH 7.2 with KOH	

1 x Resuspension buffer working solution

make fresh	
10 ml	2 x resuspension buffer st.
10 ml	H_2O grade III

Percoll, 28 % (v/v)/Resuspension buffer, 1 x

28 ml	percoll
50 ml	2 x resuspension buffer st.
22 ml	H_2O grade III

Sucrose, 2 M

85.575 g	sucrose
dissolved in H_2O grade III to a final volume of 125 ml	

2.2.3.7 Enzyme assays

Enzyme assays with so called marker enzymes were used to ensure the peroxisome isolation. As marker enzymes serves catalase for peroxisomes, fumarase for mitochondria, and isocitrate lyase for chloroplast. The isolated peroxisomes as well as supernatants from the peroxisome isolation protocol, and crude plant extract were undertaken all three enzyme assays. And all enzyme assays included pure enzyme assays as positive controls as well as boiled probes (and sometimes also water) as negative controls. All enzyme assays were measured and monitored with the UV-VIS Recording Spectrophotometer and the appendant software UV Prob Version 1 (Shimadzu, Germany).

2.2.3.7.1 Catalase activity assay

Catalase catalyzes the decomposition of 2 H_2O_2 to 2 H_2O and O_2. The reaction can be measured by a decrease of absorbance at 240 nm. Initially the concentration of H_2O_2 - PO_4 buffer was determined by measuring its absorbance against 66 mM $KNaPO_4$ buffer (spectrometer blanked with $KNaPO_4$ buffer). The concentration was calculation by dividing the absorbance with the molecular weight of H_2O_2 (M = 34.02 g/mol). The concentration should be at least 14 mM. For measuring the decomposition of catalase quartz cuevettes were filled with 1 ml H_2O_2 - PO_4 buffer. The reaction was started by adding 50 – 100 µl catalase or enzyme sample to the reference cuvette and mixing. The kinetic time scan was stared from a blank. The reason for having the reaction in the reference and not in the sample cuevette was to obtain a positive curve increase.

Catalase working stock: 100U/ml $KNaPO_4$ buffer

<u>66 mM $KNaPO_4$ buffer</u>

3.522 g KH_2PO_4
7.268 g Na_2HPO_4
up to 1000 ml with H_2O grade III
adjust to pH 7.0 with NaOH

<u>H_2O_2 - PO_4 buffer</u>

make fresh
15 µl H_2O_2
10 ml 66 mM $KNaPO_4$ buffer

2.2.3.7.2 Fumarase activity assay

The enzymatic reaction of fumarase was measured by the formation of fumarate and H_2O from L-malate. The reaction shows an increasing absorbance at 240 nm in the first 4 minutes. Quartz cuvettes were used as reaction vessels. Both sample and reference cuevette were filled with 970 µl 50 mM L-malic acid. The reaction was started by add-

ing 30 to 100 µl enzyme sample to the sample cuevette and mixing. The reference cuevette contained the same amount of 0.1 % bovine serum albumin instead.

Fumarase working stock: 1U/ml potassium phosphate buffer

0.5 M Potassium phosphate buffer, pH 7.5

28.85 ml 1 M Na_2HPO_4
21.15 ml 1 M NaH_2PO_4
x ml H_2O grade II to 1000 ml

50 mM L-malic acid, pH 7.5

prepared with 0.5 M potassium phosphate buffer, pH 7.5

0.1 % bovine serum albumine

dissolved in 10 ml H_2O grade III

2.2.3.7.3 Isocitrate lyase activity assay

Isocitrate lyase catalyzes the cleavage of isocitrate into succinate and glyoxylate. The following formation of glyoxylate to phenylhydrazine to a complex gives a linear increase between 2 to 3 min after start at 324 nm and, therefore, can be measured with the spectrophotometer. Both reference and sample cuvette (regular one use plastic cuevettes) were filled with 10 to 100 µl enzyme sample, 100 µl phenylhydrazine-HCl up to 800 µl for the sample cuvette and up to 900 µl for the reference cuvette. The reaction was started by adding 100 µl 130 mM isocitrate to sample cuvette and mixing.

Isocitrate lyase working stock: 0.07 U/ml IL buffer

50 ml IL buffer

12.5 ml 0.2 M K H_2PO_4
12.5 ml 0.2 M $KHPO_4$
500 µl 1 M $MgCl_2$
77 mg DTT
200 µl 0.25 M EDTA
up to 50 ml with H_2O grade II
adjust to pH 6.8 with KOH if necessary

130 mM Isocitrate

168 mg isocitrate
5 ml H_2O grade III

100 mM Phenylhydrazine-HCl

make fresh
72 mg phenylhydrazine
10 ml H_2O grade III

3 Results

Peroxisomal proteins are nuclear encoded and therefore have to carry specific signals for targeting them to the peroxisomes. One possible peroxisomal targeting signal (PTS) is commonly referred to as PTS1. PTS1 contains the tripeptide motif SKL or conservative variations of it at the carboxyl-terminus (Gould et al., 1987; Gould et al., 1989; Reumann, 2004). It is rather straightforward for subcellular prediction programs to identify conserved sequences and make predictions as to their subcellular localization. PTS1 signals have proven to be a robust indicator for the targeting of the protein to the peroxisome but it is not a sufficient criterion due to limited knowledge of proper peroxisomal targeting. To clarify the true localization of a protein in the peroxisome, it actually has to be experimentally determined.

The two Arabidopsis BZLs At1g65880 and At1g65890 exhibit a carboxyl tripeptide of the type SRL, one of the major predicted PTS1 variations (Reumann, 2004). Furthermore, subcellular prediction programs indicate a likely localization of the two *A. thaliana* genes to the peroxisomes. It was my goal to obtain stronger evidence for peroxisomal targeting by using direct and indirect experimental approaches.

3.1 Results of the mutant complementation test

3.1.1 Design of transgenic lines

The mutant complementation test was chosen to localize plant BZLs to the peroxisomes in an indirect fashion. The system chosen in this case was to utilize two previously characterized T-DNA knockout lines, Salk_094196 (Alonso et al., 2003) and GABI_565B09 (Rosso et al., 2003), which both contained insertions within the gene At1g65880 (BZO1, (Kliebenstein et al., 2007)). Both lines are completely unable to produce 3- and 4-benzoyloxyglucosinolates (3BZOgls and 4BZOgls) in the homozygous knockout state (see figure 6b and c). Several different (putative) BZL genes from plants as well as a formerly characterized BZL from a bacterium were introduced into

these two lines to test weather they can complement the known BZL knockout phenotype.

Six different gene fusion constructs were used to transform the two *A. thaliana* T-DNA insertion lines Salk_094196 (Alonso et al., 2003) and GABI_565B09 (Rosso et al., 2003), and *A. thaliana* Col-0. The six gene fusion constructs contained of one of five different (putative) BZL cDNAs – the Arabidopsis At1g65880 (880) and At1g65890 (890) BZLs, putative BZLs from *Clarkia breweri* (Cbr1_N01) and *Petunia hybrida* (Petunia BZL), and a bacterial BZL from *Rhodopseudomonas palustris* (*R. palustris* BZL). In addition, a reporter gene (eGFP) under the control of the At1g65880 promoter (880Prom) was used as a control. Table 4 summarizes the eighteen transgenic lines which were made. At1g65880, At1g65890 and Cbr1_N01 exhibit a potential major PTS1 of the type SRL, while the putative Petunia BZL and the *R. palustris* BZL do not contain any obvious peroxisomal targeting signals. The nucleotide sequences of the five (putative) BZL genes, and of the At1g65880 promoter are shown in the appendix. The (putative) BZL genes, the eGFP gene, and the At1g65880 promoter were already cloned into the Gateway® cloning system (pDONR™ 207::BZL/eGFP and pDEST™::At1g65880 promoter; see 2.2.1.5).

The genes derived from the donor vectors (pDONR™ 207::BZL/eGFP) were fused to the 3'-end of the At1g65880 promoter sequence via an LR clonase reaction. Only plasmids carrying inserts without sequence errors (2.2.1.8 and table 1) were used to transform competent *Agrobacterium tumefaciens* strain GV 3850 cells (see 2.2.1.5.1). Plasmid DNA of transgenic *A. tumefaciens* was isolated and the six inserts were sequenced before being used. *A. tumefaciens* colonies carrying one of the six chimeric pDEST™::880Prom::BZL/eGFP gene fusion constructs were integrated into the genomes of three independent Arabidopsis lines, the *Arabidopsis thaliana* T-DNA insertion lines, Salk_094196 (Alonso et al., 2003) and GABI_565B09 (Rosso et al., 2003) and *Arabidopsis thaliana* Col-0. Altogether, eighteen different transgenic Arabidopsis lines were derived from six different gene fusion constructs and three Arabidopsis backgrounds. An overview of this procedure is provided in figure 4.

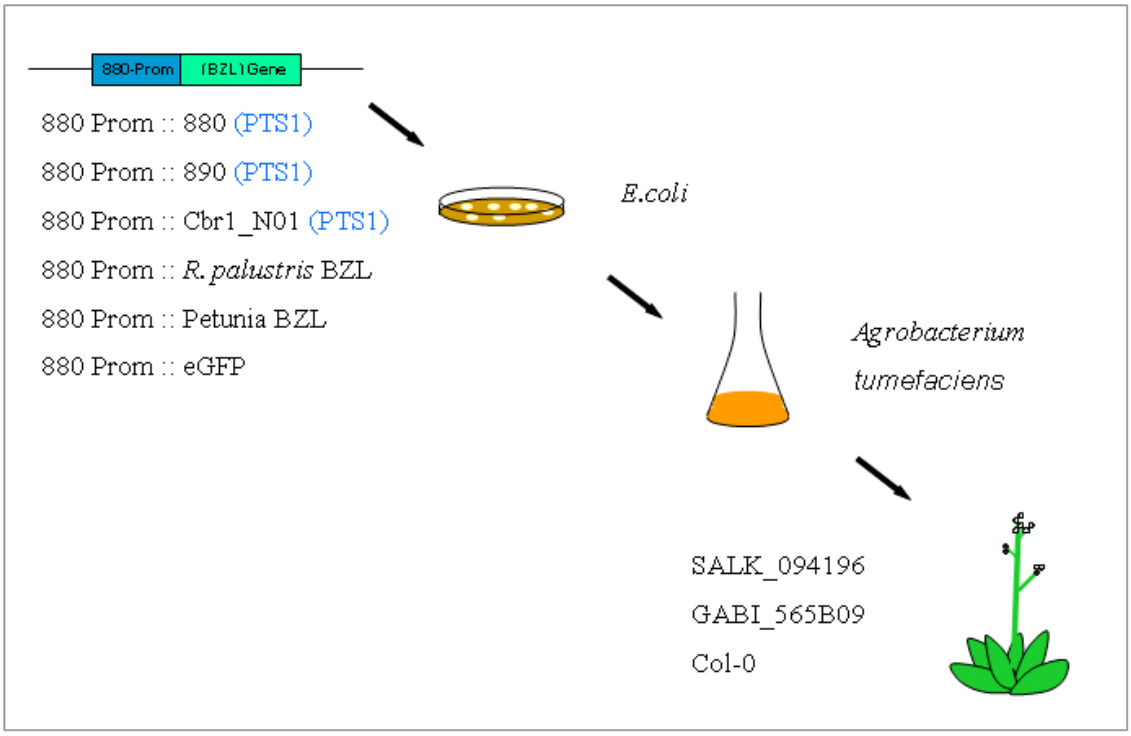

Figure 4: An overview of the procedure described in section 3.1.1.
Initially, different BZL genes (the Arabidopsis At1g65880 (880) and At1g65890 (890) BZLs, putative BZLs from *Clarkia breweri* (Cbr1_N01) and *Petunia hybrida* (Petunia BZL), and a bacterial BZL from *Rhodopseudomonas palustris* (R. palustris BZL)) and a control gene (eGFP) were cloned under the control of the At1g65880 promoter (880Prom). The gene fusion constructs were amplified in *E. coli* and transformed into *Agrobacterium tumefaciens*. The transgenic *Agrobacteria tumefaciens* carrying one of the six gene fusion constructs were used to infect two different *A. thaliana* T-DNA insertion lines, Salk_094196 (Alonso et al., 2003) and GABI_565B09 (Rosso et al., 2003) as well as wildtype *A. thaliana* (Col-0).

To identify those T0-seeds that were successfully transformed, plants were sewn in soil and selected for based on their BASTA resistance. Only resistant T1-plants were allowed to grow to maturity and self pollinate. Further analysis of the mature T1-seeds consisted of segregation analysis of the seeds after growth on MS medium containing BASTA (see 2.2.2.4). Only green healthy plants showing a 3:1 ratio of healthy green plants to yellow (dead) plants growing on the selection medium were used for further analysis. Mature T2-seeds were cleaned and tested for homozygosity in an identical fashion, this time retaining only those lines in which all the seedlings were resistant to the BASTA containing media. The end result of this analysis was the collection of several independent homozygous single insert lines per construct. Figure 5 shows an overview of this procedure.

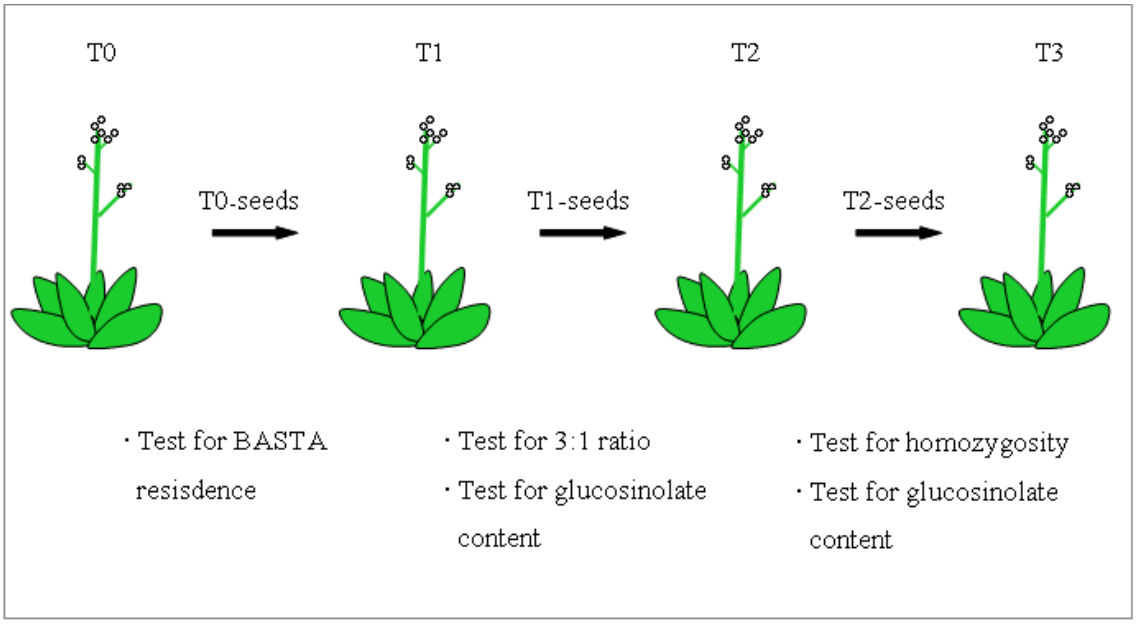

Figure 5: An overview of the transgenic selection procedure.
Seeds from T0-plants were tested for BASTA resistance. Seeds from resistant T1-plants were tested for a 3:1 resistance ratio (single insertion test). Finally, seeds from single insertion T2-plants were tested for homozygosity. Both, seeds from T1 and T2 generations, were tested for their glucosinolate content in an HPLC-based assay.

3.1.2 3- and 4-benzoyloxyglucosinolate screening in transgenic plants via HPLC-based analysis

Seeds from both the T1 and T2 generation were screened for 3- and 4-benzoyl-oxyglucosinolate levels using an HPLC-based method (see 2.2.3.1). The analysis of the HPLC-based raw data was done in cooperation with Michael Reichelt (Reichelt et al., 2002). Initially, T1-seeds of approximately 65 individuals from each of the eighteen produced transgenic lines (see above and figure 4) were screened in order to see if any rescue had occurred. Following confirmation that some lines did indeed show partial rescue, the focus became the analysis of seeds from the T2 generation (over 50 individuals per plant line). The results of the seed based glucosinolate analysis are summarized in table 4. Both the T1 and T2 generations were comparable in respect to their 3- and 4-benzoyloxyglucosinolates levels in seeds and therefore were summarized in the results.

Analysis of the untransformed parent lines revealed the complete absence of both 3- and 4-benzoyloxyglucosinolates in the insertion lines in contrast with the profile of Col-0

wildtype plants (figure 6a to c). Complete rescue to wildtype levels was only achieved with the construct containing the putative BZL gene from *Clarkia breweri* (figure 6f). Both of the insertion lines showed identical complementation patterns following transformation. In addition, 3BZOgls and 4BZOgls were also detected in SALK/GABI lines transformed with the fusion construct 880Prom::880 (figure 6d). The relative levels of 3BZOgls and 4BZOgls were lower than that of to the Col-0 control and the Cbr1_N01 rescue lines. SALK/GABI lines transformed with the fusion construct 880Prom::890 were devoid of benzoyloxyglucosinolates or contained only trace levels of either 3- or 4BZO. The pattern for this particular construct seemed inconsistent when compared to either the Clarkia or At1g65880 constructs. In some cases, the glucosinolate profile did not deviate from the untransformed knockout lines, whereas in other lines trace levels of benzoyloxyglucosinolates were found (figure 6e). Knockout lines transformed with 880Prom::*R. palustris* BZL, 880Prom::Petunia BZL, or 880Prom::eGFP displayed phenotypes identical with their untransformed counterparts (figure 6g to i). The presence of 3BZOgls and 4BZOgls in the diverse lines is summarized in table 4.

Table 4: An overview of the rescue mutant results.

In the table displayed are the three background plants and the six different gene fusion constructs they were transformed with. The eighteen transgenic lines and the three untransformed controls were undertaken of HPLC-based analysis of their seeds in the generations T1 and T2 to test weather 3- and 4-benzoyloxyglucosinolates (3BZOgls and 4BZOgls) are present.

+++: full presence compared to Col-0, ++: presence but not at Col-0 levels, -/+: absence to slight presence, -: absence

background	generation tested	gene fusion construct	3BZOgls and 4BZOgls
Col-WT	T1/T2	no transformation	+++
	T1	880Prom::880	+++
	T1	880Prom::890	+++
	T1	880Prom::Cbr1_N01	+++
	T1	880Prom::*R. palustris* BZL	+++
	T1	880Prom::Petunia BZL	+++
	T1	880Prom::eGFP	+++

Salk_094196	T1/T2	no transformation	-
	T1/T2	880Prom::880	+/++
	T1/T2	880Prom::890	-/+
	T1/T2	880Prom::Cbr1_N01	+++
	T1	880Prom::*R. palustris* BZL	-
	T1	880Prom::Petunia BZL	-
	T1/T2	880Prom::eGFP	-
GABI_565B09	T1/T2	no transformation	-
	T1/T2	880Prom::880	+/++
	T1/T2	880Prom::890	-/+
	T1/T2	880Prom::Cbr1_N01	+++
	T1	880Prom::*R. palustris* BZL	-
	T1	880Prom::Petunia BZL	-
	T1/T2	880Prom::eGFP	-

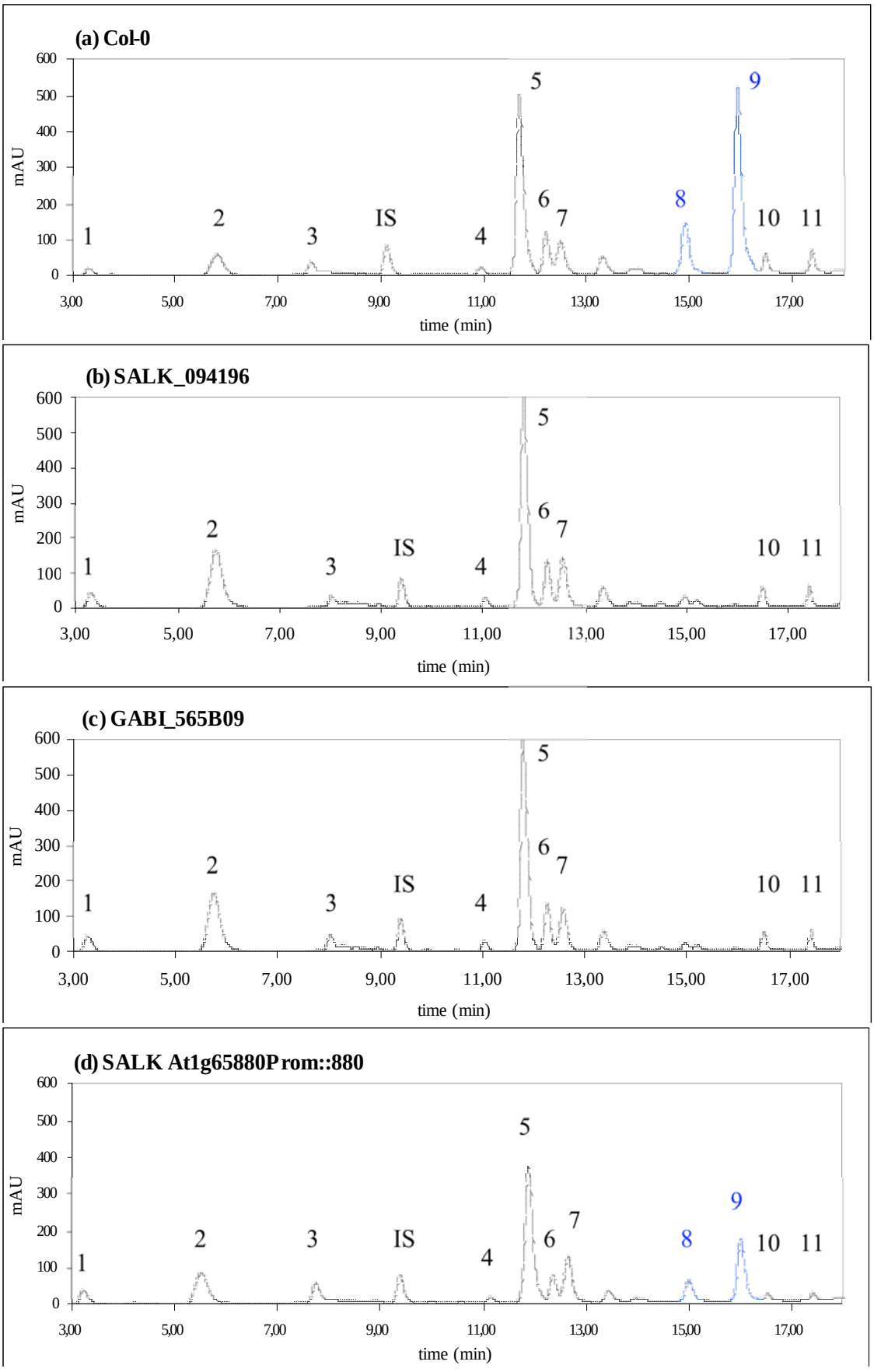
(a) Col-0
(b) SALK_094196
(c) GABI_565B09
(d) SALK At1g65880Prom::880
mAU
time (min)
1
2
3
IS
4
5
6
7
8
9
10
11

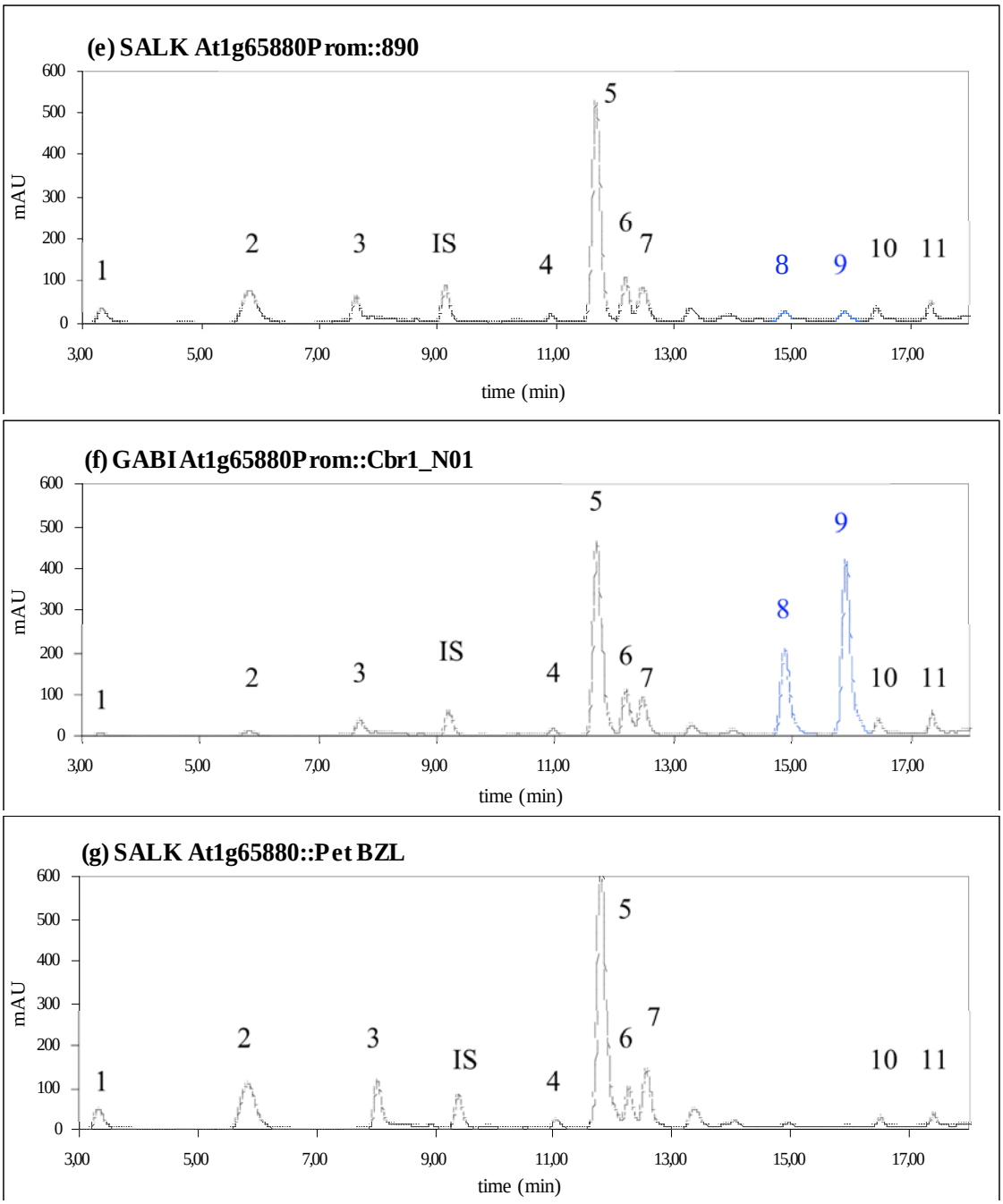
(e) SALK At1g65880Prom::890
mAU
time (min)
1
2
3
IS
4
5
6
7
8
9
10
11
(f) GABI At1g65880Prom::Cbr1_N01
mAU
time (min)
1
2
3
IS
4
5
6
7
8
9
10
11
(g) SALK At1g65880::Pet BZL
mAU
time (min)
1
2
3
IS
4
5
6
7
10
11

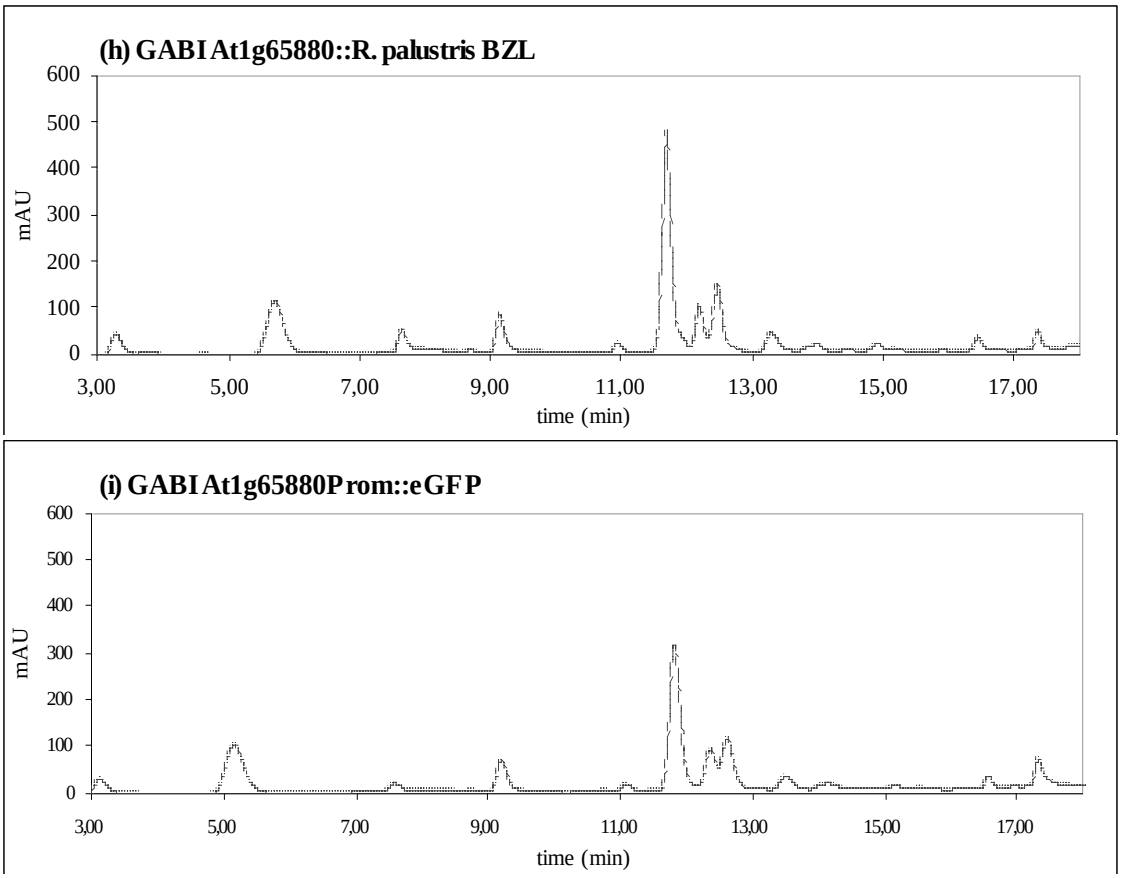

Figure 6: Representative HPLC-DAD traces of seed glucosinolate analysis.
(a) Col-O; (b) T-DNA insertion line SALK_094196;
(c) T-DNA insertion line GABI_565B09;
(d) T2 SALK line transgenic for At1g65880Prom::880;
(e) T2 SALK line transgenic for At1g65880Prom::890;
(f) T2 GABI line transgenic for At1g65880Prom::Cbr1_N01;
(g) T1 SALK line transgenic for At1g65880Prom::Pet BZL;
(h) T2 GABI line transgenic for At1g65880Prom::*R. palustris* BZL;
(i) T2 GABI line transgenic for At1g65880Prom::eGFP.
Glucosinolates were identified by absorption profile and retention time in comparison to an internal standard. Glucosinolates are as follows:
1: 3-hydroxypropylglucosinolate (3OHB);
2: 4-hydroxybutylglucosinolate (4OHB);
3: 4-methylsulfinylbutylglucosinolate (4MSOB);
4: 7-methylsulfinylbutylglucosinolate (7MSOH);
5: 4-metylthiobutylglucosinolate (4MTB);
6: 8-methylsulfininyloctylglucosinolate (8MSOH);
7: 3-indolyl-3-mythylglucosinolate (I3M);
8: 3-benzyloxypropylglucosinolate (3BZO);
9: 4-benzyloxypropylglucosinolate (4BZO);
10: 7-methylthiooctylglucosinolate (7MTH);
11: 8-methylthiooctylglucosinolate (8MTH);
IS, internal standard (p-hydroxybenzyl).

Precise calculations of the 3BZOgls and 4BZOgls contents in seeds was carried out on T2-lines which were determined to be homozygous following an extra generation of segregation analysis. The concentrations of 3BZOgls and 4BZOgls in these seeds were calculated according to the following formula.

$$concentration\ analyte = \frac{area\ analyte * response\ \ factor * amount\ of\ \ stnd}{area\ stnd * seed\ \ weight}$$

Results of the calculations are represented in figure 7. The average was taken from combining both of the transformed knockout lines since they contained similar concentrations of 3BZOgls and 4BZOgls. *Clarkia breweri* (Cbr1_N01) carrying transgenic SALK/GABI lines had 3BZOgls and 4BZOgls concentrations of approximately 8.11 µmol/g (± 1.42) and 16.89 µmol/g (± 2.46) which were nearly identical to that of to wildtype Col-0 levels (approximately 5.44 µmol/g (± 0.26; 3BZOgls) and 16.68 µmol/g (± 2.60; 4BZOgls)). Transgenic SALK/GABI lines transformed with the gene At1g65880 also showed 3BZOgls and 4BZOgls concentrations in the seeds (approximately 3.26 µmol/g (± 0.86) and 5.56 µmol/g (± 1.25)). Furthermore, the control and reporter gene transformed SALK/GABI eGFP-seeds did not have 3BZOgls and 4BZOgls similar to their At1g65880 knockout parents. Transgenic At1g65890-lines had slightly enhanced 3BZOgls and 4BZOgls concentrations (approximately 1.29 µmol/g (± 0.86) and 0.72 µmol/g (± 0.32)) compared to the knockout parents.

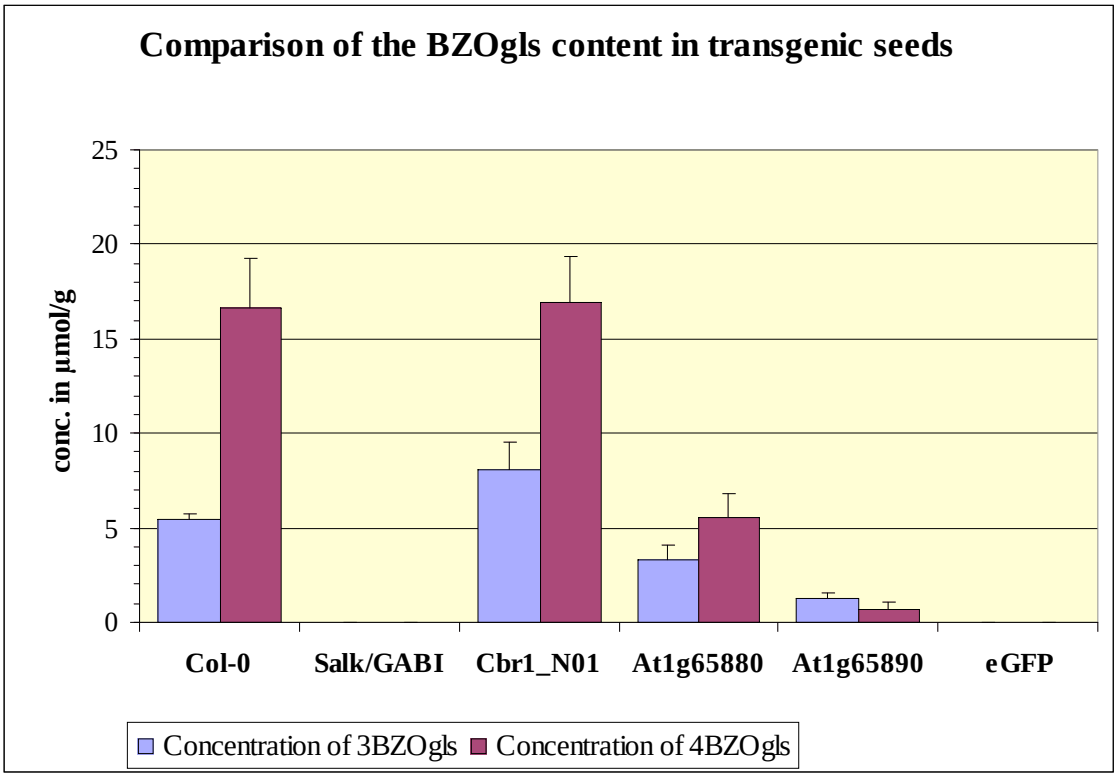

Figure 7: Concentrations of 3- and 4-benzoyloxyglucosinolates (3BZOgls and 4BZOgls) in transgenic plants.
The averaged concentrations of 3BZOgls and 4BZOgls were derived through HPLC-based analysis of several homozygous representatives of the transgenic lines SALK/GABI 880Prom::Cbr1_N01 (sample size: n = 15), SALK/GABI 880Prom::At1g65880 (sample size: n = 29), SALK/GABI 880Prom::At1g65890 (sample size: n = 13) and SALK/GABI 880Prom::eGFP (sample size: n = 10), and of Col-0 (sample size: n = 2) and the T-DNA insertion lines Salk_094196 and GABI_565B09 (sample size: n = 4) is displayd.

3.1.3 Verification of transcription activity for transgene constructs

RT-PCR experiments were used in order to determine whether or not the transgenes used during this study were transcriptionally active. Total RNA was isolated from mature T2-seeds of Salk_094196 and GABI_565B09 transgenics carrying the gene fusion constructs 880Prom::At1g65880, 880Prom::At1g65890, 880Prom::Cbr1_N01, or 880Prom::eGFP (see 2.2.1.1). T2-lines that were determined to be homozygous after T3 screening were chosen for RT-PCR reactions of total RNA and following primer-specific PCR reactions to detect the transgenes in the total cDNA. Furthermore, the gene APT1 encoding for adenine phosphate transferase was used as a positive control for the reverse transcriptase reaction. Purified binary vector plasmids were included to serve as further controls for fragment size. The negative controls consisted of cDNAs

synthesized from RNA of the untransformed Col-0, Salk_094196 and GABI_565B09 lines. Primers were designed to achieve fragments including parts of both the plasmid and the transgene by using a gene specific primer in combination with a plasmid specific primer. Results for the other constructs are displayed in figure 8. For each primer combination a transgene specific fragment of the expected size was obtained. A reamplification of the fragment was necessary to obtain enough DNA for sequencing purposes. The transgenes of the eGFP-lines were deteted by using gene specific primers (eGFP F1 + eGFP R1 figure 9). The sequence analysis didn’t reveal any sequence errors and the potential PTS1 was present.

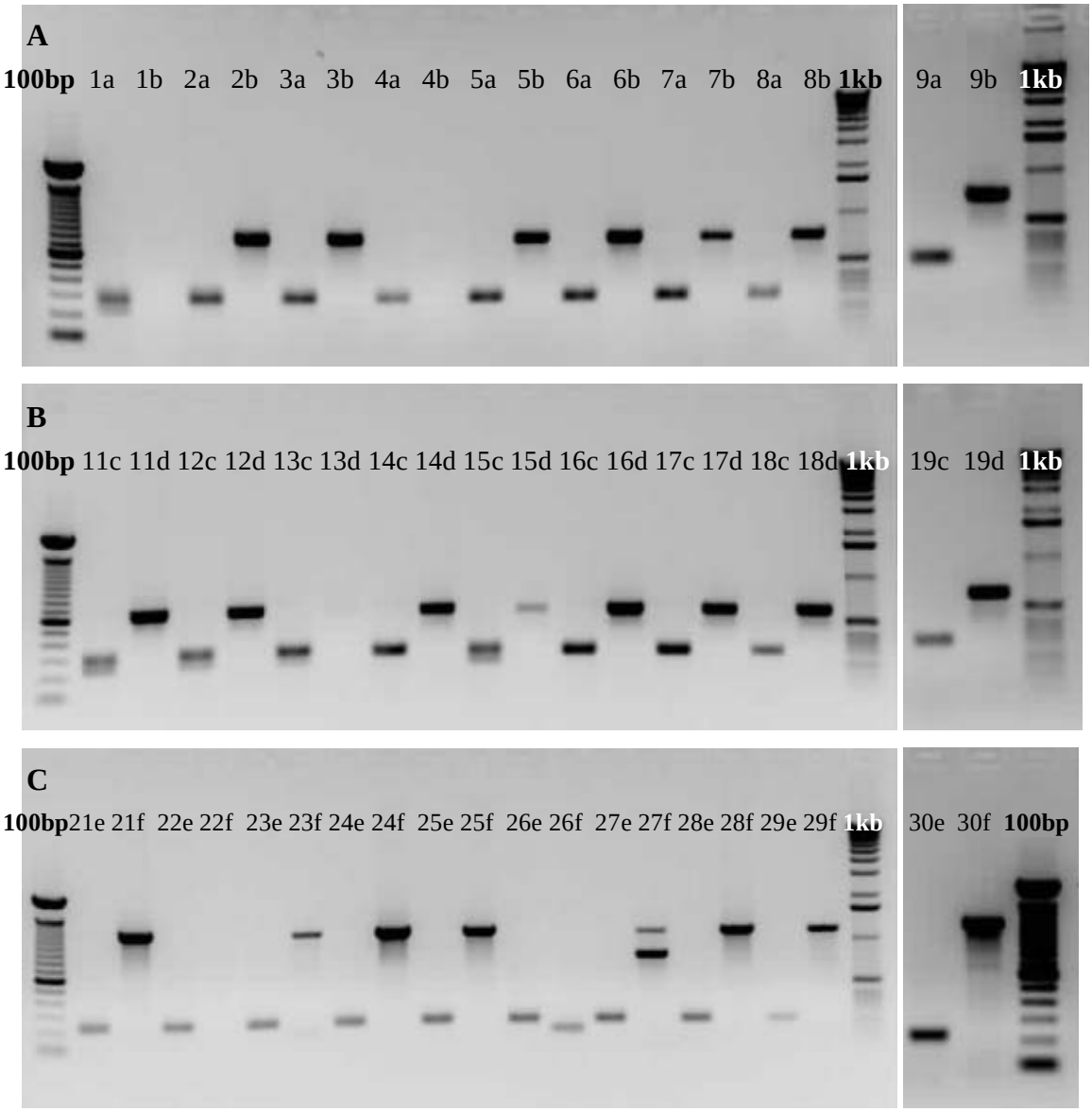

Figure 8: Screening of transgenic Arabidopsis plants by RT-PCR.
Total RNA was extracted from independent transgenic *A. thaliana* lines homozygous for one of three fusion constructs. The resulting cDNA was used as template in PCR reactions performed with different primer combinations for each cDNA. Reamplifications of the PCR products were carried out using 1 µl PCR reaction as template with the same primer combinations as before. DNA (number); Primer pair (small letter)/approximate fragment size:

A: pDEST^{TM}::880Prom::880 in Salk_094196 (1 to 3) or GABI_565B09 (4 to 8),
pDEST^{TM}::880Prom::880 plasmid (9),
a) pDest 880 fwd + 880 Seq R4 (730 bp), b) 880 Seq 4 + OCS 3' rev (250 bp);

B: pDEST^{TM}::880Prom::890 in Salk_094196 (11 to 13) or GABI_565B09 (14 to 18),
pDEST^{TM}::880Prom::890 plasmid (9),
c) pDest 880 fwd + 890 Seq R4 (600 bp), d) 890 Seq F4 + OCS 3' rev (260 bp);

C: pDEST^{TM}::880Prom::Cbr1_N01 in Salk_094196 (11 to 24) or GABI_565B09 (25 to 29),
pDEST^{TM}::880Prom::Cbr1_N01 plasmid (9),
e) pDest 880 fwd + Cbr1_N01 Seq R4 (1160 bp), f) Cbr1_N01 Seq F4 + OCS 3' rev (200 bp).

Ladder: 100 bp DNA ladder left, 1 kb DNA ladder middle and right.

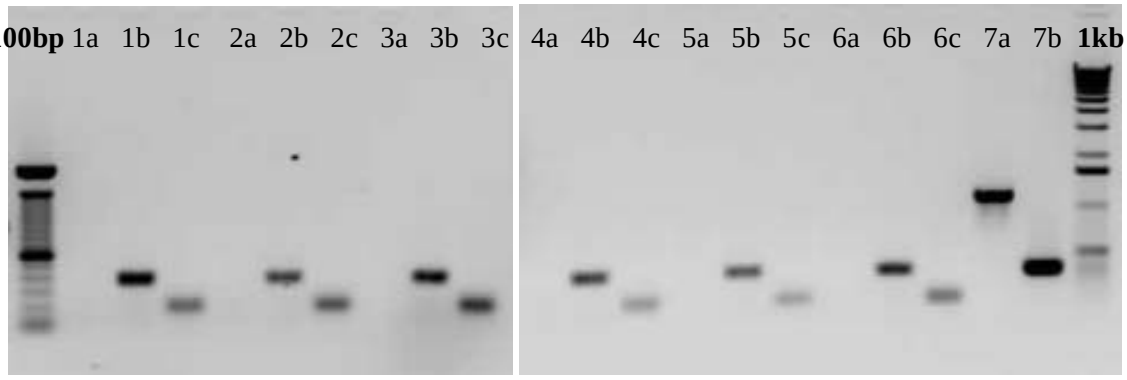

Figure 9: Screening of the pDESTTM::880Prom::eGFP gene fusion construct in transgenic Arabidopsis plants.
Total RNA was extracted from independent lines of transgenic *A. thaliana* plants with the background Salk_094196 (1 to 3) or GABI_565B09 (4 to 6) homozygous for pDEST^{TM}::880Prom::eGFP. The resulting cDNA was used as template in PCR reactions performed with the primer combinations: a) pDest 880 fwd + OCS3' rev 4, b) eGFP F1 + eGFP R1, c) APT1 F and APT1 R; resulting in product length' of approximately a) 1120 bp, b) 370 bp, and c) 200 bp. The same PCR reactions were carried out with the appropriate plasmid DNA pDEST^{TM}::880Prom::eGFP for fragment size control.
Ladder: 100 bp DNA ladder left, 1 kb DNA ladder right.

3.1.4 Confirmation of promoter activity using eGFP

At1g65880 promoter::eGFP studies were carried out to test At1g65880 promoter specific expression in embryonic tissue in cooperation with John D'Auria. Transgenic *A. thaliana* (Col-0 background) lines carrying the gene fusion construct At1g65880 promoter::eGFP in their genome were studied for eGFP expression using the Axiovert 200 microscope. The specific expression of eGFP in embryonic tissue controlled by the At1g65880 promoter is displayed in figure 10. eGFP activity was found in intact seeds and in embryos freed from the seed coat.

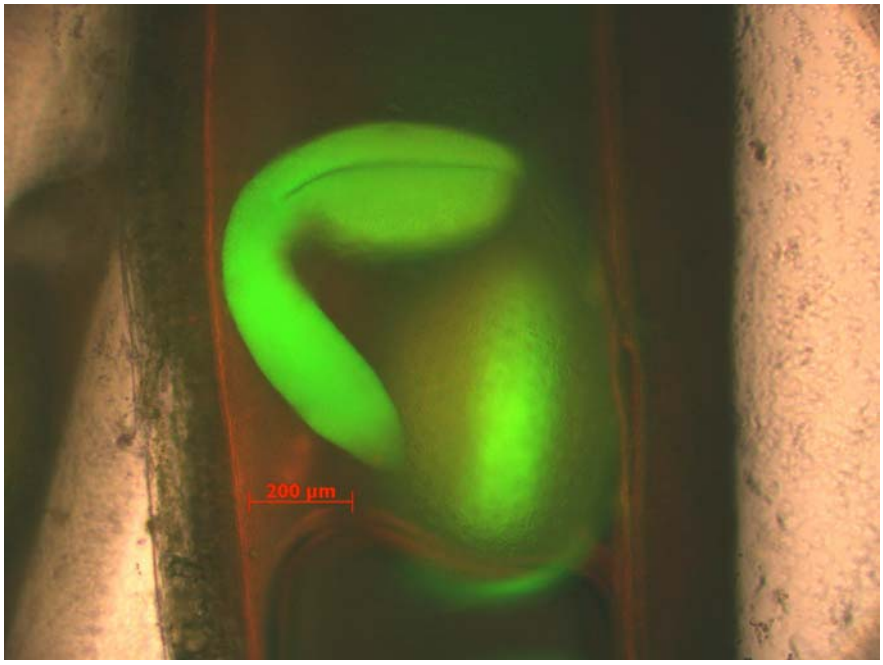

Figure 10: At1g65880 promoter::eGFP studies on embryonic tissue of A. thaliana. eGFP activity.
eGFP activity is found in intact seeds and in the whole embryo without seed coat. Red plant tissue belongs to the siliques.
The scale bar displays 200 µm.

3.2 Subcellular localization of Arabidopsis BZL using a density gradient

Differential and percoll/sucrose density gradient centrifugation was used to isolate peroxisomes of *A. thaliana* in order to directly locate plant BZLs in the peroxisomes. Transgenic *A. thaliana* plants carrying a constitutively overexpressed At1g65880 or At1g65890 gene that contained an introduced epitope tag at the 5'-end of the vector construct were used for the peroxisome isolation. The epitope tag used was obtained from *Human influenza virus*. The putative BZL proteins can subsequently be detected by separation of total proteins from the purified peroxisome fractions followed by detection using western immunoblot analysis with antibodies specific for detection of the HA-tag.

Seeds of transgenic *A. thaliana* Col-0 lines homozygous for the gene fusion constructs 35S::HA-tag-At1g65880 or 35S::HA-tag-At1g65890 respectively, where kindly re-

ceived from John D'Auria. The unrelated HA-tag is a short 27 bp long sequence (5'-tacccatacgatgttccagattacgct -3') from the *Human influenza virus.* The At1g65880 and At1g65890 sequences are shown in the appendix.

3.2.1 Verification of expression of the transgenic Arabidopsis BZL genes exhibiting a 5' HA-tag via RT-PCR

To test whether transgenic BZL is properly expressed and contains the full length HA-tag as well as the potential PTS1 tripeptide sequence total RNA was isolated from 10 day old transgenic seedling homozygous for the gene fusion construct pEarly-Gate201::35S::HA-At1g65880 or pEarlyGate201::35S::HA-At1g65890 (five of each line; see 2.2.1.1). The transgenic seedlings were grown on selective MS plates containing BASTA allowing only transgenic plants to grow. The isolated total RNA was reverse transcribed to cDNA. The PCR reactions were performed with transgene specific primers allowing the detection of the regions of interest. Verification of the reverse transcriptase reaction and control for the PCR reaction itself was achieved through the use of primers designed against the APT1 gene (see above). As a positive control for the expected fragments, the appropriate plasmid::insert DNAs, pEarlyGate201::35S::HA-At1g65880 or pEarlyGate201::35S::HA-At1g65890, were also included in the PCR reactions. cDNA of 10 day old Col-0 seedlings derived through the a similar growth on MS plates (without BASTA) severed as a negative control for transgene expression. The primer combination pEARLEY201_35_HA_fwd + OCS3' rev binding pEarlyGate201 vector DNA, the 35S promoter and parts of the HA-tag and enclosing the HA-BZL insert did not yield any observable products. New primers were designed in between the two BZL ORFs: A forward primer close to the 3' end (880 Seq 4, 890 Seq F4) used in combination with OCS3' rev and a reverse primer close to the 5' end (880 Seq R4, 890 Seq R4) used in combination with pEARLEY201_35_HA_fwd. Both primer combinations specifically amplified fragments of expected length of the cDNA of each transgenic line (figure 11). The untransformed Col-0 cDNA did not yield any fragments specific for the insertion of a transgene. To further confirm that both HA-tag and potential PTS1 are intact in the transgenic lines, representatives of the fragments derived from the PCR of the upstream and downstream vector::gene-ends were TOPO TA cloned and sequenced using the same primers as in the PCR reactions. The sequence

analysis confirmed both the presence of the HA tag as well as the presence of the PTS1 signal sequence at the 3'-end.

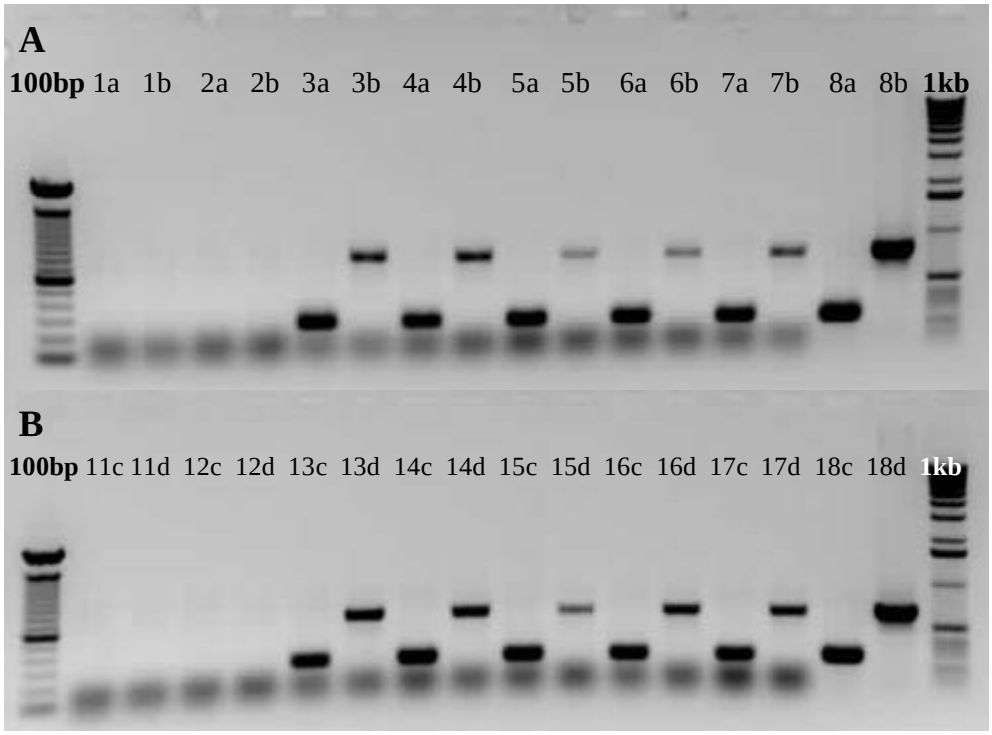

Figure 11: Screening of transgenic BZL in A. thaliana plants.
Total RNA was extracted from five of each transgenic *A. thaliana* lines homozygous for pEarlyGate201::35S::HA-At1g65880 (A: 3 to 7) or for pEarlyGate201::35S::HA-At1g65890 (B: 13 to 17) and from two Col-0 lines (A: 1 and 2, B: 11 and 12) at the age of 10 day old seedlings and reverse transcribed. The resulting cDNA was used as template in PCR reactions performed with two different primer combinations for each cDNA: a) pEARLEY201_35_HA_fwd + 880 Seq R4, b) 880 Seq 4 + OCS3' rev, and c) pEARLEY201_35_HA_fwd + 890 Seq R4, d) 890 Seq F4 + OCS3' rev. The same PCR reactions were carried out with the appropriate plasmid DNAs pEarlyGate201::35S::HA-At1g65880 (A: 8) or pEarlyGate201::35S::HA-At1g65890 (B: 18) for fragment size controls and therefore represented a positive control in the PCR reactions while the Col-WT cDNA represented a negative control.

3.2.2 Verification of proper Antibody-binding

To verify proper antibody-binding to the 5' HA-tag of two transgenic *A. thaliana* BZL HA-At1g65880 and HA-At1g65890, the HA-tag was fused to the two BZL ORFs and the fusion protein was heterologously expressed in *E. coli.*

The HA-tagged BZLs expressed in *E. coli* were detected with monoclonal HA-tag antibodies produced in rabbits. A band of approximately 70 kDa was detected in both pellet and supernatant samples, but with higher signals obtained with protein from the pellet

samples (figure 12). Vector only controls did not yield any signals regardless of the antibody concentrations used. Various concentrations of heterologously expressed proteins were used in order to determine the detection limit of the primary antibodies. Both pellet and supernatant samples were loaded onto polyacrylamide gels using 5, 10 and 15 µl of each protein sample. In addition, a dilution series of the antibodies was also used in order to optimize the visualization conditions of the immunoblot (figure 13). The optimal dilutions were found to be 1:10,000 for the primary antibody and 1:15000 for the alkaline phosphatise coupled secondary antibody.

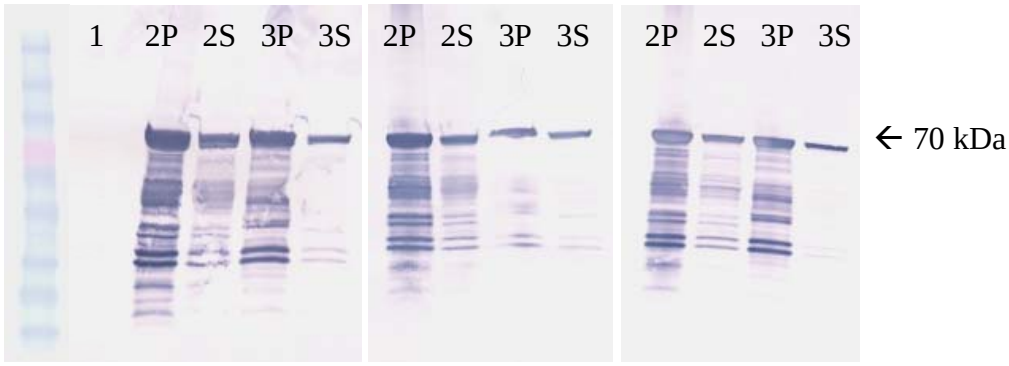

Figure 12: Immunoblot analysis of transgenic BZLs carrying an unrelated HA-tag.
SDS-polyacrylamide gels were loaded with A: 15, B: 10 and C: 5 µl of proteins samples overexpressed in BL21(DE3) *E. coli*: (1) empty pH9GW vector control, (2) HA-tag-At1g65880-protein and (3) HA-tag-At1g65890-protein.
P: resuspended pellet, S: supernatant

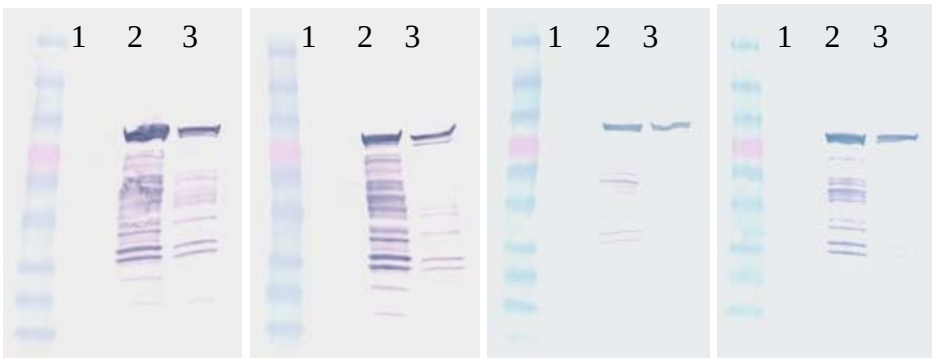

A	B	C	D	
1:3000	1:3000	1:10,000	1:5000	dil. pAb
1:5000	1:10,000	1:15,000	1:10,000	dil. sAb

Figure 13: Immunoblot analysis of transgenic BZLs carrying an introduced N-terminal HA-tag.
SDS-polyacrylamide gels were loaded with 5 µl of protein overexpressed in BL21(DE3) *E. coli*: (1) empty pH9GW vector control, (2) HA-tag-At1g65880-protein and (3) HA-tag-At1g65890-protein. The gels were used in western immunoblot analysis with different dilutions of the primary and the secondary antibodies to detect the HA-tag.
dil. pAb: dilution of the primary antibody; dil. sAb: dilution of the secondary antibody

3.2.3 Verification of proper marker enzyme activity

Commercially available preparations of the marker enzymes necessary for this study were obtained in order to develop optimized conditions for their detection. These enzymes consisted of catalase for peroxisomes, fumarase for mitochondria and isocitrate lyase for chloroplast (see 2.2.3.7). All three purified enzymes showed proper activity in their respective assays and can further be used as positive controls. To test the activity of the three marker enzymes in *A. thaliana,* a crude extract of mature leaves of 4 to 6 week old Col-0 plants was prepared. All three marker enzymes were found to be active within the crude extract compared to the positive control of each pure enzyme sample and to the negative controls of boiled extract sample or samples in which water was substituted for crude protein.

3.2.4 Verification of the isolation of peroxisomes from *Arabidopsis thaliana*

Mature leaves of 4 to 6 week old *A. thaliana* Col-0 plants were used to verify that the protocol for isolation of glyoxysomes from pumpkin cotyledons (Olsen and Harrison-Lowe, 2005) can be used for *A. thaliana*. Several different quantities of leaves were homogenized in order to extract and purify the peroxisomes (see 2.2.3.6). Only 1 to 5 g of Col-0 leaves yielded a visible yellowish band of peroxisomes as reported in the established protocol from L. Olsen laboratory (figure 14). The visible yellowish band was taken as an indicator for isolated peroxisomes.

Figure 14: Peroxisome isolation on a percoll/sucrose density gradient.
2.5 g of Col-0 leaf tissue was differential and density gradient centrifugation on a gradient of 2 M sucrose (bottom) and 28 % percoll (top). A yellowish band consisting of peroxisomes at the sucrose/percoll surface was obtained. The green band on top of the gradient contains cell debris.

The overall yield of isolated peroxisomes obtained from a gradient with 2.5 to 5 g leaf material was not enough to perform all of the necessary marker enzyme assays. Therefore, two gradients each consisting of 2.5 g leaf material were used. As predicted, the peroxisome fraction contained catalase activity (figure 15A). No activity was detected for fumarase as a marker enzyme for mitochondria and isocitrate lyase as a marker enzyme for chloroplast the isolated peroxisome fraction (figure 15B and C).

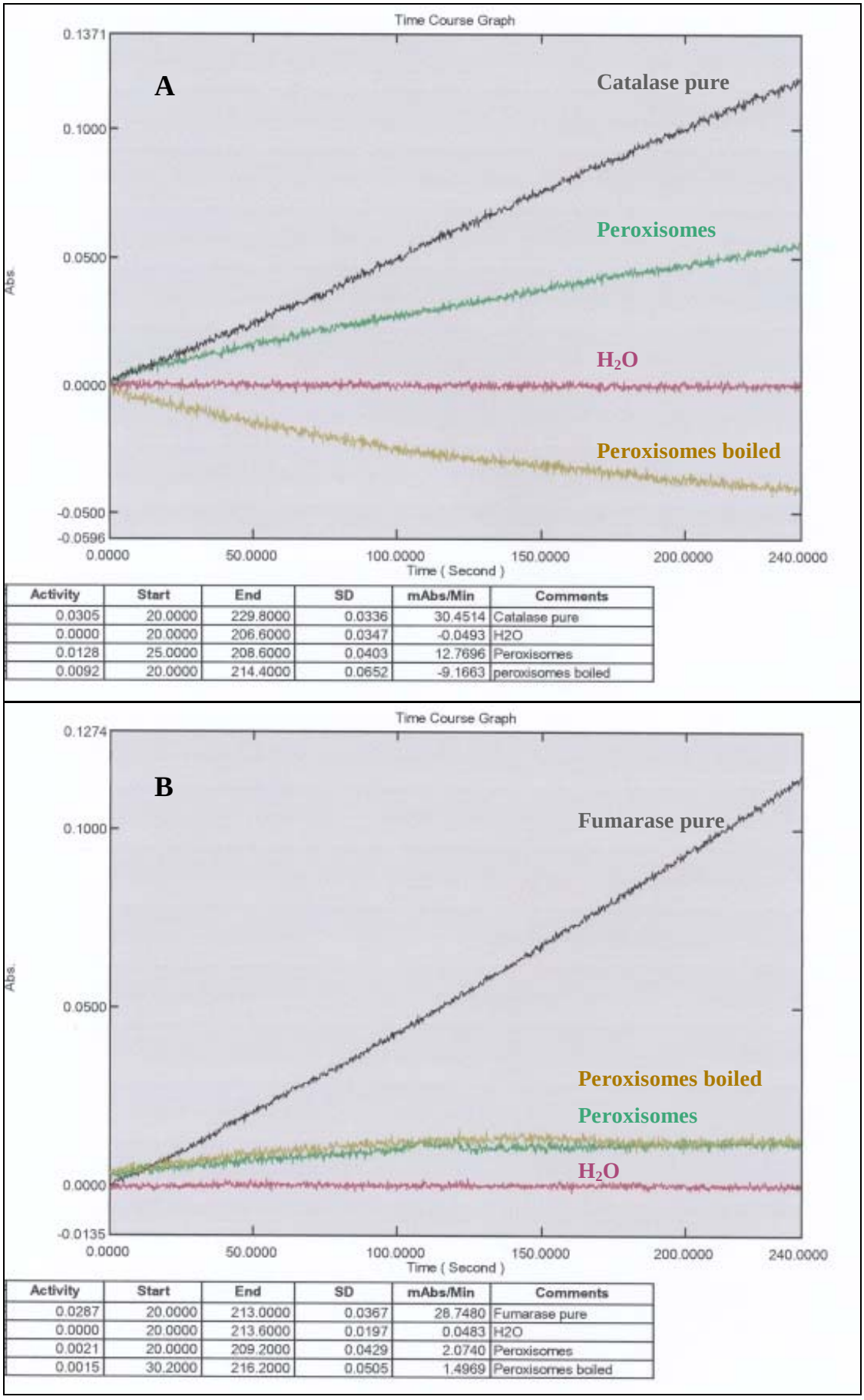

Activity	Start	End	SD	mAbs/Min	Comments
0.0305	20.0000	229.8000	0.0336	30.4514	Catalase pure
0.0000	20.0000	206.6000	0.0347	-0.0493	H2O
0.0128	25.0000	208.6000	0.0403	12.7696	Peroxisomes
0.0092	20.0000	214.4000	0.0652	-9.1663	peroxisomes boiled

Activity	Start	End	SD	mAbs/Min	Comments
0.0287	20.0000	213.0000	0.0367	28.7480	Fumarase pure
0.0000	20.0000	213.6000	0.0197	0.0483	H2O
0.0021	20.0000	209.2000	0.0429	2.0740	Peroxisomes
0.0015	30.2000	216.2000	0.0505	1.4969	Peroxisomes boiled

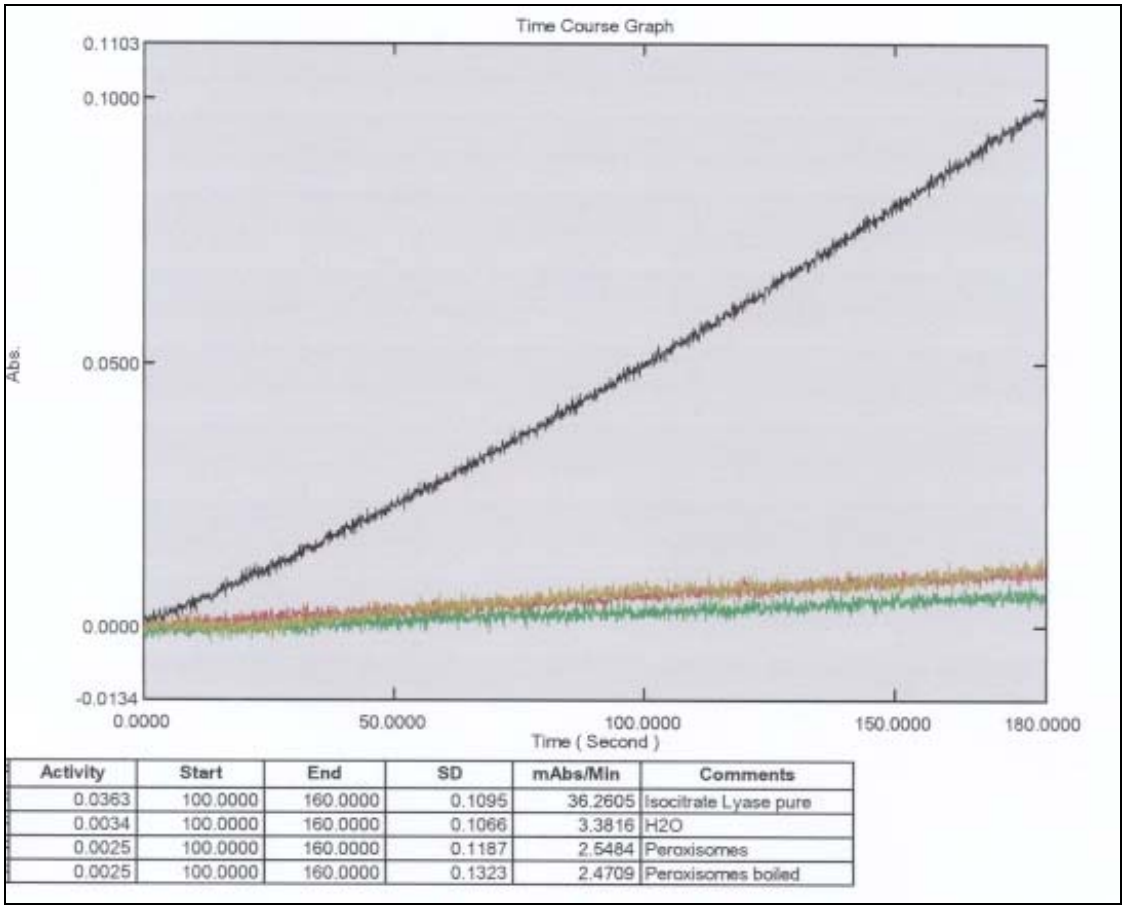

Activity	Start	End	SD	mAbs/Min	Comments
0.0363	100.0000	160.0000	0.1095	36.2605	Isocitrate Lyase pure
0.0034	100.0000	160.0000	0.1066	3.3816	H2O
0.0025	100.0000	160.0000	0.1187	2.5484	Peroxisomes
0.0025	100.0000	160.0000	0.1323	2.4709	Peroxisomes boiled

Figure 15: Marker enzyme assays on isolated peroxisome fractions obtained using a sucrose percoll gradient.
The activities for the enzymes (A) catalase, (B) fumarase and (C) isocitrate lyase were obtained from isolated peroxisomes using 2.5 g Col-0 leaf tissue. The activities are displayed in absorption over time. A: The absorbance was measured at a wavelength of 240 nm for 240 seconds. B: The absorbance was measured at a wavelength of 240 nm for 240 seconds. C: The absorbance was measured at wavelength of 324 nm for 180 seconds. Each assay included commercially available enzyme preparations as a positive control as well as boiled peroxisome samples and water as negative activity controls.

3.2.5 Isolation of peroxisomes from transgenic *Arabidopsis thaliana* carrying an overexpressed tagged BZL gene

In order to locate transgenic BZL to the peroxisomes via a 5' fused foreign HA-tag, the peroxisomes had to be isolated from transgenic *Arabidopsis thaliana* Col-0 plants carrying the fusion product HA-tag-At1g65880 or HA-tag-At1g65890.

Seedlings approximately two weeks of age from the two individual transgenic lines per construct and from Col-0 were chosen for the isolation of the peroxisomes. 2.5, 5 and

10 g of seedling material failed to yield a visible yellowish band of peroxisomes at the sucrose/percoll surface as previously observed in section 3.2.4 (figure 14). Therefore, it was deemed necessary to repeat the assay with mature 4 to 6 weeks old plants. Due to problems arising from herbivore infestation and time constraints, the experiment could not be completed.

3.3 Results of the At1g65890 promoter activity time course

Despite available expression data which suggests that the *A. thaliana* gene At1g65890 is most highly expressed in embryonic tissue (Zimmermann et al., 2004), its actual spatial and temporal expression pattern and its function in plant metabolism is not known. At1g65890 is closely related to the *A. thaliana* gene At1g65880, which was shown to play an important role in seed-specific accumulation of benzoyl-oxyglucosinolates (Kliebenstein et al., 2007). The two genes are tandemly duplicated having >90 % nucleotide sequence identity and they are members of the superfamily of acyl-activating enzymes (AAE; (Shockey et al., 2003)). Furthermore, At1g65890, as well as At1g65880, was shown to be an active BZL ((Kliebenstein et al., 2007); unpublished data).

A promoter::GUS fusion experiment was chosen to obtain a better understanding of the potential sites of spatial and temporal expression of the At1g65890 in the development of an *A. thaliana* plant.

The 5'-flanking promoter region of the At1g65890 gene was used to construct a chimeric fusion with the GUS reporter gene. The sequence of the At1g65890 promoter is shown in the appendix. Using the Gateway® Cloning system (see 2.2.1.5) the construct was designed in such a way that the promoter's +1 site was retained with that of the ATG of the GUS reporter. After amplification in *E. coli* and sequencing to select for clones without sequence errors, *A. thaliana* Col-0 plants were transformed with a chimeric At1g65890 promoter::GUS gene fusion construct using the *Agrobacterium tumefaciens* system (see 2.2.2.2). I kindly received *A. thaliana* Col-0 seeds already transformed with the At1g65890 promoter::GUS gene fusion construct from John D'Auria. The seeds were of the T2-generation. Therefore, I screened the transgenic T2-seeds (growing to T3 plants) for homozygosity. The seeds were sterilized, planted on BASTA

containing MS plates and evaluated for their ratio of dead plants to green healthy plants (see 2.2.2.3 and 2.2.2.4). Only seeds of transgenic At1g65890 promoter::GUS lines having all green seedlings in the T3 generation were used. Seeds of three homozygous lines were sterilized and planted onto BASTA containing MS plates. To synchronize germination the seeds were incubated at 4 °C for two days. The incubation time was counted as day 0 and the day of transferring the plants into a growth chamber was counted as day 1 for purposes of this time course. Samples for the time course were taken every two days starting from day 0 (untreated seeds) and proceeded to day 22 (approximately 20 seeds, 10-15 plantlets). In addition, a subset of plate grown seedlings were transferred into soil at the age of two weeks (for plant growth conditions see 2.2.2.1) and used for GUS staining after 31 days. Col-0 seeds/plants were raised under identical conditions and used as a negative control. Plant tissue samples (seeds, seedlings, or plants, respectively) were incubated in GUS staining solution for 4 h to detect tissue specific constitutive promoter activity (see 2.2.2.5).

All three transgenic lines harbouring the At1g65890 promoter::GUS gene fusion construct showed a consistent pattern of GUS staining during the time course. Although, the intensity of the staining was relatively variable among the three lines, the patterns of the reporter gene activity remained the same. The Col-0 controls, exhibited either no staining or a faint blue background in all tissues.

During the time course and the development of the plant, the pattern of GUS activity changed. Day 0-seeds and germinating day 2-seeds as well as day 2-embryos are displayed in figure 16A and B. No GUS activity was detectable during day 0 and day 2. Due to difficulties with focusing on the embryo inside intact seeds, some seed coats were mechanically sheared and the embryos were released by smashing the whole seeds between two glass slides. The tissue of the embryos was very dense and made light penetration and subsequent documentation difficult.

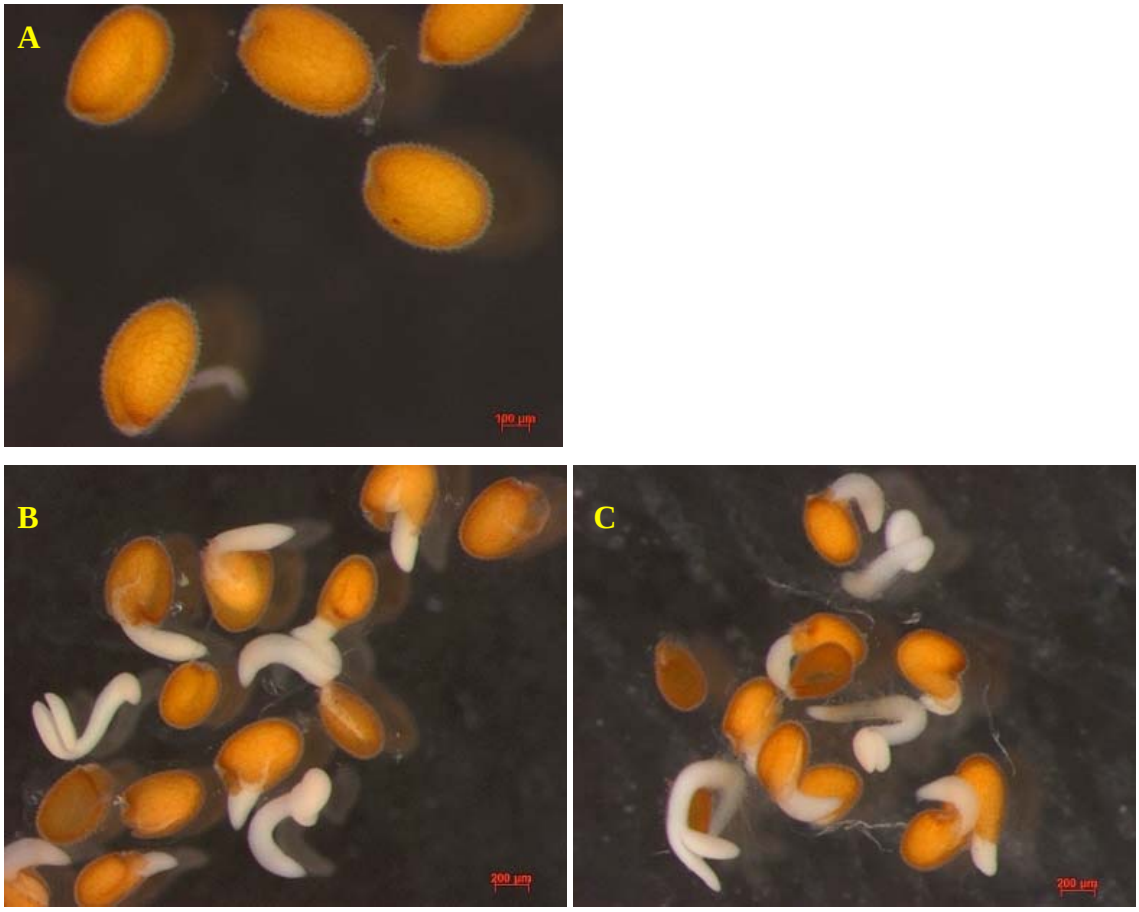

Figure 16: Histochemical analysis of At1g65890 promoter::gusA gene fusion expression.
A: mature transgenic seeds and B: 2 day old germinating transgenic seeds, and C: 2 day old untransformed germinating Col-0 seeds. B and C: Some seedlings were released of their seed coats by mechanical shearing. The samples were stained for 4 h.
(Magnification/scale bar: A: 6.6 x/100 µm; B: and C: 4 x/200 µm)

GUS activity was detected for the first time at day 4 post-germination. Two well stained transgenic seedlings plus the day 4 Col-0 control are shown in the figure 17. Seedlings of the transgenic lines were stained blue at the lower part of the hypocotyls. Additionally, some primary roots showed a pattern of blocked staining, which developed stronger later during the time course.

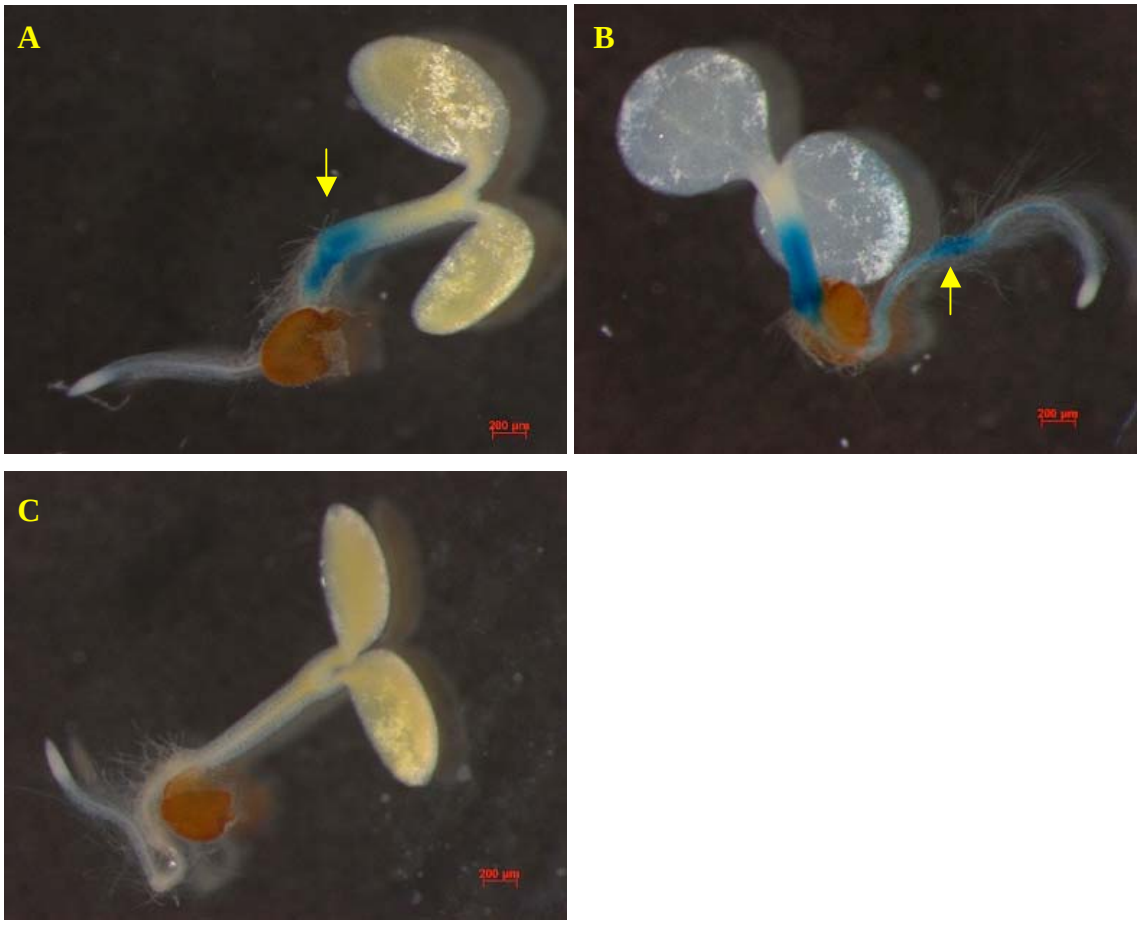

Figure 17: Histochemical analysis of At1g65890 promoter::gusA gene fusion expression.
A: and B: 4 day old seedlings, and C: 4 day old untransformed Col-0 seedlings. The samples were stained for 4 h. A and B: Arrows are pointing to the stained parts of the transgenic seedlings which consist of the lower hypocotyl and parts of the root.
(Magnification/scale bar: A, B and C: 4 x/200 µm)

The observed staining pattern of day 4 transgenic seedlings remained the same for the day 6 seedlings. Stained transgenic seedlings of day 6 plus the unstained Col-0 control are shown in the figures 18A, B and C. The base or lower parts of the hypocotyls were stained as well as the elongation zone of the primary root. The staining pattern of the roots in some day 6 seedlings showed an intermittent striped pattern with zones of more intense colour interspersed by zones with weak or no colour at all, while the root tip including the root meristem, elongation and specialization zone were devoid of signal. Furthermore, petioles of both the cotyledons and the base of developing primary leaves exhibited GUS activity.

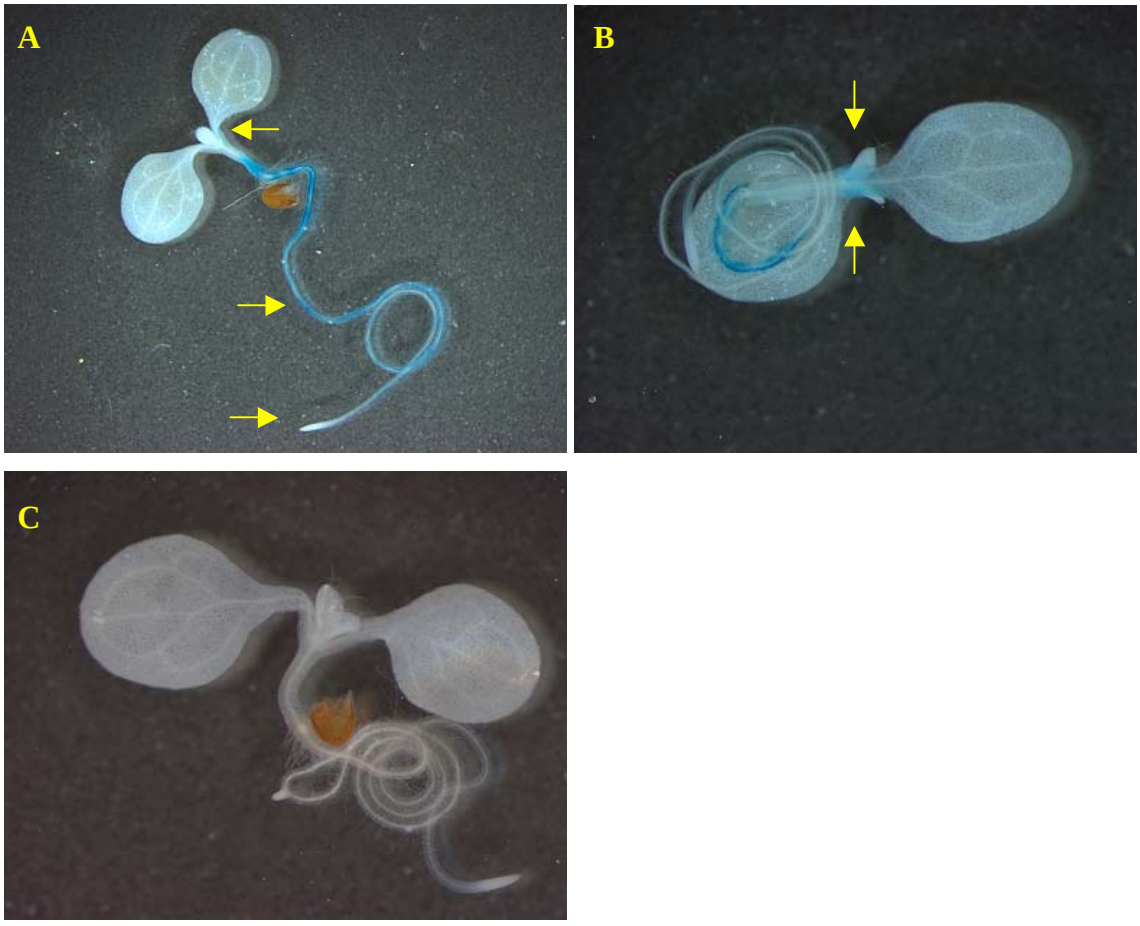

Figure 18: Histochemical analysis of At1g65890 promoter::gusA gene fusion expression.
A and B: 6 day old seedlings, and C: 6 day old untransformed Col-0 seedlings. The samples were stained for 4 h. A: Arrows are pointing to a stained petiole of a cotyledon and to the striped GUS-pattern of primary root with an unstained root tip. B: Arrows are pointing to the stained petioles of the cotyledons and the stained lower part of the developing primary leaves. (Magnification: A: 1.2 x; B and C: 2.5 x)

The staining patterns observed at day 6 post-germination persisted throughout the time course. All findings from day 8 until day 22 plus day 31 are summarized in figure 19 and figure 20. The largest difference observed as the plants matured was the loss of dark staining at the base of the hypocotyl. The blocked staining in the root persisted along with the development of a striped pattern as lateral root formation progressed. Additional staining patterns became apparent in the newly developing tissue of the inflorescences. Blue staining was found at the base of cauline leaves and at the abscission zones of flowers and siliques. Roots of 31 day old plants could not be observed due to the damage which occurred whilst trying to free the mature plants from the soil.

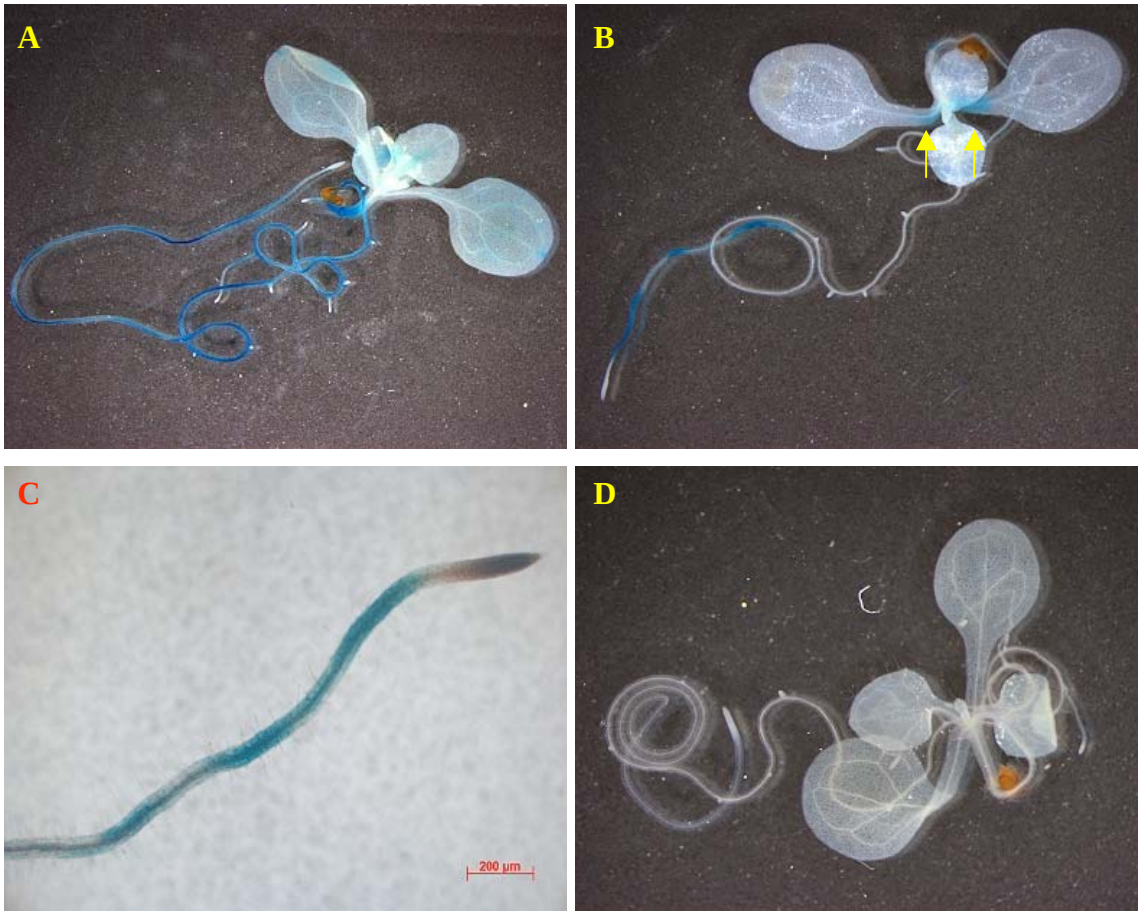

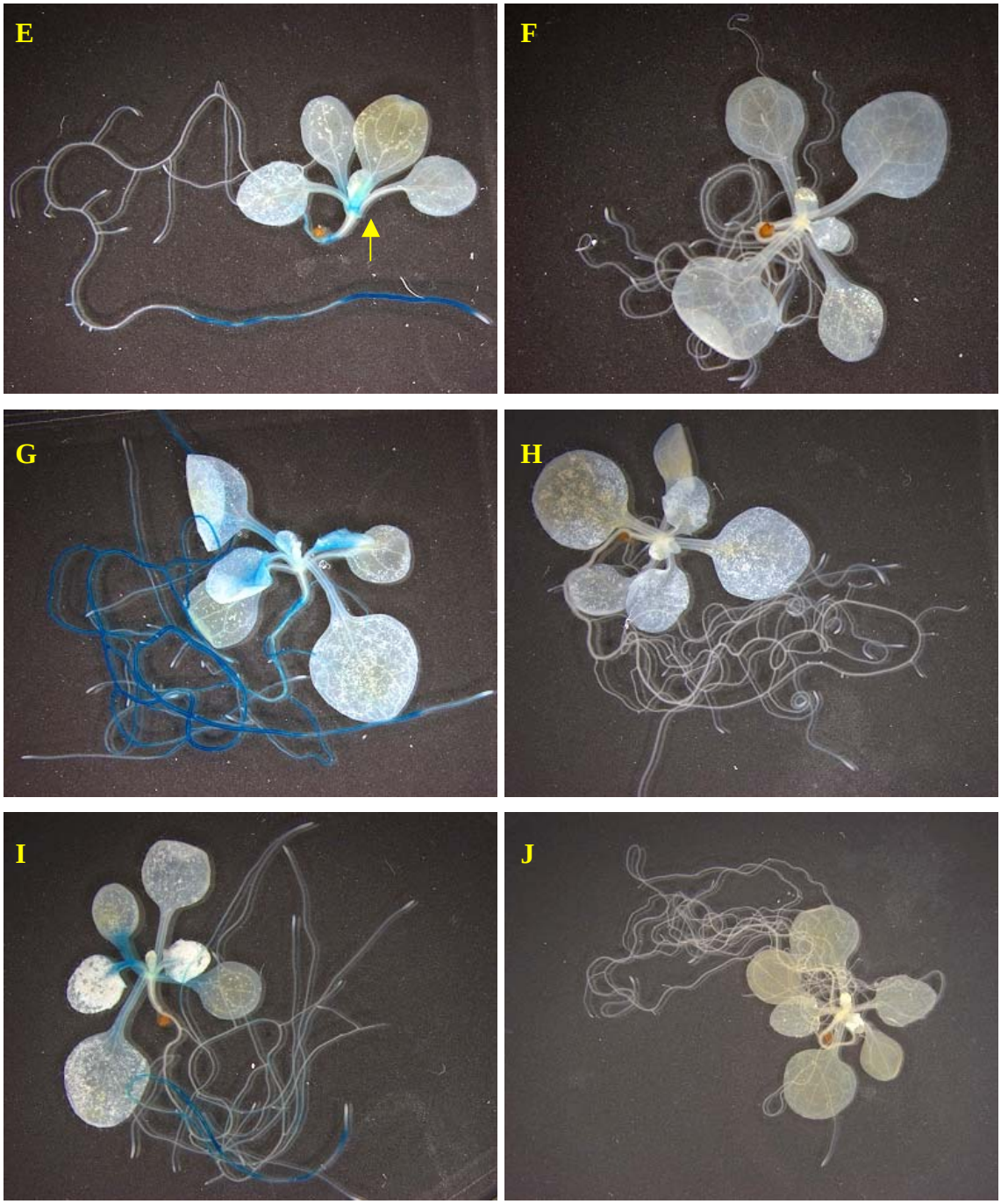
E
F
G
H
I
J

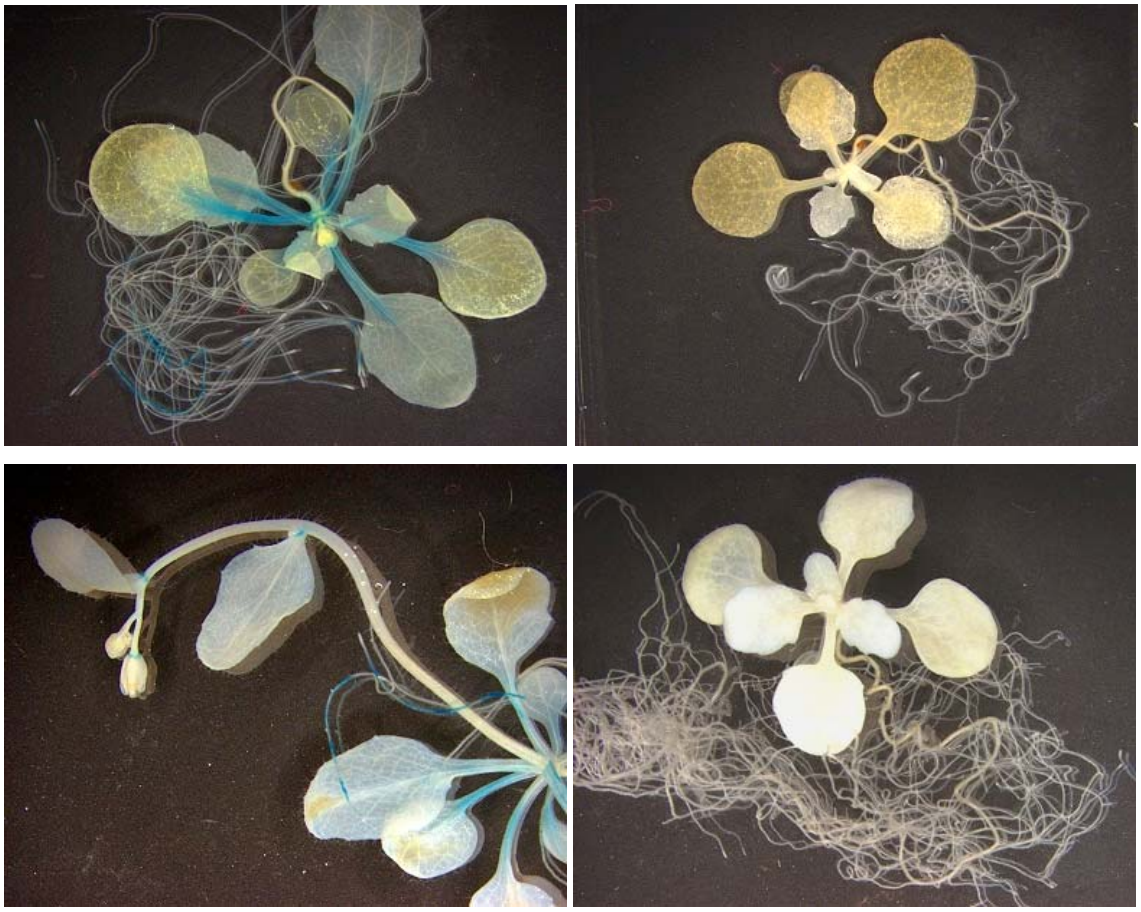

Figure 19: Histochemical analysis of At1g65890 promoter::gusA gene fusion expression in transgenic plants of different developing stages and of untransformed Col-0 controls.
The samples were stained for 4 h. A to C: 8 day old transgenic plants, C: close-up of the primary root and D: 8 day old Col-0 control; E: 10 day old transgenic plants and F: 10 day old Col-0 control; G: 12 day old transgenic plants and H: 12 day old Col-0 control; I: 14 day old transgenic plant and J: 14 day old Col-0 control; K: 16 day old transgenic plant and L: 16 day old Col-0 control; M: 22 day old transgenic plant and N: 22 day old Col-0 control. Arrows mark GUS staining at: B and E: Petioles; M: Abscission sites of flowers and the base of cauline leaves.
(Magnification: 0.6 x: I to N; 0.8 x: E, G and H; 1 x: A and F; 1.2 x: B; 1.6 x: C; 4 x: D; scale bar C: 200 µm)

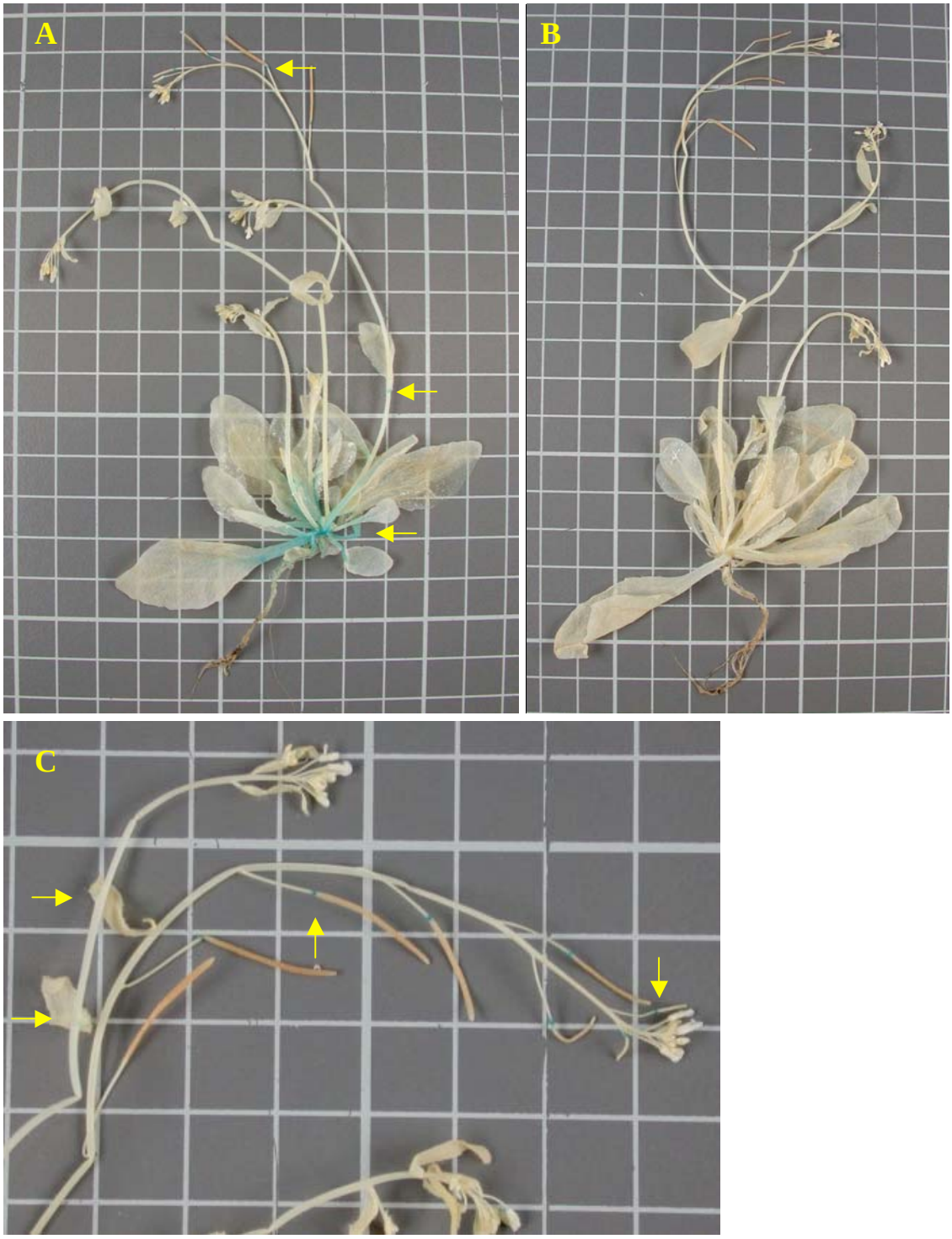
A
B
C

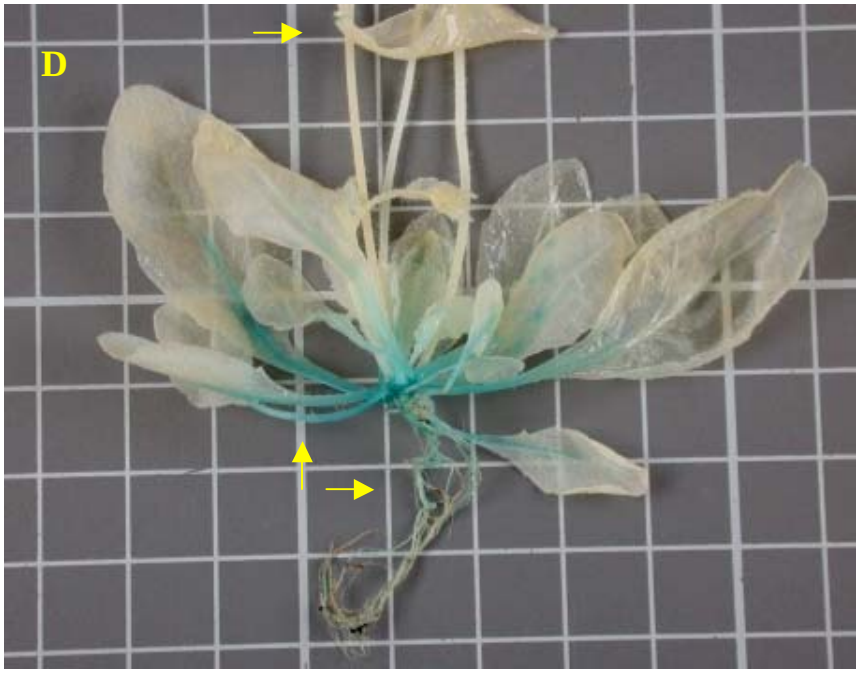

Figure 20: Histochemical analysis of At1g65890 promoter::gusA gene fusion expression in 31 day old transgenic plants and of a 31 day untransformed Col-0 control plant.
The samples were stained for 4 h. A: Whole transgenic plant. B: Whole Col-0 control. C: A close-up of the inflorescence of a transgenic plant. D: A close-up of the rosette leaves of a transgenic plant. Arrows mark stained tissue: Petiole, root, and the abscission sites of cauline leaves and siliques.
(A square displays 1 cm^2)

Tissue from 31 day old plants was dissected from the plant and visualized according to their tissue types (figure 21). GUS staining was apparent at the excision sites in addition to the normal patterns observed for non-wounded or non-dissected plants.

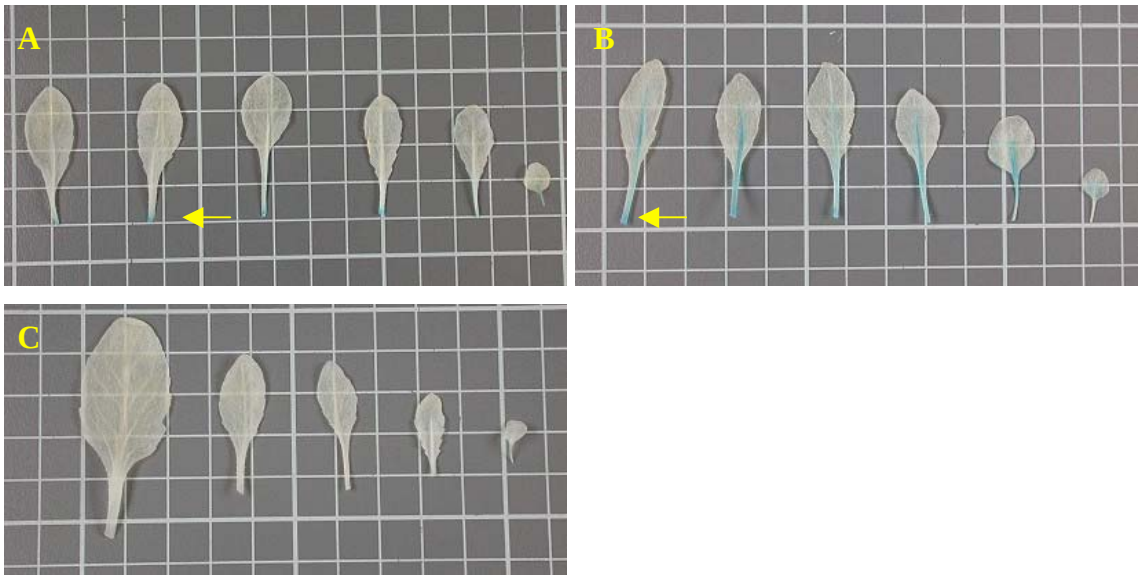

Figure 21: Histochemical analysis of At1g65890 promoter::gusA gene fusion expression in 31 day old transgenic leaves and of 31 day old untransformed Col-0 control leaves.
Leaves were ripped of the plants and stained for 4 h. A and B: Leaves of transgenic plants. Arrows mark GUS activity at the excision sites. C: Leaves of the Col-0 control.
(A square displays 1 cm^2)

4 Discussion

The aim of the present diploma work was to test the hypothesis that benzonate:CoA ligases (BZL) in plants are localized to the peroxisomes. The hypothesis was founded upon the analysis of two genes in *Arabidopsis thaliana*, At1g65880 and At1g65890, that have been shown to function as BZLs ((Kliebenstein et al., 2007); unpublished data by John D'Auria) and exhibit a carboxyl-terminal potential PTS1 of the type SRL (Gould et al., 1987; Gould et al., 1989; Reumann, 2004). The localisation to the peroxisomes was further strengthened by subcellular prediction programs (PSORT, (Nakai and Horton, 1999); TargetP, (Emanuelsson et al., 2000); and AraPerox, (Reumann et al., 2004)). The prediction by such programs can only be used as preliminary evidence due to the lack of knowledge which still surrounds the necessary and sufficient signals that target proteins to the peroxisomes. Demonstration of the proper targeting of plant BZL to the peroxisomes would provide evidence for the potential role of the *β*-oxidative like pathway of bezenoid biosynthesis in plants (see figure 1; (Boatright et al., 2004)).

4.1 At1g65890 promoter activity time course

The At1g65890 gene is a member of the large superfamily of acyl-activating enzymes (AAEs) in *Arabidopsis thaliana* (Shockey et al., 2003). Enzymes of this superfamily contain an AMP-binding motif and activate their respective carboxylic acid substrates with Coenzyme A through pyrophosphorylysis of ATP. At1g65890 belongs to an undescribed subclade consisting of 14-members. The members which consist of clade VI are more closely related to those enzymes which have been biochemically shown to be long-chain acyl-CoA synthetase (LACS) enzymes. In addition to the LACS family, members of clade VI share some similarity with known members of the 4-coumarate:CoA ligases (4CL). Recently, the function of At1g65880 a member of clade VI was biochemically determined. At1g65880 shares > 90 % nucleotide sequence identity with At1g65890. Furthermore, this gene was shown to play a significant role in the seed-specific accumulation of benzoyloxyglucosinolates by acting as a BZL enzyme (Kliebenstein et al., 2007). At1g56890 is also capable of producing benzoyl-CoA when

tested *in vitro* (unpublished data by John D'Auria). A disabled At1g65880 gene yields a chemotype in the seeds in which 3- and 4-benzoyloxyglucosinolates are completely missing. In contrast, the T-DNA insertion line GABI_751B10 with a disruption of the adjacent At1g65890 does not show any obvious phenotypic effects. Expression data suggests that seeds are the tissue type with the highest expression of one or both genes (Zimmermann et al., 2004); however, affimetrix microarrays may not be able to differentiate between At1g65880 and At1g65890 due to their high sequence similarities. Therefore, the function of the At1g65890 in plant metabolism remains unclear.

A promoter::*β*-glucuronidase (GUS) reporter gene assay was chosen as a valuable tool to detect the potential sites of spatial and temporal expression of the At1g65890 gene during the development of *A. thaliana*. The sites where At1g65890 is expressed might provide insight into the specific function At1g65890 plays within the plants metabolism. *A. thaliana* ecotype Col-0 plants transformed with a chimeric At1g65890 promoter::GUS fusion construct were used in a time course experiment testing plants for GUS staining every two days post-germination starting at day 0 (untreated seeds) up to day 22. In addition, plants aged 31 days post-germination were also tested for GUS staining. Only plants containing a single insert and were segregating as homozygous for the transgene were studied. Transgenic constructs might be expressed differently due to the chromosomal environment around the insertion event, leading to spurious and inconsistent results. High expression of the GUS gene as a result of several insertion events can cause the blue stain to diffuse through the tissue and into sites where it is actually not expressed.

A total of three independent homozygous At1g65890 promoter::GUS lines were tested and revealed qualitatively similar patterns of expression. The intensity of the staining between the three lines was often variable. These differences in GUS activity among independent lines transformed with the same chimeric promoter::GUS fusion construct can be explained by the 'position effect'. T-DNA is mostly randomly integrated into the plant's genome. As a result of the position and the chromosomal environment the activity of the chimeric promoter::GUS fusion construct can be influenced either positively or negatively (Dean et al., 1988). The slight differences observed in GUS activity among one transgenic line can be explained by the phenomena that transgenic plants occasionally inactivate transgenes (Matzke and Matzke, 1995). Testing different inde-

pendently transformed lines ensures a correct interpretation of the GUS activity pattern when that pattern remains consistent between the lines.

A GUS activity pattern completely different from the known activity of At1g65880 was found for the At1g65890 promoter. While At1g65880 has exclusively high expression in embryonic tissue, no At1g65890 promoter::GUS activity was detected in transgenic seeds and 2 day old germinating seeds (figure 16). Instead, high At1g65890 promoter::GUS activity was found in other tissues following germination and later on during the plant's development. Therefore, it can be established that At1g65890 has different expression patterns when compared with the expression of At1g65880.

The earliest GUS expression was seen in the lower part of the hypocotyl of day 4-seedlings (see figure 17). In addition, a blocked staining pattern of the fully differentiated part of the primary root was observed. The root tip, including the meristematic, elongation, and specialization zones were devoid of GUS activity. In addition, there was also an absence of GUS activity in the root hairs. This root pattern of intermittent blocked staining was observed throughout the entire time course (figure 17 to 20 and figure 19C). The lateral roots also developed this pattern during day 8 post-germination (figure 19A and G). No distinct zones were identified which might delineate the tissue types responsible for the intermittent pattern of GUS staining observed. For example, the junctions between the lateral root and the primary root were inconsistently stained and no obvious pattern was found. GUS staining was also found in the petioles as early as day 6 post-germination (see figure 18A, figure 19B, E and K, and figure 20D). Inflorescences developed strong GUS staining at the base of cauline leaves and in the abscission zone of flowers and immature siliques (see figures 19M and 20D). Tissue of dividing cell types (meristems) never showed any staining indicating no involvement of the At1g65890 gene in processes in actively differentiating cells. No distinct relationships were established for the deduced function between the different sites that showed GUS activity in the time course. An exhaustive search of the literature did not reveal any examples in which similar patterns of GUS expression were observed with other genes that were observed with At1g65890.

GUS activity in our lines was observed in the abscission zones of flowers and siliques during inflorescence development. Abscission zones are anatomically distinct bands of cells for the abscission of organ systems such as petals, sepals, and stamens (Addicott, 1982; Bleecker and Patterson, 1997). At1g65890 may be involved in the processes of

protecting wound surfaces which appear in the abscission zones following the shedding of organs. We also observed high At1g65890 promoter::GUS activity at the excision sites of dissected plant organs (figure 21). The phytohormone jasmonic acid is known for its impact on induction of defence related genes due to elicitor- and wound-induced responses (Wallis and Browse, 2002; Devoto and Turner, 2004; Li et al., 2004). JA is also considered to be involved in abscission processes as a signal hormone during the induction of plant defence (Kubigsteltig et al., 1999). The biosynthesis of JA terminates in three cycles of β-oxidation in the peroxisomes (Sanders et al., 2000; Stintzi and Browse, 2000; Schaller, 2001; Weber, 2002). In contrast to all other steps of JA biosynthesis, enzymes participating in these peroxisomal β-oxidation reactions of JA precursors have not been established. Emerging evidence indicates that plant peroxisomes are involved in a diverse array of plant defensive functions ranging from protection against herbivous insects as well as pathogen attack and that several *A. thaliana* proteins with putative PTS are involved in these defensive mechanisms. It is believed that peroxisomal biosynthetic and possibly catabolic reactions of aromatic and cyclic plant hormones are involved (Reumann, 2004; Reumann et al., 2004; Taler et al., 2004; Koh et al., 2005; Lipka et al., 2005). Such proteins that are hypothesized to function in the biosynthetic β-oxidation of plant hormones by activating their substrates to their corresponding CoA derivates are peroxisomal AAEs (Staswick et al., 2002; Shockey et al., 2003). At1g65890 as a member of the AAEs possesses a potential major PTS1 (Gould et al., 1987; Gould et al., 1989; Reumann, 2004) and was targeted to peroxisomes by subcellular prediction programs. Therefore, At1g65890 could be one of the candidate AAEs with a role in the biosynthetic β-oxidation of aromatic and cyclic plant hormones such as JA, auxin, and salicylic acid (SA). A connection between an up-regulation of the At1g65890 gene with phytohormones could be tested by GUS assays or quantitative RT-PCR with a hormonal treatment (JA, SA and auxin) of the plants.

Alternatively, the At1g65890 gene may be involved in the accumulation of protective secondary metabolites such as benzoyloxyglucosinolates (Reichelt et al., 2002). This would be in agreement with the function of At1g65880, the tandemly duclicated gene which provides benzoyl-CoA for the accumulation of seed specific 3- and 4-benzoyloxyglucosinolates. At1g65890 if functioning as an active BZL might provide benzoyl-CoA for the accumulation of non-seed specific benzoyloxyglucosinolates or other benzenoid derived secondary metabolites (D'Auria and Gershenzon, 2005).

It is also a possibility that At1g65890 has a redundant function in the metabolism of *A. thaliana* ecotype Col-0. Firstly, the high nucleotide sequence identity between At1g65880 and At1g65890 indicates that a gene duplication event has recently occurred. While At1g65880 has a distinct metabolic function, it could be that the tissues in which At1g65890 is expressed do not require activated benzenoid compounds. This would explain why no clear phenotype has yet to be identified for plant lines harbouring a T-DNA insertion within At1g65890. The evolution of enzymes involved in plant secondary metabolism need not begin immediately with the appearance of a new biochemical activity. Spatial and temporal changes in a gene's expression may also lead to the evolution of new biochemical functions for genes and the enzymes they encode (Pichersky and Gang, 2000). In addition, it may be that the function of At1g65890 may only be observed in another ecotype of *A. thaliana*. It may be that Col-0 may not actually have the metabolic machinery to utilize the products supplied by the At1g65890 enzyme. It is well known that chemotype differences exist between ecotypes. What is now required is a more in depth study which spans multiple *A. thaliana* ecotypes and focusses on the chemical analysis of those tissues which were identified as having high At1g65890 promoter activity.

4.2 Mutant Complementation

The question posed during the course of this particular experiment was whether plant BZLs are peroxisomal targeted and whether the function of a plant BZL is required to be localized to the peroxisomes. Therefore, an experiment was devised to observe whether several different putative BZL genes could rescue a known BZL phenotype in plants. Several of these genes had previously been shown to be active BZL enzymes in *in vitro* assays. In addition, some of the enzymes contained putative PTS1 signal peptides. The working hypothesis of this experiment was that only those BZL enzymes with PTS1 signal peptides would be able to complement the mutant phenotype, whereas the others, due to the lack of a PTS1 signal would be unable to complement.

The commercially available T-DNA insertion lines Salk_094196 (Alonso et al., 2003) and GABI_565B09 (Rosso et al., 2003) were chosen as host plant systems in the experiment. The two lines have a disabled *A. thaliana* Col-0 At1g65880 gene that as men-

tioned earlier was established to encode a functional BZL which provides bonzoyl-CoA for the seed-specific production of benzoyloxyglucosinolates. The At1g65880-BZL exhibits the tripeptide SRL indicaticng a potential PTS1 site at its carboxyl-terminal end and is believed to function in phenylpropanoid metabolism. Due to the functional loss of the At1g65880-BZL, the two knockout lines lack the production of 3- and 4-benzoyloxyglucosinolate in embryonic tissue what becomes apparent in HPLC-based analysis of the glucosinolate content of the seeds (figure 6b and c). The At1g65880 promoter was chosen to yield seed specific expression of the transgenes.

The first chimeric construct expressed by the At1g65880 promoter in transgenic knock-out lines, was the native *A. thaliana* Col-0 At1g65880 gene itself. It was assumed that introducing the At1g65880 gene back into the knockout lines would rescue the phenotype as the integrated gene substitutes the function of the disrupted gene. And indeed HPLC-DAD analysis revealed the production of 3- and 4-benzoyloxyglucosinolates in the transgenic seeds (figure 6d).

The second chimeric construct that was chosen to investigate the potential of a BZL containing a potential PTS1 to rescue the knockout phenotype, was the *A. thaliana* Col-0 At1g65890 gene expressed by the At1g65880 promoter. At1g65890 also encodes an active BZL exhibiting the potential PTS1 SRL, but with no known metabolic function in the plant (see above). Therefore, it was assumed that At1g65890 can substitute the function of the disrupted At1g65880 as well. Unexpectedly, 3- and 4-benzoyloxyglucosinolates were either not found at all in the transgenic seeds of the At1g65890-lines or only found in trace levels (figure 6e).

A third chimeric construct was designed with a putative BZL gene from *Clarkia breweri* (Cbr1_N01). Since a BZL was partially purified and characterized from *Clarkia breweri* flowers (Beuerle and Pichersky, 2002) the database was searched by sequence homology using the *A. thaliana* At1g65890 and At1g65890 genes. The homology search revealed a gene of 59 % amino acid sequence identity also exhibiting a carboxyl-terminal SRL. The cDNA of the potential *Clarkia breweri* BZL was fused downstream to the At1g65880 promoter for seed-specific expression and introduced in the genomes of the two T-DNA insertion lines. Because of the high sequence identity, the knowledge of the existence of a BZL activity in *Clarkia breweri*, and the presence of a potential PTS1, the potential Cbr1_N01-BZL gene was assumed to rescue the mutant phenotype. HPLC-DAD analysis of the glucosinolate content of the transgenic

seeds revealed with the production of wildtype amounts of both 3- and 4-benzoyloxyglucosinolates (figure 6a and f).

The fourth chimeric gene fusion construct contained a putative BZL from *Petunia hybrida* (Petunia BZL), which also was found through sequence homology search using the *A. thaliana* At1g65890 and At1g65890 genes. Petunia has been a useful model organism for studies on the biochemistry and enzymology of the floral scent (Negre et al., 2003; Boatright et al., 2004; Orlova et al., 2006). As a result of this research, biosynthetic pathways leading to some benzenoid compounds in petunia were proposed (see figure 1; (Boatright et al., 2004)). It was determined that both the oxidative and non-oxidative pathways of benzoic acid biosynthesis exist in petunia flowers. This therefore became the reason to search the Petunia flower database for a potential BZL. Interestingly, a putative BZL similar to those in *A. thaliana* was identified. However, this particular gene encoded an enzyme without any identifiable PTS1. Because of the lack of an obvious peroxisomal targeting signal it was assumed that no substitution of the disrupted At1g65880 gene can be derived through the introduction of the putative Petunia BZL in the mutant backgrounds. In fact, the HPLC-spectrum of the transgenic Petunia BZL-seeds revealed no differences compared to that of the Salk_094196 and GABI_565B09 (figure 6a, b and g).

A BZL gene for the fifth chimeric gene fusion construct was taken from the bacteria *Rhodopseudomonas palustris* (*R. palustris* BZL). The gene *badA* from *R. palustris* catalyzes the esterification of BA with CoA during the anaerobic growth of the bacterium on benzoate (Egland et al., 1995). As a functionally active BZL, the *R. palustris badA* gene has the potential to substitute the function of the knocked out *A. thaliana* BZL, but due to a missing known peroxisomal targeting signal no rescuing to a Col-0 phenotype was expected. If the *badA* gene would function for the disrupted At1g65880 gene in the transgenic lines, this would provide strong evidence for the capability of this BZL in the cytosol and provide evidence that it is not necessary to have a peroxisomal targeted BZL. The spectrum of transgenic *R. palustris* BZL-seeds were identical to that of untransformed knockout mutants (figure 6h).

A last sixth chimeric gene fusion construct contained an eGFP reporter gene driven by the At1g65880 promoter. The promoter::reporter gene fusion was chosen as a negative vector control as well as a positive control as a reporter for the seed-specific expression of the At1g65880 promoter. The 3- and 4-benzoyloxyglucosinolate-free HPLC-analysis

of transgenic eGFP-seeds is shown in figure 6i and the activity of the eGFP gene in seeds is shown in figure 10. The control with eGFP demonstrated the activity of the At1g65880 promoter and revealed no background production of 3- and 4-benzoyloxyglucosinolates.

In addition to the transgenic lines made in the backgrounds of the Salk_094196 and GABI_565B09 lines, all six chimeric constructs were also integrated into the genome of *A. thaliana* ecotype Col-0. The reason to do this was to see if the constructs would induce variations in glucosinolate profiles as a result of either gene silencing or other transformation related events. The HPLC-analysis of these transgenic lines didn't indicate any changes in the glucosinolate content of the seed compared to that of untransformed Col-0 seeds. Therefore, no changes in the seed glucosinolates are expected through the transformation with the six different chimeric constructs except if they are caused by a functional BZL.

We have been able to establish that the putative BZL gene isolated from *Clarkia breweri* flowers encodes a functional BZL by rescuing the known BZL mutation in *Arabidopsis thaliana*. A BZL was partially purified from *Clarkia breweri* where it showed highest activity in sepals and petals (Beuerle and Pichersky, 2002). In flowers of this species BZL probably provides benzoyl-CoA for the formation of benzylbenzonate, a component of this species floral scent (Raguso and Pichersky, 1995; Dudareva et al., 1998a). Since *Clarkia breweri* does not contain glucosinolates or related compounds, the full rescue of the glucosinolate phenotype in the *A. thaliana* T-DNA knockout lines should be due to an epistatic gene in the pathway. This strongly argues for the role of the enzyme encoded by the Clarkia gene as a biosynthetically active BZL. There are multiple examples of secondary plant metabolites requiring BA as a biosynthetic building block and, in particular, of its activated thioester benzyol-CoA being needed for the acetyltransferase catalyzation of benzoylation (Bjorklund and Leete, 1992; Yang et al., 1997; Walker and Croteau, 2000; Graser et al., 2001). This further provides evidence for the existence of the biosynthetic pathways of the phenylpropanoid metabolism in plants (Boatright et al., 2004). Both the native At1g65880 and *C. breweri* BZL proteins posses a potential PTS1 signal. The fact that rescue was not achieved with the *R. palustris* BZL or the Petunia clone strongly suggests that peroxisomal targeting is a necessary requirement for the function of BZL in plants. A cytosolic localization for plant BZLs may also be required. However, it is not sufficient in this particular case to

have an active BZL in the cytosol. The peroxisomal targeting again provides evidence for the existence of a peroxisomal *β*-oxidative-like pathway for the production of benzoic acid derived compounds.

The results obtained from the transgenic knockout lines carrying the rescue construct with At1g65890 gene were unexpected. At1g65890 exhibits *in vitro* BZL activity as well as containing a PTS1 signal identical to At1g65880. The HPLC-DAD analysis revealed that very little rescue occurred, if at all. To test wether the lack of functional substitution is due to an inoperative chimeric construct, RT-PCR was performed. RNA of the transgene was found to be transcribed in the transgenic At1g65890-plants (figure 8B), but it can not be excluded that the transcription is on a very low level yielding little to no translated protein. Quantitative RT-PCR would provide an answer to the question of the quantity of transgenic transcript, but was not part of the current experimental plan. Another possible likelihood explaining the inability of At1g65890 to complement the knockout phenotype would be gene silencing (Flavell, 1994; Hsieh and Fire, 2000). Nothing is known about the metabolic function of the At1g65890 gene. A promoter::GUS reporter assay was included within this study to understand the activity of the At1g65890 promoter in more detail. The assay revealed that At1g65880 and At1g65890 are differentially expressed. While At1g65880 is most highly expressed in seeds, At1g65890 showed no GUS activity in embryonic tissue. That suggests that expression of At1g65890 in this particular tissue is very low or simply inactive. The GUS reporter system is often limited in its sensibility. Finding no GUS staining does not necessarily mean that transcriptional activity is absent. Therefore, At1g65890 might still be expressed in seeds of Salk_094196 and GABI_565B09 causing gene silencing to the introduced At1g65890 gene yielding in a low or completely inhibited translation. The assumption of gene silencing through an active native At1g65890 gene is further supported by the finding that At1g65880 complements the knockout phenotype but does not rescue the phenotype to wildtype levels. While Col-0 seeds had concentrations of approximately 5.44 µmol/g (± 0.26; 3BZOgls) and 16.68 µmol/g (± 2.60; 4BZOgls) and transgenic Cbr1_N01-seeds also showed comparable amounts (approximately 8.11 µmol/g (± 1.42) and 16.89 µmol/g (± 2.46)), the transgenic At1g65880-seed measured was barely half those levels (approximately 3.26 µmol/g (± 0.86) and 5.56 µmol/g (± 1.25)) (figure 7). At1g65880 and At1g65890 share a very high sequence homology. Therefore, it is a very likely that a background of native At1g65890 tran-

scription causes gene silencing to both of the tandemly duplicated genes, yielding in reduced At1g65880-protein and almost no At1g65890-protein.

Further ongoing experiments should build upon the lessons learned during this work. In particular, it would be useful to fuse a PTS1 (e.g. SRL) to the 3'-end of (potential) BZLs that do not obviously exhibit such a signal (*R. palustris* BZL and Petunia BZL). Complementation by these constructs would provide even stronger evidence for the necessity of BZL to be targeted to the peroxisomes. Conversely, the potential PTS1 could be removed from those genes that were able to rescue the phenotype (Cbr1_N01 and At1g65880). If the truncated BZL genes can not rescue the At1g65880-kockout phenotype anymore this would lead to the same assumption: The carboxyl-terminal tripeptide SRL of these genes is an active PTS necessary and sufficient to enable the function of the BZL.

4.3 The subcellular localization of Arabidopsis BZL using a density gradient

Differential and density gradient centrifugation techniques allow for the isolation of peroxisomes from other organelles based upon their density (Olsen et al., 1993; Brickner et al., 1997; Brickner and Olsen, 1998; Liepman and Olsen, 2001; Johnson and Olsen, 2003; Liepman and Olsen, 2003). Isolated peroxisomes provide the potential for further studies of peroxisomal protein content. An available basic protocol for the isolation of glyoxysomes of pumpkin cotyledons (Olsen and Harrison-Lowe, 2005) was chosen for the isolation of peroxisomes in *Arabidopsis thaliana* in this experiment. The protocol recommends its usage with minor modification on multiple plant tissues and species. For the identification of a plant BZL in the content of isolated peroxisomes, transgenic *A. thaliana* ecotype Col-0 lines constitutively overexpressing either an At1g65880 or an At1g65890 gene that contained a 5' terminal HA-tag fusion were chosen. After the isolation of the peroxisomes of the transgenic lines, the HA-tag of the fused BZLs can be detected via immunoblot analysis. Localization of the tagged BZLs in the isolated peroxisomes would provide direct evidence of the targeting of these *A thaliana* BZLs to the peroxisomes and also provide evidence for the *β*-oxidative like pathway for BA biosynthesis.

Two week old transgenic seedlings were initially chosen for the isolation of peroxisomes due to the ease of gathering large amounts of tissue in a short amount of time. In addition, seedlings are known to be rich in peroxisomes, notably glyoxysomes which are active in the β-oxidative pathway of fatty acid metabolism. The isolation of peroxisomes from seedlings was performed the same way as it was done with the initial control experiments using mature leaves of *A. thaliana* Col-0 (see 3.4.4). However, the preparation and proceeding density gradient centrifugation did not yield a visible yellowish band of peroxisomes at the sucrose/percoll interface. According to the protocol, peroxisomes leave a visible yellowish band at the sucrose/percoll interface when successfully separated. Such a yellowish band was obtained after using Col-0 leaf tissue (figure 14). Therefore, it was assumed that peroxisomes were not successfully isolated from the transgenic seedlings. *A. thaliana* peroxisomes show an extreme fragility in aqueous extracts probably due to the high concentration of secondary metabolites which have organelle-destabilizing effects. Furthermore, it is known that peroxisomes in *Brassicaceae* physically associate with chloroplasts and mitochondria, making it even harder to isolate pure peroxisomes (Reumann et al., 2007). It was decided to repeat the assay with mature leaves, because the isolation of peroxisomes from leaf tissue had previously yielded positive results. Unfortunately, the plants grown for the assay became infected by aphids and had to be treated with anti-pest solution to avoid contamination of the growth chambers. The pest treatment caused damage to the leaves and as a result, the plants could not be used for further experimentation. At this point, the experimental time allotted for the diplom work had run out and further experiments were cancelled.

I am confident that given the extra time this part of the project would have yielded interesting results. All controls performed prior to the actual assay worked and therefore gave positive indications for successful ongoing experiments. The isolation of peroxisomes from mature leaves of 4 to 6 week old *A. thaliana* Col-0 plants yielded positive results in that an optimal tissue amount in the range of 2.5 g (figure 14) was determined. Furthermore, the yield as well as the purity of isolated peroxisomes was confirmed with functioning marker enzyme assays. The enzymes fumarase and isocitrate lyase were chosen as markers for mitochondria and chloroplast. Neither of these enzyme activities were found within the samples of isolated peroxisomes (figure 15B and C), whereas they had activity in a control of crude leaf extract before the onset of the density gradi-

ent protocol. Catalase, a marker enzyme for isolated peroxisomes showed significant activity in the same samples (figure 15A).

Within the protocol, the step following the density gradient centrifugation which calls for the removal of sugar in the peroxisomal fraction proved to be problematic. In this step, the peroxisomal fraction was diluted in resuspension buffer and centrifuged resulting in a pellet containing the purified peroxisomes. The pellet was nearly impossible to visualize and it became evident that total loss of the peroxisomes at this step would likely occur. Additionally, the yield of peroxisome material following a single preparation is not enough to perform all necessary assays. Therefore, for future experiments it was found to be necessary to perform several preparations and pool the resulting isolated peroxisome yields.

Given the meticulous analysis of transcripts for the transgenic plants by detection of the chimeric transgenes HA-At1g65880 and HA-At1g65890 via RT-PCR (figure 11) and the sequencing of those amplified fragments, we were able to confirm that both the PTS1 and HA-tag were present. Only an actively transcribed transgenic BZL exhibiting an intact HA-tag and with the potential of peroxisomal targeting can possibly be found in isolated peroxisomes of this assay. Additionally, immunoblot assays for the detection of the HA-tagged BZL were optimized by using heterologously expressed BZL protein in conjuction with HA specific antibodies (see figure 12 and 13 in 3.2.2). HA-tag-BZLs were heterologously expressed in the *E. coli* BL21(DE3) system and were detected as clear protein bands of approximately 70 kDA with higher protein concentration (stronger bands) in the pellet samples in each case. A BZL that was purified from *Clarkia breweri* flowers had the approximately size of 59-64.5 kDa (Beuerle and Pichersky, 2002). According to the given controls I am confident that in future I would have been able to isolate peroxisomes from mature leaves of transgenic plants and to locate transgenic BZL protein in isolated peroxisomes by detecting the fused foreign HA-tag through immunoblot analysis.

4.4 Future perspectives

The classical methods reported in the literature in which peroxisomal targeting of proteins is demonstrated rely mostly on the isolation of peroxisomes and determination of

their contents via immunoblot analysis. Further approaches include the use of immunogold localization experiments or fluorescent protein fusion constructs (Olsen et al., 1993; Brickner et al., 1997; Brickner and Olsen, 1998; Johnson and Olsen, 2003; Liepman and Olsen, 2003; Orth et al., 2007). A protocol for the isolation of highly purified peroxisomes from mature *A. thaliana* leaves was recently established (Reumann et al., 2007). The highly pure peroxisomes were used to analyze the proteome by complementary gel-based and gel-free approaches to identify novel peroxisomal targeted proteins as well as novel functional PTSs. The analysis revealed multiple unknown peroxisome targeted protein providing a base for future studies. Included in this list of identified proteins were enzymes that support the emerging evidence for an important role of the leaf peroxisomes in defence against pathogens and herbivores, e.g. *β*-glucosidases and myrosinases. This may provide insights into a possible metabolic function of the At1g65890 gene since it is transcriptionally active in abscission zones of flowers and siliques and at the excision sites of dissected plant organs (discussed above). Other tools which circumvent the necessity for the isolation or fractionation of peroxisomes to study targeting processes are in development. For example, a series of fluorescent organelle markers based on well-established targeting sequences was recently generated for co-localization studies on plant cell organelles including peroxisomes (Nelson et al., 2007). The usefulness of the markers in testing predicted subcellular localizations was demonstrated by determining the intracellular distribution of three previously uncharacterized proteins. Such a marker system may be employed in future studies focusing on the roles peroxisomes play in benzoic acid biosynthesis.

5 Abstract

Despite their importance in plant secondary metabolism, surprisingly little is known about the biochemical pathways leading to the formation of simple benzenoid compounds. The enzyme benzonate:Coenzyme A ligase (BZL) catalyzes the activation of benzoic acid (BA). The identification of potential peroxisomal targeting signals (PTS) in two *A. thaliana* BZLs led to the hypothesis that the peroxisomes are an important site for benzoic acid biosynthesis. If BZL enzymes could be shown to be targeted to the peroxisomes, it would provide strong evidence for the potential role of the *β*-oxidative like pathway of benzenoid biosynthesis in plants.

Results of this present study have been able to establish that a putative BZL gene isolated from *Clarkia breweri* flowers encodes a functional BZL by rescuing a known BZL loss of function mutation in *A. thaliana*. Furthermore, it was shown that the only genes capable of rescuing the BZL knockout plants were those containing a PTS1 signal. These findings strongly suggest that peroxisomal targeting is a necessary requirement for the function of BZL in plants. A further approach for the localization of plant BZLs to the peroxisomes by differential and density gradient centrifugation techniques could not be finished due to given time limitations. However, given the present work the usefulness and expectation of yielding interesting results through this approach was shown.

A promoter::*β*-glucuronidase (GUS) reporter gene assay was chosen to detect the potential sites of spatial and temporal expression of the At1g65890 gene during the development of *A. thaliana*. The function of the At1g65890-BZL in plant metabolism is unknown. The GUS assay revealed that At1g65890 has different expression patterns when compared with the expression of its tandemly duplicated relative, At1g65880, a gene with established function in the accumulation of seed-specific benzoyloxyglucosinolates.

6 Abbreviations

880	At1g65880
890	At1g65890
AAE12	At1g65890
AMP	adenosinemonophosphate
A. thalinana	*Arabidopsis thaliana*
ATP	adenosinetriphosphate
BA	benzoic acid
BASTA	glufosinate-ammonium
bp	base pairs
BZL	benzoate:CoA ligase
BZOgls	benzyloxyglucosinolates
CA	cinnamic acid
Cbr1_N01	*Clarkia breweri* BZL gene
cDNA	copy DNA (complementary to mRNA)
CoA	acetyl coenzyme A
Col-0	Columbia-0
DMSO	dimethyl sulfoxide
DNA	deoxyribonucleic acid
dNTP	deoxynucleotide triphosphate
DTT	dithiothreitol
E. coli	*Escherischia coli*
EDTA	ethylendiamintetra acetic acid
eGFP	enhanced green fluorescent protein
EtOH	ethanol
Gent	gentamicin
GUS	*β*-glucuronidase
HPLC	High Performance Liquid Chromatography
IPTG	Isopropyl-*β*-thiogalactopyranosid
JA	jasmonic acid
Kan	kanamycin

kb	kilo base
kDa	kilo dalton
LB-agar	Luria-Bertani (broth) agar
mRNA	messenger RNA
M&S salts	Murasheege Skoog salts
NEB	New England Biolabs
PAL	phenylalanine ammonia lyase
PCR	polymerase chain reaction
Pex	peroxins
Pfu	*Pyrococcus furiosus*
Phe	phenylalanine
Pol	polymerase
Prom	promoter
PTS	peroxisomal targeting signal
Rif	rifampicin
RNA	ribonucleic acid
RNase	ribonuclease
R. pal	*Rhodopseudomonas palustris*
RT-PCR	reverse transcriptase PCR
SA	salic acid
Spec	spectinomycin
stnd	standart
Taq	*Thermophilus aquaticus*
Tim	timentin
U	Units
UV	ultraviolet
V	volts
v/v	volume per volume
WT	wild type
w/v	weight per volume

7 Literature

Addicott, F.T. (1982). Abscission. Berkeley: University of California Press.

Albertini, M., Rehling, P., Erdmann, R., Girzalsky, W., Kiel, J.A., Veenhuis, M., and Kunau, W.H. (1997). Pex14p, a peroxisomal membrane protein binding both receptors of the two PTS-dependent import pathways. Cell **89,** 83-92.

Alonso, J.M., Stepanova, A.N., Leisse, T.J., Kim, C.J., Chen, H., Shinn, P., Stevenson, D.K., Zimmerman, J., Barajas, P., Cheuk, R., Gadrinab, C., Heller, C., Jeske, A., Koesema, E., Meyers, C.C., Parker, H., Prednis, L., Ansari, Y., Choy, N., Deen, H., Geralt, M., Hazari, N., Hom, E., Karnes, M., Mulholland, C., Ndubaku, R., Schmidt, I., Guzman, P., Aguilar-Henonin, L., Schmid, M., Weigel, D., Carter, D.E., Marchand, T., Risseeuw, E., Brogden, D., Zeko, A., Crosby, W.L., Berry, C.C., and Ecker, J.R. (2003). Genome-wide insertional mutagenesis of *Arabidopsis thaliana*. Science **301,** 653-657.

Beuerle, T., and Pichersky, E. (2002). Purification and characterization of benzoate:coenzyme A ligase from *Clarkia breweri*. Arch Biochem Biophys **400,** 258-264.

Bjorklund, J.A., and Leete, E. (1992). Biosynthesis of the benzoyl moiety of cocaine from cinnamic acid via (*R*)-(+)-3-hydroxy-3-phenylpropanoic acid. Phytochemistry **31,** 3883-3887.

Bleecker, A.B., and Patterson, S.E. (1997). Last exit: senescence, abscission, and meristem arrest in Arabidopsis. Plant Cell **9,** 1169-1179.

Boatright, J., Negre, F., Chen, X., Kish, C.M., Wood, B., Peel, G., Orlova, I., Gang, D., Rhodes, D., and Dudareva, N. (2004). Understanding *in vivo* benzenoid metabolism in petunia petal tissue. Plant Physiol **135,** 1993-2011.

Bones, A.M., and Rossiter, J.T. (1996). The myrosinase–glucosinolate system, its organisation and biochemistry. Physiologia Plantarum **97,** 194-208.

Brickner, D.G., and Olsen, L.J. (1998). Nucleotide triphosphates are required for the transport of glycolate oxidase into peroxisomes. Plant Physiol **116,** 309-317.

Brickner, D.G., Harada, J.J., and Olsen, L.J. (1997). Protein transport into higher plant peroxisomes. *In vitro* import assay provides evidence for receptor involvement. Plant Physiol **113,** 1213-1221.

Brocard, C., Lametschwandtner, G., Koudelka, R., and Hartig, A. (1997). Pex14p is a member of the protein linkage map of Pex5p. Embo J **16,** 5491-5500.

Brown, P.D., Tokuhisa, J.G., Reichelt, M., and Gershenzon, J. (2003). Variation of glucosinolate accumulation among different organs and developmental stages of *Arabidopsis thaliana*. Phytochemistry **62,** 471-481.

Crookes, W.J., and Olsen, L.J. (1999). Peroxin puzzles and folded freight: peroxisomal protein import in review. Naturwissenschaften **86,** 51-61.

D'Auria, J.C., and Gershenzon, J. (2005). The secondary metabolism of Arabidopsis thaliana: growing like a weed. Curr Opin Plant Biol **8,** 308-316.

D'Auria, J.C., Chen, F., and Pichersky, E. (2002). Characterization of an acyltransferase capable of synthesizing benzylbenzoate and other volatile esters in flowers and damaged leaves of *Clarkia breweri*. Plant Physiol **130,** 466-476.

Dean, C., Jones, J., Favreau, M., Dunsmuir, P., and Bedbrook, J. (1988). Influence of flanking sequences on variability in expression levels of an introduced gene in transgenic tobacco plants. Nucleic Acids Res **16,** 9267-9283.

Devoto, A., and Turner, J.G. (2004). Jasmonate-regulated Arabidopsis stress signalling network. Physiologia Plantarum **16,** 126-143.

Dudareva, N., Raguso, R.A., Wang, J., Ross, J.R., and Pichersky, E. (1998a). Floral scent production in *Clarkia breweri*. III. Enzymatic synthesis and emission of benzenoid esters. Plant Physiol **116,** 599-604.

Dudareva, N., D'Auria, J.C., Nam, K.H., Raguso, R.A., and Pichersky, E. (1998b). Acetyl-CoA:benzylalcohol acetyltransferase--an enzyme involved in floral scent production in *Clarkia breweri*. Plant J **14,** 297-304.

Dudareva, N., Murfitt, L.M., Mann, C.J., Gorenstein, N., Kolosova, N., Kish, C.M., Bonham, C., and Wood, K. (2000). Developmental regulation of methyl benzoate biosynthesis and emission in snapdragon flowers. Plant Cell **12,** 949-961.

Egland, P.G., Gibson, J., and Harwood, C.S. (1995). Benzoate-coenzyme A ligase, encoded by *badA*, is one of three ligases able to catalyze benzoyl-coenzyme A formation during anaerobic growth of *Rhodopseudomonas palustris* on benzoate. J Bacteriol **177,** 6545-6551.

Eilers, T., Schwarz, G., Brinkmann, H., Witt, C., Richter, T., Nieder, J., Koch, B., Hille, R., Hansch, R., and Mendel, R.R. (2001). Identification and biochemical characterization of *Arabidopsis thaliana* sulfite oxidase. A new player in plant sulfur metabolism. J Biol Chem **276,** 46989-46994.

Emanuelsson, O., Nielsen, H., Brunak, S., and von Heijne, G. (2000). Predicting subcellular localization of proteins based on their N-terminal amino acid sequence. J Mol Biol **300,** 1005-1016.

Emanuelsson, O., Elofsson, A., von Heijne, G., and Cristobal, S. (2003). *In silico* prediction of the peroxisomal proteome in fungi, plants and animals. J Mol Biol **330,** 443-456.

Feussner, I., and Wasternack, C. (2002). The lipoxygenase pathway. Annu Rev Plant Biol **53,** 275-297.

Flavell, R.B. (1994). Inactivation of gene expression in plants as a consequence of specific sequence duplication. Proc Natl Acad Sci U S A **91,** 3490-3496.

Gehring, A.M., Bradley, K.A., and Walsh, C.T. (1997). Enterobactin biosynthesis in *Escherichia coli*: isochorismate lyase (EntB) is a bifunctional enzyme that is phosphopantetheinylated by EntD and then acylated by EntE using ATP and 2,3-dihydroxybenzoate. Biochemistry **36,** 8495-8503.

Glover, J.R., Andrews, D.W., Subramani, S., and Rachubinski, R.A. (1994). Mutagenesis of the amino targeting signal of *Saccharomyces cerevisiae* 3-ketoacyl-CoA thiolase reveals conserved amino acids required for import into peroxisomes *in vivo*. J Biol Chem **269,** 7558-7563.

Gould, S.G., Keller, G.A., and Subramani, S. (1987). Identification of a peroxisomal targeting signal at the carboxy terminus of firefly luciferase. J Cell Biol **105,** 2923-2931.

Gould, S.J., Keller, G.A., Hosken, N., Wilkinson, J., and Subramani, S. (1989). A conserved tripeptide sorts proteins to peroxisomes. J Cell Biol **108,** 1657-1664.

Graser, G., Oldham, N.J., Brown, P.D., Temp, U., and Gershenzon, J. (2001). The biosynthesis of benzoic acid glucosinolate esters in *Arabidopsis thaliana*. Phytochemistry **57,** 23-32.

Hsieh, J., and Fire, A. (2000). Recognition and silencing of repeated DNA. Annu Rev Genet **34,** 187-204.

Johnson, T.L., and Olsen, L.J. (2001). Building new models for peroxisome biogenesis. Plant Physiol **127,** 731-739.

Johnson, T.L., and Olsen, L.J. (2003). Import of the peroxisomal targeting signal type 2 protein 3-ketoacyl-coenzyme a thiolase into glyoxysomes. Plant Physiol **133,** 1991-1999.

Kliebenstein, D.J., D'Auria, J.C., Behere, A.S., Kim, J.H., Gunderson, K.L., Breen, J.N., Lee, G., Gershenzon, J., Last, R.L., and Jander, G. (2007). Characterization of seed-specific benzoyloxyglucosinolate mutations in *Arabidopsis thaliana*. Plant J.

Koh, S., Andre, A., Edwards, H., Ehrhardt, D., and Somerville, S. (2005). *Arabidopsis thaliana* subcellular responses to compatible *Erysiphe cichoracearum* infections. Plant J **44,** 516-529.

Komori, M., Rasmussen, S.W., Kiel, J.A., Baerends, R.J., Cregg, J.M., van der Klei, I.J., and Veenhuis, M. (1997). The Hansenula polymorpha PEX14 gene encodes a novel peroxisomal membrane protein essential for peroxisome biogenesis. Embo J **16,** 44-53.

Koo, A.J., Chung, H.S., Kobayashi, Y., and Howe, G.A. (2006). Identification of a peroxisomal acyl-activating enzyme involved in the biosynthesis of jasmonic acid in Arabidopsis. J Biol Chem **281,** 33511-33520.

Kragler, F., Lametschwandtner, G., Christmann, J., Hartig, A., and Harada, J.J. (1998). Identification and analysis of the plant peroxisomal targeting signal 1 receptor NtPEX5. Proc Natl Acad Sci U S A **95,** 13336-13341.

Kubigsteltig, I., Laudert, D., and Weiler, E.W. (1999). Structure and regulation of the *Arabidopsis thaliana* allene oxide synthase gene. Planta **208,** 463-471.

Li, L., Zhao, Y., McCaig, B.C., Wingerd, B.A., Wang, J., Whalon, M.E., Pichersky, E., and Howe, G.A. (2004). The tomato homolog of CORONATINE-INSENSITIVE1 is required for the maternal control of seed maturation, jasmonate-signaled defense responses, and glandular trichome development. Plant Cell **16,** 126-143.

Liepman, A.H., and Olsen, L.J. (2001). Peroxisomal alanine : glyoxylate aminotransferase (AGT1) is a photorespiratory enzyme with multiple substrates in *Arabidopsis thaliana*. Plant J **25,** 487-498.

Liepman, A.H., and Olsen, L.J. (2003). Alanine aminotransferase homologs catalyze the glutamate:glyoxylate aminotransferase reaction in peroxisomes of Arabidopsis. Plant Physiol **131,** 215-227.

Lipka, V., Dittgen, J., Bednarek, P., Bhat, R., Wiermer, M., Stein, M., Landtag, J., Brandt, W., Rosahl, S., Scheel, D., Llorente, F., Molina, A., Parker, J., Somerville, S., and Schulze-Lefert, P. (2005). Pre- and postinvasion defenses both contribute to nonhost resistance in Arabidopsis. Science **310,** 1180-1183.

Marzioch, M., Erdmann, R., Veenhuis, M., and Kunau, W.H. (1994). *PAS7* encodes a novel yeast member of the WD-40 protein family essential for import of 3-oxoacyl-CoA thiolase, a PTS2-containing protein, into peroxisomes. Embo J **13,** 4908-4918.

Matzke, M.A., and Matzke, A. (1995). How and why do plants inactivate homologous (trans)genes? Plant Physiol **107,** 679-685.

Murfitt, L.M., Kolosova, N., Mann, C.J., and Dudareva, N. (2000). Purification and characterization of *S*-adenosyl-*L*-methionine:benzoic acid carboxyl methyltransferase, the enzyme responsible for biosynthesis of the volatile ester methyl benzoate in flowers of *Antirrhinum majus*. Arch Biochem Biophys **382,** 145-151.

Nakai, K., and Horton, P. (1999). PSORT: a program for detecting sorting signals in proteins and predicting their subcellular localization. Trends Biochem Sci **24,** 34-36.

Nakamura, T., Meyer, C., and Sano, H. (2002). Molecular cloning and characterization of plant genes encoding novel peroxisomal molybdoenzymes of the sulphite oxidase family. J Exp Bot **53,** 1833-1836.

Negre, F., Kish, C.M., Boatright, J., Underwood, B., Shibuya, K., Wagner, C., Clark, D.G., and Dudareva, N. (2003). Regulation of methylbenzoate emission after pollination in snapdragon and petunia flowers. Plant Cell **15,** 2992-3006.

Nelson, B.K., Cai, X., and Nebenfuhr, A. (2007). A multicolored set of *in vivo* organelle markers for co-localization studies in Arabidopsis and other plants. Plant J **51,** 1126-1136.

Neuberger, G., Maurer-Stroh, S., Eisenhaber, B., Hartig, A., and Eisenhaber, F. (2003). Prediction of peroxisomal targeting signal 1 containing proteins from amino acid sequence. J Mol Biol **328,** 581-592.

Nowak, K., Luniak, N., Witt, C., Wustefeld, Y., Wachter, A., Mendel, R.R., and Hansch, R. (2004). Peroxisomal localization of sulfite oxidase separates it from chloroplast-based sulfur assimilation. Plant Cell Physiol **45,** 1889-1894.

Obel, N., and Scheller, H.V. (2000). Enzymatic synthesis and purification of caffeoyl-CoA, *p*-coumaroyl-CoA, and feruloyl-CoA. Anal Biochem **286,** 38-44.

Olsen, L.J. (1998). The surprising complexity of peroxisome biogenesis. Plant Mol Biol **38,** 163-189.

Olsen, L.J., and Harrison-Lowe, N. (2005). Isolation of glyoxysomes from pumpkin cotyledons. Current Protocols in Cell Biology**,** 3.19.11-13.19.18.

Olsen, L.J., Ettinger, W.F., Damsz, B., Matsudaira, K., Webb, M.A., and Harada, J.J. (1993). Targeting of glyoxysomal proteins to peroxisomes in leaves and roots of a higher plant. Plant Cell **5,** 941-952.

Orlova, I., Marshall-Colon, A., Schnepp, J., Wood, B., Varbanova, M., Fridman, E., Blakeslee, J.J., Peer, W.A., Murphy, A.S., Rhodes, D., Pichersky, E., and Dudareva, N. (2006). Reduction of benzenoid synthesis in petunia flowers reveals multiple pathways to benzoic acid and enhancement in auxin transport. Plant Cell **18,** 3458-3475.

Orth, T., Reumann, S., Zhang, X., Fan, J., Wenzel, D., Quan, S., and Hu, J. (2007). The PEROXIN11 protein family controls peroxisome proliferation in Arabidopsis. Plant Cell **19,** 333-350.

Petersen, B.L., Chen, S., Hansen, C.H., Olsen, C.E., and Halkier, B.A. (2002). Composition and content of glucosinolates in developing *Arabidopsis thaliana*. Planta **214,** 562-571.

Pichersky, E., and Gang, D.R. (2000). Genetics and biochemistry of secondary metabolites in plants: an evolutionary perspective. Trends Plant Sci **5,** 439-445.

Raguso, R., and Pichersky, E. (1995). Floral volatiles of *Clarkia breweri* and *C. concinna* (*Onagraceae*): recent evolution of floral aroma and moth pollination. Plant Systematics and Evolution **194,** 55-67.

Rask, L., Andreasson, E., Ekbom, B., Eriksson, S., Pontoppidan, B., and Meijer, J. (2000). Myrosinase: gene family evolution and herbivore defense in *Brassicaceae*. Plant Mol Biol **42,** 93-113.

Rehling, P., Marzioch, M., Niesen, F., Wittke, E., Veenhuis, M., and Kunau, W.H. (1996). The import receptor for the peroxisomal targeting signal 2 (PTS2) in *Saccharomyces cerevisiae* is encoded by the *PAS7* gene. Embo J **15,** 2901-2913.

Reichelt, M., Brown, P.D., Schneider, B., Oldham, N.J., Stauber, E., Tokuhisa, J., Kliebenstein, D.J., Mitchell-Olds, T., and Gershenzon, J. (2002). Benzoic acid glucosinolate esters and other glucosinolates from *Arabidopsis thaliana*. Phytochemistry **59,** 663-671.

Reumann, S. (2004). Specification of the peroxisome targeting signals type 1 and type 2 of plant peroxisomes by bioinformatics analyses. Plant Physiol **135,** 783-800.

Reumann, S., Ma, C., Lemke, S., and Babujee, L. (2004). AraPerox. A database of putative Arabidopsis proteins from plant peroxisomes. Plant Physiol **136,** 2587-2608.

Reumann, S., Babujee, L., Ma, C., Wienkoop, S., Siemsen, T., Antonicelli, G.E., Rasche, N., Luder, F., Weckwerth, W., and Jahn, O. (2007). Proteome analysis of Arabidopsis leaf peroxisomes reveals novel targeting peptides, metabolic pathways, and defense mechanisms. Plant Cell **19,** 3170-3193.

Ross, J.R., Nam, K.H., D'Auria, J.C., and Pichersky, E. (1999). *S*-Adenosyl-*L*-methionine:salicylic acid carboxyl methyltransferase, an enzyme involved in floral scent production and plant defense, represents a new class of plant methyltransferases. Arch Biochem Biophys **367,** 9-16.

Rosso, M.G., Li, Y., Strizhov, N., Reiss, B., Dekker, K., and Weisshaar, B. (2003). An *Arabidopsis thaliana* T-DNA mutagenized population (GABI-Kat) for flanking sequence tag-based reverse genetics. Plant Mol Biol **53,** 247-259.

Sanders, P.M., Lee, P.Y., Biesgen, C., Boone, J.D., Beals, T.P., Weiler, E.W., and Goldberg, R.B. (2000). The arabidopsis DELAYED DEHISCENCE1 gene encodes an enzyme in the jasmonic acid synthesis pathway. Plant Cell **12,** 1041-1061.

Schaller, F. (2001). Enzymes of the biosynthesis of octadecanoid-derived signalling molecules. J Exp Bot **52,** 11-23.

Schopfer, P., and A., B. (2006). Pflanzenphysiologie. (Spektrum Akademischer Verlag).

Serino, L., Reimmann, C., Baur, H., Beyeler, M., Visca, P., and Haas, D. (1995). Structural genes for salicylate biosynthesis from chorismate in *Pseudomonas aeruginosa*. Mol Gen Genet **249,** 217-228.

Shockey, J.M., Fulda, M.S., and Browse, J. (2003). Arabidopsis contains a large superfamily of acyl-activating enzymes. Phylogenetic and biochemical analysis reveals a new class of acyl-coenzyme a synthetases. Plant Physiol **132,** 1065-1076.

Staswick, P.E., Tiryaki, I., and Rowe, M.L. (2002). Jasmonate Response Locus *JAR1* and several related Arabidopsis genes encode enzymes of the firefly luciferase superfamily that show activity on jasmonic, salicylic, and indole-3-acetic acids in an assay for adenylation. Plant Cell **14,** 1405-1415.

Stintzi, A., and Browse, J. (2000). The Arabidopsis male-sterile mutant, opr3, lacks the 12-oxophytodienoic acid reductase required for jasmonate synthesis. Proc Natl Acad Sci U S A **97,** 10625-10630.

Strassner, J., Schaller, F., Frick, U.B., Howe, G.A., Weiler, E.W., Amrhein, N., Macheroux, P., and Schaller, A. (2002). Characterization and cDNA-microarray expression analysis of 12-oxophytodienoate reductases reveals differential roles for octadecanoid biosynthesis in the local versus the systemic wound response. Plant J **32,** 585-601.

Swinkels, B.W., Gould, S.J., Bodnar, A.G., Rachubinski, R.A., and Subramani, S. (1991). A novel, cleavable peroxisomal targeting signal at the amino-terminus of the rat 3-ketoacyl-CoA thiolase. Embo J **10,** 3255-3262.

Taler, D., Galperin, M., Benjamin, I., Cohen, Y., and Kenigsbuch, D. (2004). Plant eR genes that encode photorespiratory enzymes confer resistance against disease. Plant Cell **16,** 172-184.

Van der Leij, I., Franse, M.M., Elgersma, Y., Distel, B., and Tabak, H.F. (1993). PAS10 is a tetratricopeptide-repeat protein that is essential for the import of

most matrix proteins into peroxisomes of *Saccharomyces cerevisiae*. Proc Natl Acad Sci U S A **90,** 11782-11786.

Verleur, N., Hettema, E.H., van Roermund, C.W., Tabak, H.F., and Wanders, R.J. (1997). Transport of activated fatty acids by the peroxisomal ATP-binding-cassette transporter Pxa2 in a semi-intact yeast cell system. Eur J Biochem **249,** 657-661.

Walker, K., and Croteau, R. (2000). Taxol biosynthesis: Molecular cloning of a benzoyl- CoA:taxane 2*alpha* -*O*-benzoyltransferase cDNA from Taxus and functional expression in *Escherichia coli*. Proceedings of the National Academy of Sciences **97,** 13591-13596.

Walker, K., Schoendorf, A., and Croteau, R. (2000). Molecular cloning of a *taxa*-4(20),11(12)-dien-5*alpha*-ol-*O*-acetyl transferase cDNA from Taxus and functional expression in *Escherichia coli*. Arch Biochem Biophys **374,** 371-380.

Wallis, J.G., and Browse, J. (2002). Mutants of Arabidopsis reveal many roles for membrane lipids. Prog Lipid Res **41,** 254-278.

Wang, C.-Z., Maier, U.H., Eisenreich, W., Adam, P., Obersteiner, I., Keil, M., Bacher, A., and Zenk, M.H. (2001). Unexpected biosynthetic precursors of amarogentin — a retrobiosynthetic 13C NMR study. European Journal of Organic Chemistry **2001,** 1459-1465.

Weber, H. (2002). Fatty acid-derived signals in plants. Trends Plant Sci **7,** 217-224.

Werner, I., Bacher, A., and Eisenreich, W. (1997). Retrobiosynthetic NMR studies with 13C-labeled glucose. Formation of gallic acid in plants and fungi. J Biol Chem **272,** 25474-25482.

Wildermuth, M.C. (2006). Variations on a theme: synthesis and modification of plant benzoic acids. Curr Opin Plant Biol **9,** 288-296.

Wildermuth, M.C., Dewdney, J., Wu, G., and Ausubel, F.M. (2001). Isochorismate synthase is required to synthesize salicylic acid for plant defence. Nature **414,** 562-565.

Wimmer, C., Schmid, M., Veenhuis, M., and Gietl, C. (1998). The plant PTS1 receptor: similarities and differences to its human and yeast counterparts. Plant J **16,** 453-464.

Yang, Q., Reinhard, K., Schiltz, E., and Matern, U. (1997). Characterization and heterologous expression of hydroxycinnamoyl/benzoyl-CoA:anthranilate *N*-hydroxycinnamoyl/benzoyltransferase from elicited cell cultures of carnation, Dianthus caryophyllus L. Plant Mol Biol **35,** 777-789.

Zambryski, P., Joos, H., Genetello, C., Leemans, J., Montagu, M.V., and Schell, J. (1983). Ti plasmid vector for the introduction of DNA into plant cells without alteration of their normal regeneration capacity. Embo J **2,** 2143-2150.

Zimmermann, P., Hirsch-Hoffmann, M., Hennig, L., and Gruissem, W. (2004). GENEVESTIGATOR. Arabidopsis microarray database and analysis toolbox. Plant Physiol **136,** 2621-2632.

Zolman, B.K., Monroe-Augustus, M., Thompson, B., Hawes, J.W., Krukenberg, K.A., Matsuda, S.P., and Bartel, B. (2001). chy1, an Arabidopsis mutant with impaired *beta*-oxidation, is defective in a peroxisomal *beta*-hydroxyisobutyryl-CoA hydrolase. J Biol Chem **276,** 31037-31046.

Appendix

GATTATACAT CTCCGACTTA TAAATATGTA TGTATGGTTG TCTATTAAAG CACCTTAGCT TCATTGAAGG

TCTTAAGAGA GTCTCTCAAC AATTATGTAT GGTTGTCTAT ATATATAGTA ATGATAAAAT TGTGATTCTC

CATTGATGGA CAGTCAAAAC ATTGACCAAA GTAATCAATT ATGTACGTAG TTATTAAAAT GACATTTAAA

ATTTAAAATT TCTTACCATT TTTTATCACC CACACATTTA AACAAAAACA ATATTCTCCA ATTCATAATT

CTAGCACGGG AAACATTGAA CATATTATTA GGCAATGAGA GATTTTGATC TCGTCCAAGA TTACCGAGGA

ATTAATTATG CATGGCAATT CTGAGTTGTG ACTACCATGT TTTTTTTATT AGTCTTCTTT TATTTACATT

AATCATGTGA CTACAAAGTT GCCGTTTATC CAGTTCTAAA AGGGAGTGAA AATGAACTTA ATCAAATACC

AATATAAGCC ACGCAATTCT TGAATCTTTT CGAAGTTCAT GAAGACGAGA TTGTATCTGA AATCCTTACC

TGCGAACCAA CTGGATGTGG ATCATAATAG ATTTCAGGTT ATTTTAAAAT TTCATTTTGG TTAACCGATC

AGTTTGGATG AATCCAAAAT TGAAGTGGAT ATGGAAACTG GATGAGAAGG TAGTTACCTA AAAGTTAGGT

TTAGACCGAG TCGACTTGAA ATGAGCCGGT TCAGATATTG TAGTTCTACT TAGATCGACC AATCATTTTT

AATGCAAAAC ACAAACTCTT CAGAATAATT GACAAGTGCA AGGGACCGGT TGATGTCCAC TTGACCTTTC

GAGTTATTTA TCACTTTTTC AGAAGTCAAG TGGACATCGC CCGGCCTCTT TAGCTCGTCG ATTCTTCTCG

ATAGTTTGTG TATTTGCATT AAAATGATCG GTTGATCAGT GGAAATAGTT TATATTCATC ACCTTTTGGG

TCAGTCTTTA AGACGTTTAG TCAGTCACCT CATTTCTTCT ACAATTATCG TTGCACTTTA TCTACGCATC

AGAATATCAT AAGTTCATTA CTTTTGTCTT TACCTTTTGA TCTGCCGGTT GATATTAGTT GAAACACCGG

AAAATCTTTT TTGGTAGGAA ATTAAACATC ACTGGCTAGT TGAAACTCAA CCTCGTACTA TAGCTATCCA

AACTTCAATA AATTTTAATG GTAGGAAATT TACATCCCAC ATTATGTTTT AGACGCTTTT GTATGATCCT

ATATCATTAT TTTCTTCACT TGCATCCAAA TGAAAACCTT ACAAGATAAT AATGCTCAAA ACACAAAAGA

ATGATACACA AAGAACAAGG GGGGGGGGGG GGGGGGGGGG GGGTTGGTGG GGAGTCGAAA CAAAAGGTTG

TAAGAACATC AGTCACATCT GGATTTAAAT TTGACGGAGA AAAAGAATTT ATTTCTTAAT GATTTATGAG

TAAATAATGA TGGATACAAA TGTATGGATC AACCTTGTCG GTGAGTAACA GAGATAAAAC GTGTTCGTCC

AATTCTGTTGA AACCTGACCA CATAAAAATG TTGATAAACG TAAACGCCTA TTTATGTAG AATTAAAATT

GAGAGATTTT TTGTTAAAAA AAGTAAAGGA AGAGGACCGT TGCTATAATT TCCTTTTAAG TAATTGCCAT

AATTGAGCGA CGGATTATTT TGAATTCCCA ATTTTAGCCA TTTTTTACAT CTACTTCCGA AAAATATATG

ACTTGTTTAT TCTCATTAAT TTTCTTTATA TACTATATCG TTGCACATCC CTTTTCTCTC ACATCAACAT

TCATTTAACA CATTACACAA AGTAGAAGAA GAAGAAGAAG

Figure 22: At1g65880 promoter sequence.
The 1860 bp long At1g65880 promoter sequence is shown in 5’ to 3’ orientation.

AACGTGAAAA TAAGGTCTCG AACACCTCTT TGACGACCTC AAATGTGGAA AAAGCTTGAA TGAGTTCAAT

ACGAAATTTG AGTTGAAAGG TGATTCTACA CCGGAAAATC TTTTTTGGTT GAAACTCAAC TTCATACTAT

ACTGTCCAAA TTTCAATAAA TTTGCATGGT AAGTAAGTTT ACATCCCAGC AGATGATCTT TTAGATGCTT

TTGCATGATA ATCATATATC ATTATTTTGC TTACTTGCAT CCAAATGACA ACCAAATAAG ATAAAAAAAA

TACCCAAAAC ACAAAAGAAT GATAAGAAAA GAAAAAACTA AAGAAACAAA AAGCTGAAAT AAAAGTTATA

AGAAGGTAAA AACGAATCAT CATCAGTCAC CATCTGGATT TAAATTGACG AAAAAAATAA TTTAGCTCTG

TTGGATTTAT TGAGTAAATG AAGAGGGATA CAAACAGTAT GGATCAACCT TGTCGGTCAG TAGCTGAGAT

AAATCGTGGT TCGTGGAAAT CACTCAATTC CAAATTTTTT TGAAACCTGA CCACAAAAAA ATGTTGAGAA

GGAAAAGGAC CCTTGCAATA ATTTCCTTTC AATAATTGCA AGCGACAGAT TATTTTTATT TCCAAAATTA

GCCGCGTTTT ACATTTAGGG GTGTTCCTAT TTAATAAATT TTCATGACTT TAATAAAATC ATAGAAAAAT

GAATGAATGA ATGGTTTTAA ACTATCTTGT AAATTTTCTC AAACAATTTT TTTATTTTGA TGATATTTTT

CATTATTTTA TTTTGTGAAG AAAAGTATAT AAAGTTATAA ACCAATAACA CAATAATTTA ATTTATTAAC

AATCATAAAT TCTTTTTGTT TTAATTGAAT AACAAAAAAA GTTTTGTTAA CTTTATAAAA GAAGAAATCC

AATAACTTAA GATTTTAGAT TATTTTTTAC AAATATTAAA CTAATATCAC CAAACTTTAC CAAAATTTTA

AAAAATCTTG ATTAAATAAC AACAAATTCT ACATAACATT TAAGTCATTA AAACTTTATT TAAATCACAC

ACCAATAATT AAGTGACAAA TTATTTTTCT TACTTTTTAG TTTTAGCCAC GTTTTACATA TAGTTCTTAA

AATATGACTT GTTGATTCTC ATTATTTTTC TATATATACA TTATATCTTT GTGTATCCCT TTTCCCACAC

ATAAACGTTC ATTAAACACA AAGAATAACC AGACGAAGAA GAAG

Figure 23: At1g65890 promoter sequence.
The 1234 bp long At1g65890 promoter sequence is shown in 5’ to 3’ orientation.

ATGGATGATT TGGCATTATG TGAAGCAAAC AATGTTCCTC TAACCCCCAT GACGTTCTTG AAGAGAGCTT
CAGAGTGTTA TCCAAATCGA ACTTCAATAA TCTACGGAAA AACTCGTTTC ACTTGGCCTC AGACCTATGA
CCGTTGTTGT CGTCTAGCCG CTTCTCTAAT CTCTCTTAAC ATCTCCAAGA ACGATGTGGT ATCAGTTATG
GCTCCAAACA CACCCGCCTT GTATGAAATG CACTTTGCCG TTCCCATGGC TGGAGCTGTA CTTAACCCTA
TCAACACTCG TCTAGACGCA ACATCCATTG CCGCAATCCT CCGCCACGCC AAGCCCAAGA TCTTATTCCT
AGACCGCAGT TTTGAGGCCT TGGCTAGAGA AAGCCTCCAT TTATTATCAT CTGAAGACTC AAACCTAAAC
TTGCCGGTCA TATTTATCCA CGAGAACGAT TTTCCTAAAA GGGCTTCATT CGAGGAGTTA GACTACGAGT
GTCTCATCCA GAGGGGAGAG CCTACGCCCT CGATGGTGGC ACGCATGTTC CGTATTCAAG ACGAGCATGA
TCCAATCTCC TTAAACTACA CATCGGGTAC CACTGCCGAC CCAAAAGGTG TTGTGATTAG CCACCGAGGA
GCATATTTGT GCACATTAAG CGCGATTATT GGTTGGGAAA TGGGGACCTG CCCTGTCTAC CTTTGGACTC
TGCCTATGTT TCATTGCAAT GGATGGACGT TTACATGGGG AACCGCGGCG CGTGGGGGTA CCAGTGTGTG
TATGAGGCAC GTGACTGCCC CGGAGATCTA TAAAAACATA GAAATGCATA ACGTGACACA TATGTGTTGT
GTTCCTACGG TTTTCAACAT TCTTCTGAAA GGAAATTCAC TTGACCTGTC ACCTAGATCT GGACCGGTCC
ATGTGCTTAC CGGAGGTTCA CCGCCTCCCG CTGCTCTTGT CAAGAAAGTT CAACGGTTGG GGTTTCAAGT
GATGCATGCC TATGGGCAGA CCGAGGCCAC TGGTCCAATT TTGTTTTGTG AGTGGCAAGA TGAGTGGAAT
AGATTACCAG AGAATCAACA GATGGAATTA AAAGCCAGGC AAGGGATAAG CATCTTAGGC CTAGCTGACG
TTGACGTGAA AAACAAGGAA ACGCAAAAGA GTGCTCCGCG CGATGGAAAG ACAATGGGAG AAATCCTCAT
TAAAGGAAGT AGCATAATGA AAGGGTATCT AAAAAATCCC AAAGCTACAT TTGAGGCATT TAAACACGGA
TGGCTCAACA CAGGAGATGT AGGTGTGATT CACCCTGATG GGCACGTCGA GATCAAAGAT CGGTCAAAAG
ACATAATCAT ATCGGGAGGC GAAAACATTA GTAGTGTTGA GGTCGAGAAT GTTCTTTATA AGTACCCAAA
AGTCCTTGAG ACTGCAGTTG TGGCCATGCC TCACCCTACG TGGGGTGAAA CCCCGTGTGC GTTTGTTGTT
CTAGAAAAGA GTGAGACTAC TATTAAAGAA GATCGTGTTG ATAAATTTCA GACCAGAGAG AGAAATCTGA
TTGAGTATTG CCGTGAAAAT CTGCCACATT TTATGTGTCC GAGAAAAGTG GTGTTTTTGG AAGAACTGCC
CAAAAACGGG AATGGAAAGA TCCTTAAGCC TAAGCTAAGA GACATTGCTA AAGGTTTGGT TGTTGAGGAT
GAGATCAATG TTATAGCTAA AGAAGTTAAA CGGCCGGTTG GACATTTTAT TTCGCGGCTT TGA

Figure 24: At1g65880 BZL sequence.
The 1743 bp long At1g65880 gene sequence is shown in 5’ to 3’ orientation.

ATGGATAATT TGGCGTTATG TGAAGCAAAC AATGTTCCTC TAACTCCCAT AACGTTCTTG AAGAGAGCTT
CGGAGTGTTA TCCGAATCGA ACTTCGATAA TATACGGAAA AACTCGTTTC ACTTGGCCTC AGACCTATGA
CCGTTGCTGT CGTCTAGCCG CTTCTCTCAT ATCTCTTAAT ATCGGCAAGA ACGATGTGGT ATCCGTTGTT
GCTCCAAACA CACCGGCCAT GTATGAGATG CACTTTGCCG TTCCCATGGC TGGAGCTGTA CTTAACCCTA
TCAACACTCG TCTAGACGCA ACATCCATTG CCGCAATCCT CCGCCACGCC AAGCCCAAGA TTTTATTCAT
ATACCGCAGT TTTGAGCCAT TGGCTCGAGA AATCCTCCAG TTATTATCAT CTGAAGACTC AAACCTAAAC
TTGCCGGTCA TATTTATCCA CGAGATTGAT TTCCCTAAAA GGGTTTCGTC CGAGGAGTCA GACTACGAGT
GTCTCATCCA GAGGGGAGAG CCTACGCCCT TGTTGTTGGC ACGCATGTTC TGTATTCAAG ACGAGCATGA
TCCAATCTCT TTAAACTACA CATCGGGTAC CACAGCCGAC CCAAAAGGTG TTGTGATTAG CCACCGAGGA
GCATATTTAA GCACATTAAG CGCGATTATT GGTTGGGAAA TGGGGACATG CCCTGTCTAC CTTTGGACTC
TGCCTATGTT TCATTGCAAT GGATGGACGT TTACATGGGG AACTGCGGCC CGTGGGGGTA CTAGTGTGTG
TATGAGGCAT GTGACTGCCC CGGAGATCTA TAAAAACATA GAAATGCATA ACGTGACGCA TATGTGTTGT
GTTCCTACGG TTTTTAACAT TCTTCTGAAA GGAAATTCAC TTGACCTGTC ACATAGGTCT GGGCCGGTCC
ATGTTCTTAC CGGAGGTTCA CCGCCTCCCG CTGCTCTTGT CAAGAAAGTT CAGCGGTTGG GGTTTCAAGT
GATGCATGCC TATGGTTTGA CCGAGGCCAC TGGTCCGGTT CTGTTTTGTG AGTGGCAAGA TGAGTGGAAC
AGATTACCTG AGAATCAACA GATGGAGTTA AAAGCAAGGC AAGGGCTAAG CATCTTAGGC CTAACTGAAG
TTGACGTGAG AAACAAGGAA ACTCAAGAGA GTGTTCCGCG AGATGGGAAG ACGATGGGAG AAATCGTTAT
GAAAGGAAGC AGCATAATGA AAGGCTATCT GAAGAATCCC AAAGCTACAT ATGAAGCATT TAAACACGGA
TGGCTCAACT CAGGAGACGT AGGTGTGATT CATCCTGATG GACACGTAGA GATCAAAGAT CGGTCCAAAG
ACATAATCAT ATCTGGAGGC GAAAACATTA GTAGTGTTGA AGTCGAGAAT ATTATTTATA AGTACCCAAA
AGTGCTTGAG ACTGCCGTCG TGGCCATGCC TCACCCTACA TGGGGAGAAA CCCCATGTGC ATTTGTTGTT
CTAGAAAAGG GTGAGACTAA TAATGAAGAT CGTGAAGATA AACTTGTGAC CAAAGAGAGA GATTTGATTG
AGTATTGCCG TGAAAATCTT CCACATTTTA TGTGTCCGAG AAAAGTGGTG TTTTTGGATG AATTGCCCAA
AAACGGGAAT GGAAAGATCC TTAAGCCTAA GCTAAGAGAC ATTGCTAAAG GTTTGGTTGC TGAGGATGAG
GTCAATGTTA GATCTAAAGT TCAACGGCCG GTTGAACACT TTACTTCGCG GCTTTGA

Figure 25: At1g65890 BZL sequence.
The 1737 bp long At1g65890 gene sequence is shown in 5’ to 3’ orientation.

ATGGATGTAC TTCCAAAGTG TAGCGCAAAT TACGTTCCTC TTACTCCTCT CACTTTCTTG AAGAGAGCTG
CTTTCTCTTA CGCCGATCGA ACTTCTTTGA TTTACGAGCA TCTCCGCTTC ACTTGGCGCC AAACCTACCA
CCGCTGCTCT CGCCTCGCCG CCGCGCTCAC TAATATCCTC AACGTCCGAA AAAACGACGT CGTATCTGTG
TTGGCTCCAA ATATTCCGGC GGTCTACGAG ATGCATTTCG CGGTGCCGAT GGCTCGAGCC GTCCTAAACA
CGATCAACAC CCGACTCGAC GCTCATACCG TCTCGACAAT TCTCCGCCAC TCCGGCACCA AAATCCTCTT
TGTCGATTGC CAGTTCGTGT TATTAGCCCG ACAAGCTCTC GCCTTATTGA ACCACCCGAT CCGGCTCGTC
ATTATCAATG ATGAGACCCT CGCCCTTTCG GCACCGATCG GAGCCGGGGA AGTCGAATAC GAACATCTGA
TCTCGGAAAC GGGTTTCGCT GACGTGGACG ATCAGATAAT GAGCGTGGAC GATGAGTGGG ACCCGATCGC
GCTAAACTAC ACCTCCGGCA CCACGTCGGA GCCGAAAGGA GTGGTGTACA GCCACCGTGG GGCCTACCTC
AGCACCCTCA GCCTCATCCT AGGGTGGGAA ATGGGGAGCG AGCCGGTCTA CCTGTGGACC CTACCGATGT
TCCACTGTAA CGGCTGGACC TTCACGTGGG GGATCGCCGC CCGCGGCGGA ACTAATGTCT GCATGCGTAA
CCCTACGGCG GAGGGTATTT ACCGGAATAT CGCCGTTCAC AAGGTTACCC ACATGTGTTG CGCTCCGATC
ATCTTTAATA TTCTTCTCGA GGAAGAGAAT CGTATCCCGT TGACCTCCGC GGTCAATATC TTGACCGGCG
GCGCTCCGCC TCCCGCCGCC CTGTTGCAGA GCATTGAGAG TCTAGGGTTC CACGTCACGC ACGCCTATGG
CTTGACCGAA GCCACGGGGC CCGCGTTGTT ATGCGAGTGG CAGTCGAAGT GGAACGGGCT GTCTAGTGGC
GACCGGGCGA GGCTCAAGGC CCGGCAGGGG ATCAACGTGT GACGGTGGCT GACAGTTGAC GTGAAGGACC
CCAATAACAT GAAGAGCGTC GCTCATGACG GTACCACAAT GGGCGAAATC ATGCTACGGG GCAGCGGCAT
CATGAAAGGA TACTACAAGG ACCCAAAAGC CACATCCGAT GCCTTCAAAG GCGGGTGGTT CTTCACCGGC
GATGTCGGGG TAATTCATCC CGACGGGTAC GTCGAAATCA AGGACCGGTC AAAAGACGTG ATTATATCCG
GCGGAGAGAA CATAAGCAGC ATCGAGCTCG AGGAAGTGCT CTATAAGCAT CCTCGGGTTC TAGAAGCGGC
GGTGGTGGCA ATGCCGCACC CTCGGTGGGG TGAGAGCCCT TGCGCTTTTA TCGCCGTTAA GAAAAACCCT
AACGGGTTTC GGGGCGATGA GGTTACGGAG GCGGAGATCG TGTCGTTTTG TAAAAAGAAT GTTCCGAATT
TTATGGTTCC GAAGAAGGTG GAGTTTTTGG ACAGTTTGCC GAAGACTTCG ACGGGGAAGA TTCAGAAGTT
TCAGTTAAGG GCTTTGGCTA AGGCGTTGGT GGTTACGGAA AAGAGTGTTA ACAAGAACAA CCTTAAAACA
CAACTACCGC AGCAGCACTA CGATCATTCT CAGCATCAAC AACAACAGAT TCTTGCACAA TCTCGACTTT
AA

Figure 26: Sequence of a putative *Clarkia breweri* BZL gene.
The 1752 bp long *Clarkia breweri* gene is shown in 5’ to 3’ orientation.

ATGTCTAGAT CAACAAGTTT GTACAAAAAA GCAGGCTTAC TGGTTCCGCG TGGTTCCATG GACGAGTTAC
CAAAATGTGG AGCAAACTAT GTGCCTCTAA CTCCTCTAAC CTTCTTAACA AGAGCCTTCA AATCTTATGC
TAATCGGACC TCCATCATTT ATGCTGGTGC GCGTTTCACA TGGGAGCAAA CCTACAAGAG GTGTTGTCGT
CTCGCATCCT CTCTCCAATC CTTAAACATT GTCAAGAACG ACGTTGTTTC AGTGTTAGCA CCTAATGTGC
CAGCAACGTA CGAAATGCAT TTTGCTGTAC CAATGGCAGG GGCTGTGCTA AACACAATTA ATACAAGGCT
AGACCCTATG AACATTGCAA TTATTCTCAA ACATTCTGAA GCAAAGCTCT TATTTGTGGA CTATGAATAC
CTTGAAAAGG CACGAAAGGC CCTTGAACTG CTAATGTCAA CCAACTTTAT CACAGCCCAA AATTCTAAGA
AAATTTCAAT GCCTCAAGTC ATTCTCATTG ATGACCTCTA CTCTCCAACC AGAATCCAAC AACAAGATCA
GCTCGAGTAC GAGCAACTTG TTCACCAAGG CAATCCTGAA TATGCTCCCG AGAATATTGT TGACGACGAG
TGGGATCCAA TTGTGTTGAA CTATACATCA GGTACAACTT CAGAGCCCAA AGGAGTTGTG TACAGTCACA
GAGGAGCTTT TTTAAGCACT TTGAACACAA TTATGGGATG GGAGATGGGA ACTGAGCCTG TGTACTTATG
GTCTCTTCCA ATGTTCCATA TCAATGGCTG GACTTTGACA TGGGGCATAG CGGCACGAGG TGGAACCAAC
GTTTGCATCC GCAACACTAC AGCTCAAGAA ATCTACTCCA ACATAACGTT ACATAAGGTT ACACATATGT
GTTGTGCCCC TACTGTTTTC AACATCCTCC TTGAGGCCAA GCCACACGAG CGTCGCGAAA TAACGACTCC
CGTCCAAGTA ATGGTTGGCG GAGCACCACC ACCTACAACA CTTATTGGGA AAATCGAGGA GCTCGGATTC
CACGTTGTAC ACTGTTATGG AATCACAGAG GCTGGGGGGA CGACCCTCGT GTGCGAGTGG CAGTCCGAAT
GGAACAAACT ATCTAGGGAA GATCAGGCCA ATTTGAAGGC TAGACAAGGA ATCAGCGTAC TAGCACTTGA
AGATGTTGAT GTGAAAAACT CCAAGACTAT GCAAAGTGTA CCACATAATG GAAAAACAAT GGGGGAGATA
TGCCTTCGGG GGAGTAGCAT CATGAAAGGG TACTTCAAGA ATGACAAGGC AAATTCACAA GTATTCAAAA
ATGGTTGGTT CCTCACAGGA GATGTCGCTG TCATTCACCA AGATGGATAC TTGGAAATAA AGGATAGATG
CAAGGATATC ATTATTTCAG GCGGAGAGAA TATTAGTAGC ATTGAAGTGG AAAATGCAAT TTTAAAGCAT
CCAAGTGTGA TAGAGGCAGC TGTTGTGGCC ATGCCACATC CTAGGTGGGG TGAAACTCCT TGTGCCTTTG
TCATAAAGAC CAAAAATCCA GAGATCAAAG AAGCAGATAT TATCGTACAT TGTAAGAAAG AATTACCAGG
ATTCATGGTG CCAAAGCATG TGCAATTTCT AGAAGAGTTA CCAAAAACTG GAACTGGGAA AGTAAAGAAA
CTACAGCTCA GAGAAATGGC CAAGTCATTT GGCATATTTG ATAATGCAAA TCAAACGTCC CAGATTCTTG
ATTTGCCAGC TCGTCTG

Figure 27: Sequence of a putative *Petunia hybridia* BZL gene.
The 1767 bp long Petunia gene is shown in 5’ to 3’ orientation.

ATGAATGCAG CCGCGGTCAC GCCGCCACCC GAGAAGTTTA ATTTTGCCGA GCACCTGCTG CAGACCAATC
GCGTGCGGCC GGACAAGACG GCGTTCGTCG ACGACATCTC GTCGCTGAGC TTCGCGCAAC TCGAAGCTCA
GACGCGTCAG CTCGCCGCCG CCTTACGCGC GATCGGGGTG AAACGCGAAG AGCGCGTGCT GCTGCTGATG
CTCGACGGCA CGGATTGGCC GGTGGCGTTT CTCGGCGCAA TCTACGCCGG CATCGTGCCG GTCGCGGTCA
ATACGCTGCT GACGGCGGAC GACTACGCCT ACATGCTCGA GCATTCGCGG GCTCAGGCCG TGCTGGTCAG
CGGCGCGCTG CACCCGGTGC TCAAGGCAGC GCTGACCAAG AGCGATCACG AGGTGCAGCG AGTGATCGTT
TCGCGCCCAG CGCTCCGCTG GAGCCGGGCG AGGTCGACTT CGCTGAGTCG GCGCACATCG CTTGAGAAGC
CTGCCGCTAC GCAAGCGGAC GATCCGGCGT TCTGGCTGTA TTCGTCGGGT TCTACCGGGC GGCCGAAGGG
CGTGGTGCAC ACTCACGCCA ATCCGTACTG GACCTCGGAG CTGTACGGCC GCAACACGCT GCATCTGCGC
GAAGACGACG TCTGCTTTTC GGCGGCCAAA CTGTTTTTCG CTTACGGCCT CGGCAACGCG CTGACGTTTC
CGATGACGGT CGGCGCGACC ACGCTGCTGA TGGGCGAGCG ACCGACGCCG GACGCGGTGT TCAAGCGCTG
GCTCGGCGGC GTCGGCGGTG TGAAACCGAC CGTGTTCTAC GGCGCGCCCA CCGGCTACGC CGGCATGTTG
GCCGCGCCGA ACCTGCCGTC GCGCGACCAG GTGGCGTTGC GGCTCGCGTC GTCGGCGGGC GAAGCACTGC
CGGCGGAGAT TGGGCAGCGC TTCCAGCGCC ATTTCGGCCT CGACATCGTC GATGGCATCG GCTCGACCGA
GATGCTGCAC ATCTTTCTGT CGAACCTGCC AGACCGGGTG CGCTACGGCA CCACCGGATG GCCGGTGCCG
GGCTATCAGA TCGAGCTGCG CGGCGACGGC GGCGGACCGG TCGCCGACGG AGAGCCGGGC GATCTCTACA
TTCACGGCCC GTCATCGGCG ACGATGTATT GGGGCAACCG GGCCAAGAGC CGCGACACCT TCCAGGGCGG
CTGGACCAAG AGCGGCGACA AATACGTCCG CAACGACGAC GGCTCCTACA CCTATGCGGG CCGCACCGAC
GACATGCTGA AGGTCAGCGG CATCTATGTC AGCCCGTTCG AGATCGAAGC GACGCTGGTG CAGCATCCCG
GTGTGCTCGA AGCCGCAGTG GTCGGGGTCG CCGACGAACA CGGCCTGACC AAACCGAAGG CCTATGTGGT
GCCGCGGCCC GGCCAGACCC TGTCGGAGAC CGAGCTGAAG ACCTTCATCA AGGATCGACT GGCGCCGTAC
AAATATCCGC GCAGCACGGT GTTCGTCGCC GAATTGCCGA AGACGGCGAC CGGCAAGATT CAGCGCTTCA
AGCTGCGCGA GGGTGTGTTG GGCTGA

Figure 28: Sequence of the *badA* gene of *Rhodopseudomonas palustris.*
The 1566 bp long *R. palustris* BZL gene is shown in 5’ to 3’ orientation.

Aknowledgement

I thank Prof. Jonathan Gershenzon for giving me the opportunity to do my diploma work in the Department of Plant Biochemistry and Molecular Biology at the Max-Planck-Institute for Chemical Ecology in Jena.

I thank PD Dr. Klaus-J. Appenroth for evaluating and judging my work and also for having an open ear to my questions and giving me advises.

I thank my advisor John D'Auria for the offer of this exciting project, his support throughout the whole progress and his trust in me. I also thank for all the important big and small things I learned for my furture.

Thanks to everybody in our institute who helped me in the time I did my diploma work. In particular I like to thank Michael Reichelt, Bettina Raguschke, Ulrike Temp, Katrin Luck, Irmgard Seidel-Adams, Andrew Davis, Jeannette Kley and the gardeners of the institute.

Furthermore, I thank Laura Olsen for giving recomentions and by providing useful protocols.

And last but not least, thank you Daddy for your patients!

Selbstständigkeitserklärung

Hiermit versichere ich, dass ich die vorliegende Arbeit selbstständig verfasst und nur unter Verwendung der angegebenen Literatur und Hilfsmittel angefertigt habe.

Jena, den 27. Januar 2008

_____

Katrin Gruner